The type II poly(A)-binding protein PABP-2 is a downstream target of the *let-7* microRNA in the heterochronic pathway of *Caenorhabditis elegans*

Mechanisms of microRNA-mediated gene silencing in *Caenorhabditis elegans*

Inauguraldissertation

zur
Erlangung der Würde eines Doktors der Philosophie
vorgelegt der
Philosophisch-Naturwissenschaftlichen Fakultät
der Universität Basel

von

Benjamin Andreas Hurschler
aus Engelberg, Obwalden

Basel, 2012

Genehmigt von der Philosophisch-Naturwissenschaftlichen Fakultät auf Antrag von

Professor Dr. Mihaela Zavolan, Dr. Helge Grosshans und Professor Dr. Gunter Meister.

Basel, den 20. September 2011

Professor Dr. Martin Spiess

(Dekan)

creative commons

Namensnennung-Keine kommerzielle Nutzung-Keine Bearbeitung 2.5 Schweiz

---

Sie dürfen:

das Werk vervielfältigen, verbreiten und öffentlich zugänglich machen

Zu den folgenden Bedingungen:

Namensnennung. Sie müssen den Namen des Autors/Rechteinhabers in der von ihm festgelegten Weise nennen (wodurch aber nicht der Eindruck entstehen darf, Sie oder die Nutzung des Werkes durch Sie würden entlohnt).

Keine kommerzielle Nutzung. Dieses Werk darf nicht für kommerzielle Zwecke verwendet werden.

Keine Bearbeitung. Dieses Werk darf nicht bearbeitet oder in anderer Weise verändert werden.

- Im Falle einer Verbreitung müssen Sie anderen die Lizenzbedingungen, unter welche dieses Werk fällt, mitteilen. Am Einfachsten ist es, einen Link auf diese Seite einzubinden.
- Jede der vorgenannten Bedingungen kann aufgehoben werden, sofern Sie die Einwilligung des Rechteinhabers dazu erhalten.
- Diese Lizenz lässt die Urheberpersönlichkeitsrechte unberührt.

Quelle: http://creativecommons.org/licenses/by-nc-nd/2.5/ch/ Datum: 3.4.2009

Är isch mit sire Schtaffelei am Sunndig über Land,
und het es Süsche gsuecht won'är chönnt male.
Da trifft sy Künschtlerblick uf'ene Chue am Waldesrand,
är gseht, das git es Meischterwärch, nid's zahle.

Er schtellt sech uf und malt zersch links der Wald im Hintergrund,
e Hügel rächts, chli Himmel no derzue.
Druf macht'er vorne z'Gras mit vil'ne Blueme drinn und chunnt,
am Schluss zur Houptsach, nämlech zu dr Chue.

Är mischt uf syr Palette zarti Brun, mit gschickter Hand,
und dunkt der Pinsel dry, und setzt'nen'a,
doch won'er jetz e letschte Blick wirft uf sy Gägeschtand,
isch plötzlech - o herrje - d'Chue nümme da.

Das uferschandte Tier isch usegloffe us sim Bild,
kei Mönsch weis, was vo dert ihn's het vertribe,
sy isch nümm zrugg cho, ou won'är grüeft und gwunke het wie wild,
e wisse Fläck isch uf der Linwand blibe.

No lang, a sälbem Sunntig, het är gwartet a der Schtell,
het gwartet vor sir Schtaffelei, dass da,
es bruchti nid die glychi d'sy, e Chue derthäre well,
wo ihn no würd sys Bild vollände la.

Doch d'Wält isch so perfid, dass sy sech sälte oder nie,
nach Bilder, wo'mer vore gmacht hei richtet,
so hei ou uf der Matte die banousehafte Chüe,
dä Aasatz zum'ne Meischterwärch vernichtet.

Mani Matter (1936-72)
Influential constitutional lawyer and song-writer.

Acknowledgements

I wish to thank:

Helge Grosshans for giving me the opportunity to pursue my PhD studies under his supervision, for his continuous support, and for his patience at times when projects just kept refusing to work out.

All the present and past members of the lab for a friendly working atmosphere, especially Monika Fasler for support, Ingo Büssing for introducing me to *C. elegans* work, Saibal Chatterjee for discussions, Xavier Ding for sharing the up and downs of polysome profiling, and Florian Aeschimann for carrying on the project.

My thesis committee: Mihaela Zavolan, Gunter Meister and Dirk Schübeler.

Tim Roloff, Dimos Gaidatzis, Jean Hausser, Mhoshen Korshid, and Edward Oakeley for analyzing data and Michael Stadler for providing a custom made bioinformatic tool for a project that is not part of this thesis.

Iskra Katic for establishing strains.

Saibal Chatterjee, Magdalene Rausch and Matyas Ecsedi for critically reading parts of this manuscript.

The media kitchen for providing me with more than 40,000 nematode growth plates during the past five years.

The Swiss National Science Foundation, the European Research Council and the Novartis Research Foundation for financial support.

My flat mates during most of my PhD studies: Gregor for sharing the passion for free flight and Sonja for coping with two scientists that rarely came home before dinner was ready.

My parents Marianne and Hanspeter, my sisters Barbara and Raphaela, my friends, and Kristin for all her support during the weeks of writing.

Table of content

Abbreviations

bp	base pair
cDNA	complementary DNA
CDS	coding sequence
dsRNA	double-stranded RNA
eIF	eukaryotic translation initiation Factor
EV	empty vector control, insert-less RNAi vector L4440
Ex	extrachromsomal array
gf	gain-of-function
kb	kilobase
lf	loss-of-function
miRISC	miRNA-induced silencing complex
miRNA	microRNA
mRNA	messenger RNA
nt	nucleotide
ORF	open reading frame
P-body	processing body
PolII	RNA polymerase II
pre-miRNA	miRNA precursor
pri-miRNA	primary miRNA transcript
RNAi	RNA interference
rRNA	ribosomal RNA
siRNA	small interfering RNA
snoRNA	small nucleolar RNA
snRNA	small nuclear RNA
ssRNA	single-stranded RNA
TMG	trimethylguanosine
tRNA	transfer RNA
wt	wild-type

1. Summary

microRNAs (miRNAs) are a large class of small, non-coding RNAs that post-transcriptionally regulate gene expression in animals, plants and protozoa. miRNAs are genomically encoded and transcribed by RNA polymerase II. Primary transcripts are sequentially processed by two RNase III enzymes via short, approximately 70 nucleotide long stem-loop containing precursor miRNAs into mature 21 to 23 nucleotide long miRNAs. Mature miRNAs are incorporated into the miRNA-induced silencing complex (miRISC), which, in its core, consists of an Argonaute and a GW182 family protein. miRNAs serve as guide molecules to direct miRISC to target mRNAs. Typically, miRNAs interact by base-pairing with partially complementary miRNA binding sites located in the 3' untranslated regions of the targeted mRNA. Binding of miRISC ultimately prevents protein accumulation by mechanisms which are not well understood. miRNAs regulate diverse biological processes including development, proliferation, differentiation, apoptosis, host defense, and cancer. By estimation, miRNAs potentially regulate more than 60% of the human protein coding genome, leaving only few, if any, genetic pathway untouched.

The phylogenetically conserved miRNA *lethal-7 (let-7)* was first discovered as an essential developmental gene in the heterochronic pathway of the free-living nematode *Caenorhabditis elegans*. The genes of the heterochronic pathway direct the stage specific execution of cell fates during post-embryonic development of *C. elegans.*

We identified the type II poly(A)-binding protein PABP-2 in a suppressor screen for *let-7* loss-of-function lethality. Mammalian PABP2 was initially identified as an enhancer of nuclear polyadenylation. In this work we show that depletion of PABP-2 not only rescues loss of *let-7* function, but also causes *let-7* gain-of-function phenotypes in wild-type animals. Surprisingly, efficient depletion of PABP-2 leaves global translation and mRNA levels largely unaffected, but causes premature accumulation of the LIN-29 transcription factor, the most downstream factor known in the heterochronic pathway. This is not due to an effect on *let-7* biogenesis and *let-7* activity, which are not affected by the level of PABP-2. However, we find that

PABP-2 protein levels are developmentally regulated and decrease during larval development. Although PABP-2 is unlikely to be a direct target of *let-7*, decrease of PABP-2 in late larval development depends, at least in part, on *let-7* activity.

The molecular mechanism of miRNA-mediated gene silencing has been subject to intense debate. Despite a plethora of often conflicting data, the emerging consensus is that repression of translation initiation and accelerated mRNA degradation are the prevailing mechanisms. However, it is not clear whether translational repression and mRNA degradation constitute two parallel mechanisms or whether translational repression and mRNA degradation are sequential events. Work done in our lab showed, that in *C. elegans*, miRNAs regulate their cognate target genes by repression of translation at the initiation stage, which often, but not always, coincides with reduced target mRNA levels. Furthermore, repression depended on the presence of AIN-1 and AIN-2, the *C. elegans* homologs of the GW182 protein family. AIN-1 and AIN-2 are highly divergent homologs of fly and vertebrate GW182 proteins. Moreover, AIN-1 and AIN-2 show only little similarity at the level of their protein sequences. In an extension of our previous work, we studied the individual contribution of AIN-1 and AIN-2 to miRNA mediated gene silencing by analyzing *ain-1* and *ain-2* single mutant animals. We find that translational repression, but not mRNA decay, relies on the presence of AIN-1. However, overexpression of AIN-2 rescues *ain-1* specific developmental defects and restores wild-type translational repression. It is not clear why translational repression and mRNA degradation have a different requirement for overall GW182 protein levels. Thus far, our data proof that AIN-1 as well as AIN-2 act as bona fide GW182 proteins, mediating both translational repression and mRNA decay.

2. Introduction

Three decades before the first genome annotations were available Britten and Davidson proposed a stochastic model of gene regulation in higher cells, in which *activator genes* regulate the *receptor genes* of *producer genes* (Britten and Davidson, 1969). Remarkably, rather than coding for proteins with sequence specific DNA binding capacity, the activator genes were proposed to encode "RNA molecules which form a sequence-specific complex with receptor genes linked to producer genes". The base-pairing between activator and producer gene was envisioned to be imperfect, which would allow for various degrees of regulation and evolutionary flexibility to produce new tissues and organs. As a corollary, they also proposed that all eukaryotes share more or less the same set of producer genes and that it is the layer of activators that mostly explains the difference between species. However, the existence of a comprehensive network of non-coding RNAs as regulators of gene expression and preservers of genome integrity remained long time unnoticed.

microRNAs (miRNAs) are a class of small, non-coding RNAs that are transcribed as long, 5'-capped and polyadenylated primary transcripts or reside in introns of protein coding genes. After nuclear and cytoplasmic processing, mature miRNAs of ~22 nucleotides (nt) length are incorporated into a miRNA-induced silencing complex (miRISC) where they act as guide molecules by imperfectly base-pairing to the 3' untranslated region (3' UTR) of target mRNAs. Binding of miRISC ultimately prevents protein production from the targeted mRNA by target degradation and/or translational repression. Despite palpable differences, the model presented at the beginning captures central elements of miRNAs as a regulatory layer in gene expression: target recognition by imperfect base-pairing, the potential to regulate several to hundreds of genes to various degrees, and flexibility in acquiring or abandoning regulatory relationships.

In addition to miRNA biogenesis, target recognition, and miRNA mode of action, the introductory sections will also address some of the work that led to the discovery of small interfering RNAs and miRNAs, the major genetic tool and the subject throughout most of my studies. In the case of miRNAs, this is also intended to place

an emphasis on developmental timing in *C. elegans* and its close interconnection to miRNAs and miRNA pathway genes, which was an important driving force for studying PABP-2.

2.1 Short history of a short RNA: siRNAs

The strategy to reduce gene expression using RNA that contains the complementary sequence to the targeted mRNA was used since the late 80s; for instance in petunia to silence chalcone synthase, the rate limiting enzyme in the anthocyanin biosynthesis pathway, which is responsible for the purple pigmentation of the flower (van der Krol et al., 1988). The silencing was attributed to a complete hybridization of mRNA and anti-sense mRNA, thus preventing protein production. This notion was challenged when two different groups attempted to over-express chalcone synthase in petunia by providing additional cDNA in *trans*. Instead of the expected deep purple pigmentation of the flowers, the introduced gene produced white flowers and patterned flowers with white sectors (Napoli et al., 1990; van der Krol et al., 1990). Progeny testing of a plant showed that the novel color phenotype co-segrageted with the introduced CHS gene. The phenomenon was called *co-suppression*. A similar effect was observed in *Neurospora crassa*, where introduction of RNA sequences homolgous to different portions of the *albino-1* and *albino-3* gene caused *quelling* of the endogenous gene (Romano and Macino, 1992) and also in *C. elegans*, where the injection of *in vitro* synthesized *par-1* sense RNA, intended as a negative control, unexpectedly induced *par-1* mutant phenotypes (Guo and Kemphues, 1995).

The double stranded nature of the RNA silencing trigger was first recognized by Fire and Mello (Fire et al., 1998). To investigate the requirements of structure and delivery of the interfering RNA, they injected purified sense and antisense RNA against *unc-22* mRNA, which encodes an abundant but non-essential myofilament protein. Purified antisense and sense RNA exhibited only marginal interference activity, whereas a sense-antisense mixture produced highly effective interference with the endogenous gene. The effects of *RNA interference* in the injected animals were systemic, and furthermore, could also be passed from parents to progeny. Work carried out in plants (Hamilton and Baulcombe, 1999) and drosophila (Bernstein et al., 2001; Hammond et al., 2000; Zamore et al., 2000) identified low molecular weight anti-sense RNA of 21-23 nt length produced from long, double stranded RNAs (dsRNAs) as guides of a sequence-specific endonuclease activity. The process of the conversion of long dsRNAs to small interfering RNAs (siRNAs) and the subsequent

silencing of target genes has been termed RNA interference (RNAi) (Fire et al., 1998).

siRNAs were initially proposed to be a defense mechanism against RNA of exogenous origin and an endogenous, physiological role was yet unclear. However, the utility of RNAi to silence genes in flies (Kennerdell and Carthew, 1998), worms (Fire et al., 1998), plants (Hamilton and Baulcombe, 1999) and mammalian cells (Elbashir et al., 2001) drew great interest into the regulatory function of small RNAs.

2.2 Short history of a short RNA: miRNAs

In a multi-cellular organism, integration of temporal and spatial information is prerequisite to coordinate development from a fertilized egg to adulthood. Thanks to robust genetic tools, the ability to study tissues in a living organism by microscopy, and, most of all, an invariant cell-lineage that allows to keep track of developmental decisions at a single cell resolution, *C. elegans* emerged as a powerful model to study developmental timing (reviewed by Resnick et al.).

The postembryonic development of *C. elegans* proceeds through four larval stages, termed L1 to L4, followed by the adult stage. In normal development, cells divide and differentiate in a stereotypic manner, so that the somatic cell lineages of males and hermaphrodites could be mapped (Deppe et al., 1978; Kimble and Hirsh, 1979; Sulston and Horvitz, 1977). In several lineages, stage-specific execution of cell fates is controlled by a network of genes which are collectively termed the heterochronic pathway. Mutations in these heterochronic genes cause cells to adopt fates usually observed at earlier or later larval stages, resulting in a retarded or precocious heterochronic phenotype, respectively (Ambros and Horvitz, 1984). This can be particularly well studied in the seam cells, a subset of hypodermal cells that run laterally along the longitudinal axis of *C. elegans*. In each larval stage, seam cells divide in a stereotypical, stem-cell like manner: the posterior daughter cell retains the seam-cell identity, whereas the anterior daughter cell differentiates and fuses to the underlying tissue. Additionally, a subset of seam cells also undergoes a proliferative division in early L2, which increases their number. At the L4-to-adult molt, seam cells exit the cell cycle and terminally differentiate, which involves their fusion into a syncytium. Thereby, they secret a specialized cuticular structure termed alae, i.e. three lateral ridges running along the longitudinal axis of the animal. A simplified representation of the heterochronic pathway and examples of altered seam cell lineages in heterochronic mutants are presented in Figure 2.1.

lin-4 was first characterized by the isolation of a mutant allele that causes failure of temporal switches throughout the animal, showing that *lin-4* might encode a master regulator of developmental timing (Chalfie et al., 1981; Horvitz and Sulston, 1980). In

Figure 2.1

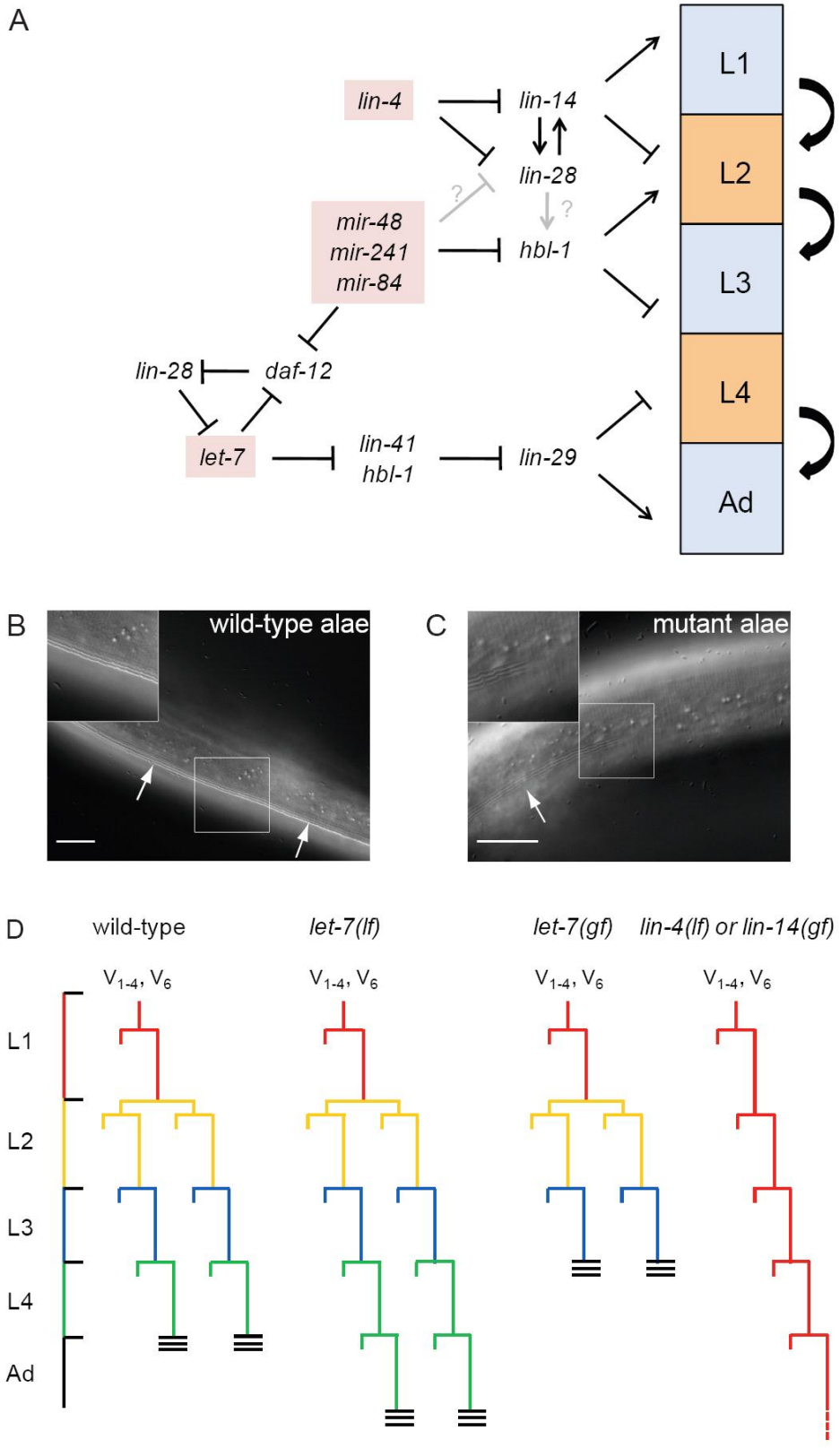
A
lin-4
lin-14
lin-28
mir-48
mir-241
mir-84
hbl-1
lin-28
daf-12
let-7
lin-41
hbl-1
lin-29
L1
L2
L3
L4
Ad
B
wild-type alae
C
mutant alae
D
wild-type
let-7(lf)
let-7(gf)
lin-4(lf) or lin-14(gf)
V1-4, V6
L1
L2
L3
L4
Ad

Figure 2.1

(A) The heterochronic pathway of *C. elegans*. For clarity, only factors discussed in this thesis are shown. miRNAs are highlighted. Three developmental switches are regulated by miRNAs: the L1 to L2 switch is mediated by repression of *lin-14* by *lin-4*, the L2 to L3 switch by *lin-4* and *let-7* sister (*mir-48*, *mir-84*, *mir-241*) mediated repression of *lin-28* and *hbl-1*, and the L4 to adult switch by *let-7* repression of *lin-41*, *daf-12*, and *hbl-1*. All regulatory relationships are supported by genetic data, however, not all are known to be direct. (B-C) DIC image of adult cuticle of a wild-type animal and an animal depleted of a miRNA pathway gene (*cbp-20*, RNAi by feeding). The alae (three lateral ridges) are indicated by arrow heads. Scale bars are 20 µm. Photo courtesy of Ingo Büssing. (D) Seam cell lineages of wild-type, *let-7(lf)*, *let-7(gf)* and *lin-4(lf)* (or *lin-14(gf)*) animals. The developmental stage is indicated at the left with the black lines indicating the molts. In the cell lineage diagrams, each cell division is represented by a horizontal line. Short horizontal lines represent the anterior, differentiating cells, long horizontal lines represent the posterior daughter cells which retain the seam-cell identity. Terminal differentiation at the L4 to adult transition is represented by three alae-like horizontal lines. A symmetrical proliferative cell division occurs in early L2, which is missing in *lin-4(lf)* or *lin-14(gf)* animals since they fail to execute L2 stage specific events. Instead, the seam cell lineage repeats L1 specific fates. In *let-7(lf)* animals, seam cells fail to exit cell cycle and repeat L4 specific events. Thus, the phenotypes of *lin-4(lf)* and *let-7(lf)* are termed retarded. *let-7(gf)* animals skip L4 specific events and terminal seam cell differentiation occurs precociously at the L3 to L4 molt.

lin-4 loss-of-function (lf) animals, certain cells reiterate L1 specific division patterns during the L2 and L3 stages. Furthermore, *lin-4(lf)* animals fail to produce an adult cuticle and hermaphrodites also lack a vulva (Chalfie et al., 1981). *lin-14* was identified as suppressor of *lin-4* associated vulva defects. Whereas *lin-14(lf)* animals exhibit phenotypes opposite to *lin-4(lf)* animals and skip L1 specific cell fates, *lin-14* gain-of-function (gf) mutations induce a similar phenotype as *lin-4(lf)* (Ambros, 1989; Ambros and Horvitz, 1987). In *lin-4(lf)* animals and also in *lin-14(gf)* animals, LIN-14 protein remains abnormally high late in development (Ruvkun and Giusto, 1989). Intriguingly, the *lin-14(gf)* mutations proved to be deletions in the *lin-14* 3' UTRs (Wightman et al., 1991) and the *lin-14* 3' UTR was shown to be necessary and sufficient for the regulation of LIN-14 protein levels by *lin-4* (Wightman et al., 1993). These findings suggested that the product of the *lin-4* gene directly or indirectly interacted with regions of the *lin-14* 3' UTR deleted in *lin-14(gf)* alleles. Surprisingly, the products of the *lin-4* gene were two small RNAs of 22 nt and 61 nt size, now known to correspond to a mature miRNA and its precursor, with partial complementarity to elements found in the *lin-14* 3' UTR. Since there was no evidence for conservation of the *lin-4* gene product beyond the genus of *Caenorhabditae*, posttranscriptional regulation of a target mRNA by a small RNA binding to partially complementary sites of its 3' UTR was rather considered a worm oddity than a new paradigm of gene regulation. Although *lin-4* related miRNAs have now been identified in mammals and flies (Lagos-Quintana et al., 2003), they are too divergent in their 3' ends to be identified by hybridization with a *lin-4* probe and thus were missed.

The canvas changed completely with the discovery of a second miRNA, *let-7*, in a screen for heterochronic mutants (Reinhart et al., 2000). Due to their regulatory function in the heterochronic pathway, *lin-4* and *let-7* were named small temporal RNAs. Soon after its discovery in nematodes, homologues of *let-7* were identified in a variety of bilaterian species, including flies, zebrafish, and humans (Pasquinelli et al., 2000), paving the way for the systematic search for miRNAs (Lagos-Quintana et al., 2001; Lau et al., 2001; Lee and Ambros, 2001).

2.3 *C. elegans let-7*: a potent model to study miRNA biology

Mature *let-7* accumulates strongly towards the end of the L3 stage (Reinhart et al., 2000). *let-7* directly represses accumulation of LIN-41, a member of the TRIM-NHL family of RNA-binding proteins (Slack et al., 2000; Vella et al., 2004). LIN-41 in turn prevents early accumulation of the zinc finger transcription factor LIN-29, the most downstream effector known in the heterochronic pathway. *lin-29* activity is required for the execution of the adult-specific terminal differentiation program including cell cycle exit, cell fusion and the formation of an adult specific cuticula (Rougvie and Ambros, 1995).

let-7 mutants develop normally until the L3-to-L4 molt, however, reiteration of L4-specific cell divisions in various tissues causes animals to die at the L4-to-adult molt by bursting at the vulva (Reinhart et al., 2000; Vella et al., 2004). Less severe mutations in *let-7* cause reiteration of L4 fates in seam cells, resulting in extra seam cell division, delay or lack of formation of the seam cell syncytium, and partial or complete lack of adult specific alae. Conversely, over-expression of *let-7* or loss-of-function in *lin-41* causes precocious execution of adult specific cell fates in L4.

Three additional members of the *let-7* family, i.e. miRNAs that share the *let-7* seed sequence, also act in developmental timing. *mir-48*, *mir-84*, and *mir-241* function together in regulating the L2-to-L3 transition by regulating the hunchback-like transcription factor *hbl-1*. Disruption of all three sister miRNAs results in reiteration of L2 specific cell fates, whereas individual deletion shows only minor phenotypes (Abbott et al., 2005; Esquela-Kerscher et al., 2005; Hayes et al., 2006).

The outstanding role of *let-7* in the proper execution of adult specific developmental programs is reflected in the fact that the individual depletion of several components of the miRNA core machinery in *C. elegans* results in heterochronic phenotypes that closely resemble the ones observed upon the loss of *let-7* miRNA. Thus, the study of such phenotypes has been instrumental in the identification of the RNase III enzyme DCR-1 (Grishok et al., 2001; Ketting et al., 2001; Knight and Bass, 2001), the Argonaute-like proteins ALG-1, ALG-2 (Grishok et al., 2001), the GW182 proteins AIN-1, AIN-2 (Ding et al., 2005; Zhang et al., 2007), the microprocessor complex

(Denli et al., 2004) and factors involved in the nuclear export of *let-7* (Bussing et al.). Conversely, individual knock-down of *let-7* target genes can partially rescue the lethal phenotype of the *let-7(n2853)* allele (Abrahante et al., 2003; Grosshans et al., 2005; Lall et al., 2006; Lin et al., 2003; Slack et al., 2000). Likewise, mutation of *lin-28* (Reinhart et al., 2000), a negative regulator of *let-7* biogenesis and depletion of XRN-2, a nuclease involved in miRNA turnover (Chatterjee and Grosshans, 2009) also rescue *let-7(n2853)* lethality by increasing the residual *let-7* activity. Therefore, we first speculated that PABP-2, the *C. elegans* orthologue of the type II poly(A)-binding protein PABP2/PABPN1 negatively interacted with *let-7* biogenesis or function when we identified *pabp-2* in a reverse genetic screen for suppression of *let-7(n2853)* associated lethality (Ding et al., 2008).

2.4 miRNA biogenesis and RISC loading in animals

miRNAs are processed from precursor molecules, which are transcribed from independent genes or represent introns of protein coding genes. Approximately 50% of mammalian miRNA loci are found in close proximity to other miRNAs. These clustered miRNAs are transcribed from a single polycistronic transcription unit, although there may be cases in which individual miRNAs are under the control of separate gene promoters (Lee et al., 2002). Transcription of most miRNA genes is mediated by RNA polymerase II (PolII) (Cai et al., 2004; Lee et al., 2004) and primary transcripts show PolII associated hallmarks like a 5' m^7GpppN-cap and a 3' poly(A) tail. A few nematode specific features of PolII transcripts will be discussed in section 2.7. However, a small group of miRNAs that are associated with Alu repeats can be transcribed by RNA polymerase III (PolIII) (Borchert et al., 2006; Gu et al., 2009b). The primary transcripts (pri-miRNAs) generated by PolII are usually several kilobases long and contain local stem-loop structures.

The initial processing is performed in the nucleus by the microprocessor complex, which consists of the RNase III type protein Drosha (Lee et al., 2003) and DGCR8 (DiGeorge syndrome critical region 8 protein) in humans or Pasha (partner of Drosha) in flies and *C. elegans* (Denli et al., 2004; Gregory et al., 2004; Han et al., 2004; Landthaler et al., 2004). DGCR8/Drosha recognizes the single-stranded RNA (ssRNA) segments and the stem, while Drosha cleaves cleaves the stem ~11 bp away from the ssRNA-dsRNA junction, releasing a ~70 nt precursor miRNA (pre-miRNA) with a 3' single-stranded overhang of 2 nt (Han et al., 2006; Zeng and Cullen, 2005). Thus, processing by the microprocessor complex defines one end of the mature miRNA. In the case of intronic miRNAs, pri-miRNA processing might be a cotranscriptional process as Drosha processing of intronic miRNA precedes splicing of the host intron (Kim and Kim, 2007; Morlando et al., 2008; Pawlicki and Steitz, 2008). Not all miRNAs depend on processing by the microprocessor complex: mirtrons reside in short introns of host mRNA genes and form a hairpin structure that resembles pre-miRNAs after splicing of the host gene (Okamura et al., 2007; Ruby et al., 2007a). Rarely, miRNAs originate also from other non-coding RNAs such as transfer RNAs (tRNAs) (Babiarz et al., 2008) or snoRNAs (Ender et al., 2008).

Following nuclear processing, pre-miRNAs are transported out of the nucleus by Exportin-5 (Exp5), a member of the nuclear transport receptor family (Bohnsack et al., 2004; Lund et al., 2004; Yi et al., 2005). However, the nematode genome lacks an orthologue of Exp-5. Instead of Exp-5, the nuclear export receptor XPO-1, possibly in conjunction with the cap-binding complex, mediates nuclear export and/or intranuclear transport of pri-miRNAs (Bussing et al., 2010). Once in the cytoplasm, pre-miRNAs are cleaved near the terminal loop by the RNase III enzyme Dicer (DCR-1 in *C. elegans*), releasing ~22 nt duplexes with 2 nt overhangs at both ends (Grishok et al., 2001; Hutvagner et al., 2001; Ketting et al., 2001).

In drosophila, Dicer-1 requires Loquacious (LOQS, also known as R3D1) as interaction partner for pre-miRNA processing and RISC loading (Forstemann et al., 2005; Jiang et al., 2005; Saito et al., 2005) and human Dicer interacts with TRBP (Chendrimada et al., 2005; Haase et al., 2005) and PACT-1 (Lee et al., 2006), which are not needed for cleavage, but appear to contribute to formation of the RISC loading complex together with an Ago protein (Chendrimada et al., 2005; Haase et al., 2005; Lee et al., 2006). To date, no such factors are known in *C. elegans*.

The RNA duplex released by dicer cleavage is loaded onto an Argonaute protein to generate the precursor of the miRNA induced silencing complex (pre-miRISC). The guide strand, i.e. the strand that will serve as the mature, single-stranded miRNA, remains in Ago whereas the opposite passenger strand (or miR*) is degraded (Aza-Blanc et al., 2003; Khvorova et al., 2003; Schwarz et al., 2003) to generate the active miRISC complex. In siRNAs, the strand with the less stable base pairs at the 5’ end is typically selected as the guide molecule whereas the other strand is cleaved by Argonaute. Possibly, the same rules apply to miRNAs as well (Han et al., 2006; Khvorova et al., 2003). Small RNAs from mismatched precursors are preferentially loaded on ALG-1 and ALG-2 in *C. elegans* (Steiner et al., 2007) and on Ago1 in drosophila (Forstemann et al., 2007; Tomari et al., 2007), whereas human Argonaute proteins do not exhibit a clear preference for miRNAs versus siRNAs.

The process of passenger strand removal is not well understood. Recent work in drosophila suggests that Argonaute loading of small RNA duplexes requires Hsc70

(Iwasaki et al., 2010) and Hsp90 (Iwasaki et al., 2010; Miyoshi et al., 2010). ATP is consumed to mediate a conformational opening of Argonaute proteins so that small RNA duplexes can fit in. Release of the tension applied to open Argonaute may then drive the strand separation without consuming ATP (Iwasaki et al., 2010). In plants, however, non-hydrolyzable ATPγS impaired passenger strand removal, but not Argonaute loading of small RNA duplexes, suggesting that ATP is consumed by Hsp90 during strand removal.

2.5 Regulation of miRNA biogenesis and miRNA turnover

Virtually all steps of miRNA biogenesis and function are subject to transcriptional and posttranscriptional regulation (Ding et al., 2009; Krol et al., 2010b). This also includes the expression and activity of many of the protein factors participating in these processes (Krol et al., 2010b). A few examples in which the abundance or integrity of the miRNA are directly affected are discussed below.

The promoter regions of independently transcribed miRNA genes are highly similar to those of protein coding genes (Corcoran et al., 2009; Ozsolak et al., 2008), such as transcription of miRNA genes can be controlled by PolII associated transcription factors, enhancing and silencing *cis*-regulatory elements, and chromatin modifications. Many miRNAs regulate their own transcription through feedback loops. For instance, *lsy-6* engages in a double negative feedback loop that operates in the asymmetric development of the *C. elegans* ASE chemosensory neurons ASE-left (ASEL) and ASE-right (ASER). *lsy-6* is expressed in ASEL and blocks the expression of the transcription factor COG-1, which represses the left-fate in ASER by stimulating the expression of *mir-273*. *mir-273* in turn targets the transcription factor DIE-1 in ASER, which would activate the expression of *lsy-6* to promote the ASEL-fate (Johnston et al., 2005).

A well documented example of post-transcriptional regulation of miRNA expression is the negative regulation of *let-7* via the pluripotency factor LIN28 in mammalian cells, which, in turn, is a target of *let-7*. *let-7* processing is inhibited by binding of LIN28 to *pri-let-7*, which interferes with cleavage of the stem-loop structure by Drosha (Newman et al., 2008; Rybak et al., 2008; Viswanathan et al., 2008). Additionally, binding of LIN28 to *pre-let-7* was also reported to block processing by Dicer. In that case, LIN28 induces 3'-terminal polyurydilation of *pre-let-7* by recruiting the terminal uridyl transferase 4 (TUT4) (Gregory et al., 2004; Hagan et al., 2009; Heo et al., 2008; Heo et al., 2009; Jones et al., 2009). Uridylation not only prevents Dicer processing but also targets *let-7* for degradation (Heo et al., 2008). A similar mechanism was also found in *C. elegans* involving the polyuridyl polymerase PUP-2 (Lehrbach et al., 2009).

Adenosine-to-inosine editing of miRNAs by ADARs, adenosine deaminases that act on dsRNA segments, can interfere with miRNA biogenesis and, if occurring in the seed sequence, even redirect miRNAs to a different set of target genes (Kawahara et al., 2007).

For a long time, it was thought that miRNAs are generally highly stable molecules. This view was based on the observed stability of miRNAs in fixed tissue samples and their long half-lives upon inhibition of miRNA biogenesis (Grosshans and Chatterjee, 2010; Krol et al., 2010b). However, the dynamic expression of miRNAs during development and the rapid and regulated decay of several miRNAs in response to dark adaptation in mouse retina (Krol et al., 2010a) support the existence of an active turn-over pathway for miRNAs.

Two kinds of nucleases involved in the degradation of miRNAs have been identified so far. In *Arabidopsis thaliana*, degradation of mature miRNAs is mediated by a family of 3' to 5' small RNA degrading nucleases, SDN1, SDN2 and SDN3 (Ramachandran and Chen, 2008). In *C. elegans*, degradation of mature miRNAs depends on the 5' to 3' exonuclease XRN-2. Depletion of XRN-2 elevates the levels of several miRNAs and rescues *let-7(n2853)* associated lethality (Chatterjee and Grosshans, 2009). Degradation by XRN-2 requires miRNAs to be released from the Argonaute protein, which may predominantly apply to idle miRISC complexes. The latter idea is based on the observation that the availability of a cognate target mRNA protects miRNAs from degradation both *in vitro* and *in vivo* (Chatterjee et al., 2011; Chatterjee and Grosshans, 2009).

2.6 miRNA target recognition

In animals, miRNAs interact with their cognate target genes by base-pairing to partially complementary target sites. Near perfect base-pairing with consequential endonucleolytic cleavage of the targeted message can occur (Davis et al., 2005; Yekta et al., 2004), but appears to constitute the figurative exception that proves the rule. The vast majority of experimentally identified or computationally inferred miRNA binding sites are positioned in the 3' UTR. However, animal miRNAs may also target 5' UTRs (Orom et al., 2008) as well as coding regions of mRNAs (Easow et al., 2007; Gu et al., 2009a). In some cases, interaction of miRNAs with 5' UTR target sites activates rather than represses translation (Henke et al., 2008; Orom et al., 2008). Binding sites in protein coding regions seem to be less robust. In line with the notion that the translation machinery would displace silencing complexes bound to these regions, inclusion of rare codons to slow down ribosomes increases the efficacy of these sites (Gu et al., 2009a).

Numerous computational and biochemical studies support that perfect base-pairing of the miRNA nucleotides 2-8 at the 5' end of the miRNA guide strand is the most important determinant of target recognition by miRNAs. (Doench and Sharp, 2004; Lewis et al., 2003; Stark et al., 2003). Due to the metaphoric view that positions 2-8 nucleate miRNA binding, they are frequently referred to as the *seed region* of the miRNA. An A across position 1 or an A or U across position 9 of the miRNA seed improve miRNA:target site interaction irrespective of whether these nucleotides engage in functional Watson-Crick base-pairing (Lewis et al., 2005; Nielsen et al., 2007). Recent structural studies of *Thermus thermophilus* Argonaute illustrate the prominence of the seed region in target recognition: Nucleotides at miRNA positions 2-6 contact Argonaute through the phosphate-ribose RNA backbone with their bases exposed for hydrogen bonding to the target mRNA. The monophosphorylated 5' terminal miRNA nucleotide is anchored in a deep pocket, which may explain why position 1 does not need to base-pair to the target-site. (Jinek and Doudna, 2009; Wang et al., 2008a; Wang et al., 2008b).

Generally, miRNA:mRNA duplexes contain mismatches and bulges in the central region (miRNA position 10-12), which explains the rare occurrence of siRNA like endonucleolytic cleavage between target nucleotides opposite to position 10 and 11. Although miRNAs can be loaded on slicing competent Argonaute proteins, they are unable to direct cleavage. Additional or supplementary pairing of the 3' end optimally centers on miRNA nucleotides 13-16 and likely plays only a modest role in target recognition (Grimson et al., 2007), apart from some exceptions. For instance, *C. elegans lin-41* contains two highly conserved 3' compensatory target sites for *let-7*, one site having a bulged nucleotide and the other one having a G:U wobble pair in the seed complementary site (Vella et al., 2004). Interestingly, only *let-7* itself, but not its family members *mir-48*, *mir-84*, and *mir-241* are capable of extensive compensatory pairing with *lin-41*. Therefore, this 3' compensatory sites may have evolved to escape premature repression of *lin-41* by the *let-7* sister miRNAs (Brennecke et al., 2005; Lewis et al., 2005). Additional features of 3' UTR context add to the functionality of possible miRNA binding sites which include (1) positioning at least 15 nt apart from the stop codon, (2) avoiding the center of long 3' UTRs, (3) an AU-rich nucleotide composition near the binding site, and (4) proximity to sites of coexpressed miRNAs (Grimson et al., 2007).

Definition of the rules of miRNA:mRNA interaction has been widely used for the generation of many miRNA target prediction tools (Betel et al., 2008; Friedman et al., 2009; Gaidatzis et al., 2007; Griffiths-Jones et al., 2008; Grimson et al., 2007; Hammell et al., 2008; Kertesz et al., 2007; Lall et al., 2006; Miranda et al., 2006; Ruby et al., 2007b; Stark et al., 2005). The majority of current target prediction programs rely on the presence of an evolutionarily conserved binding site. However, it is not known which proportion of miRNA:target interactions follow the underlying rules of the available tools.

Despite numerous large-scale studies that have been performed to identify miRNA target genes experimentally, only a modest number of functionally validated miRNA targets are known so far. Diverse experimental approaches were taken to identify miRNA-mRNA target interactions mostly in cell culture, but also *in vivo* (reviewed by Orom and Lund, 2009; Thomas et al., 2010). The fact that miRNAs down-regulate the

mRNA level of many of their target genes was exploited in numerous miRNA over-expression and inhibition studies on a transcriptome wide scale (Orom and Lund, 2009; Thomas et al., 2010). Stable isotope labeling of amino acids in cell culture (SILAC and pSILAC) has been used to identify miRNA targets on the protein level to capture targets that may mostly be inhibited at translation as well (Baek et al., 2008; Selbach et al., 2008; Vinther et al., 2006). Immunoprecipitation of Argonaute proteins (Beitzinger et al., 2007; Easow et al., 2007; Hendrickson et al., 2008; Hong et al., 2009; Karginov et al., 2007), GW182 proteins (Zhang et al., 2007) or labeled miRNAs (Hsu et al., 2009; Kedde et al., 2007; Orom and Lund, 2007; Orom et al., 2008) were used to identify miRNA target genes biochemically. Purification of UV cross-linked Argonaute (HITS-CLIP) was used to identify both Argonaute-binding site and mRNA (Chi et al., 2009; Wen et al., 2011). Ribosome profiling was used to approximate the overall effect of miRNA-mediated gene regulation on protein synthesis (Guo et al., 2010). In some cases, loss-of-function in a miRNA induces strong enough phenotypes such as suppression of these phenotypes were used in reverse genetic screens to identify target genes that substantially add to the phenotype (e.g. Mavrakis et al., 2010; Ding et al., 2008). Nevertheless: we still know far more miRNAs than validated miRNA:mRNA target interactions.

To identify target genes of *let-7* and the *let-7* family members *mir-48*, *mir-84*, and *mir-241* in the physiological context of a fully functional organism, we performed microarray studies on whole animal lysates of wild-type and miRNA mutant *C. elegans* before and after separation on polysome gradients. Despite all measures taken to improve the method, we could not overcome the lack of statistical power needed to establish a large-scale discovery tool. Nevertheless, some of our observations and our expertise in polysome profiling and qRT-PCR contributed to the study of Jovanovic et al., which describes a targeted large-scale proteomic approach to identify miRNA target genes. The published manuscript can be found in the appendix of this thesis.

2.7 Cap-dependent translation

Eukaryotic pre-mRNAs undergo extensive and tightly coupled nuclear processing before they are finally exported as mature mRNAs to the cytoplasm where they serve as templates for translation. During nuclear processing, mRNAs are spliced, acquire a m^7GpppN (monomethylguanosine) 5' terminus called 5' cap, and undergo 3'-end processing, which, except for histone-coding transcripts, involves the non-templated addition of a poly(A)-tail (Hocine et al.). The contribution of the typeII poly(A)-binding protein to nuclear polyadenylation is discussed in the introduction of my research paper in section 3.1.

Compared to fly or vertebrate cells, nuclear processing of *C. elegans* pre-mRNAs features some notable differences. An estimated ~70 percent of *C. elegans* mRNAs acquire a trans-spliced leader of 22 nt length (Blumenthal, 2005; Hastings, 2005). The spliced leader is donated by ~100 nt long RNAs that have a trimethylguanosine (TMG) cap at their 5' termini. Thus, the majority of *C. elegans* mRNAs acquires a TMG cap during nuclear processing. The same nuclear processing can also apply to individually transcribed miRNAs, such as *let-7* (Bracht et al., 2004). A 5' TMG cap in combination with a spliced leader sequence was shown to stimulate translation in nematodes (Lall et al., 2004; Maroney et al., 1995). Furthermore, many *C. elegans* mRNAs are transcribed as operons, which are disjointed to individual transcripts by trans-splicing (Blumenthal, 2005).

The process of translation can be divided into three steps: translation initiation, elongation and termination. The rate limiting step under most conditions is initiation, thus, protein synthesis is essentially regulated at the initiation step (Jackson et al., 2010). Initiation of cap-dependent translation comprises formation of a 48S initiation complex to scan the mRNA for an appropriate initiation-codon followed by recruitment of the 60S ribosomal subunit to form a translationally competent 80S ribosome. A few steps of ribosome recruitment and eukaryotic translation initiation factors (eIFs) involved in these processes are discussed below.

The 43S preinitiation complex consists of the 40S ribosomal subunit, the initiation factors eIF1, eIF1A, eIF3, and a ternary complex of eIF2-GTP together with the

initiator transferRNA (Met-tRNA$^{Met}_{i}$). eIF1 and eIF1A are recruited during disassembly and recycling of ribosomal subunits, whereas eIF3 stimulates the binding of the ternary complex. Recruitment of the 43S complex to mRNAs requires the cooperative action of translation initiation factors eIF4F and eIF4B or eIF4H. eIF4B or eIF4H help to unwind the secondary structure at the 5' cap-proximal region and thus prepare the mRNA for ribosomal attachment. eIF4F consists of the cap-binding protein eIF4E, the DEAD-box RNA helicase eIF4A, and eIF4G, a large scaffold-protein that binds eIF4E, eIF4A, and the type I poly(A)-binding protein PABPC and eIF3.

After attachment to the mRNA, the 48S complex scans the mRNA in 5' to 3' direction for the initiation codon in a process which requires association of eIF1, eIF1A and the helicase activity of eIF4A and B. Upon recognition of an initiation codon in the proper context, eIF5 activates the GTPase activity of eIF2. The subsequent GTP hydrolysis on eIF2 commits the 48S complex to the start codon. Joining of the 60S ribosomal subunit is helped by eIF5B, which mediates dissociation of eIF1, eIF1A, eIF3 and eIF2-GDP from the 48S initiation complex. The poly(A) tail functions as a translational enhancer in cap-dependent translation. By binding to both PABPC and eIF4E, eIF4G brings the poly(A) tail and the 5' cap to close proximity. This interaction is thought to induce a "closed loop" configuration of the mRNA, which is thought to facilitate ribosome recycling on the translated message.

However, there is an alternative explanation which does not require a circular structure (Jackson et al., 2010): Interaction of eIF4G with PABPC ensures that eIF4F remains on the mRNA if the contact with 5' end of the mRNA is disrupted. Thus, this interaction ensures that the eIF4F complex does not need to be recruited *de novo* to mediate further rounds of translation initiation. Histone mRNAs are efficiently translated although they lack a poly(A) tail. The stem-loop structure in the 3' end of histone mRNAs is bound by the stem-loop binding protein SLBP. SLBP interacts with the SLBP interacting protein 1 (SLIP1), which in turn interacts with eIF4G. Thus, stem-loop, SLBP and SLIP1 take on the role of PABPC and poly(A) tail in keeping the eIF4F complex on the histone mRNA (Cakmakci et al., 2008).

2.8 Publication: Translational control of endogenous miRNA target genes in *C. elegans*

Chapter 2
Translational Control of Endogenous MicroRNA Target Genes in *C. elegans*

Benjamin A. Hurschler, Xavier C. Ding, and Helge Großhans

Contents

Abstract *lin-4* and *let-7* are the founding members of the large microRNA (miRNA) family of regulatory RNAs and were originally identified as components of a *C. elegans* developmental pathway that controls temporal cell fates. Consistent with their pioneering role, *lin-4* and *let-7* were studied widely as "model miRNAs" in efforts to reveal the mode of action of miRNAs. Early work on *lin-4* thus established a paradigm that miRNAs inhibit translation of their target mRNAs at a step downstream from initiation, without affecting mRNA stability. Although some studies on mammalian miRNAs in cell culture reached similar conclusions, most of those studies indicated that miRNAs repressed translation initiation and frequently also promoted target mRNA degradation. We will discuss here what is known about

B.A. Hurschler, X.C. Ding, and H. Großhans (✉)
Friedrich Miescher Institute for Biomedical Research (FMI), Maulbeerstrasse 66, WRO-1066.1.38, CH-4002 Basel, Switzerland
e-mail: helge.groβhans@fmi.ch

R.E. Rhoads (ed.), *miRNA Regulation of the Translational Machinery*, Progress in Molecular and Subcellular Biology 50,
DOI 10.1007/978-3-642-03103-8_2, © Springer-Verlag Berlin Heidelberg 2010

modes of miRNA target gene repression in *C. elegans*, highlighting recent work that demonstrates that both mRNA degradation and repression of translation initiation are mechanisms employed in vivo by *let-7* and, unexpectedly, *lin-4* to silence their endogenous targets. We will also discuss the roles of the GW182 homologous AIN-1 and AIN-2 proteins in this process.

2.1 Introduction

lin-4 and *let-7* are the founding members of the large microRNA (miRNA) family of small noncoding RNAs and were originally identified as components of the heterochronic developmental pathway in the small roundworm *Caenorhabditis elegans* (Chalfie et al. 1981; Horvitz and Sulston 1980). *C. elegans* genetics has also been instrumental in the identification of the first miRNA target genes (Moss et al. 1997; Slack et al. 2000; Wightman et al. 1993) and the cellular machinery involved in miRNA mediated gene silencing, e.g., the RNase III enzyme DCR-1 (Dicer) (Grishok et al. 2001; Ketting et al. 2001; Knight and Bass 2001), the Argonaute-like proteins ALG-1, ALG-2 (Grishok et al. 2001), and the microprocessor complex (Denli et al. 2004). Findings in *C. elegans* have thus had a remarkable track record of guiding our understanding of miRNA biology. Indeed, the earliest work on the mechanism of action used by miRNAs to silence their target mRNAs was also performed in *C. elegans* (Olsen and Ambros 1999; Seggerson et al. 2002). It established a paradigm that miRNAs inhibited protein translation at a step downstream of initiation, without significantly affecting target mRNA stability. Surprisingly then, work in human and Drosophila cells has challenged this model of miRNA activity, by providing evidence for miRNA-mediated transcript degradation as well as repression of translation initiation. In this chapter, we discuss what is known about modes of miRNA target gene repression in *C. elegans* and how this relates to findings from other model systems. We particularly focus on recent work that demonstrates that *let-7* and *lin-4* employ both mRNA degradation and, unexpectedly, repression of translation initiation to silence their endogenous targets in vivo. We also discuss the roles of the GW182 homologous AIN-1 and AIN-2 proteins in these processes.

2.2 *lin-4* and *let-7* miRNAs in *C. elegans* Development

Postembryonic development of *C. elegans* proceeds through four larval stages, L1 through L4, each separated by a molt, until the sexually mature adult stage is reached. In a newly hatched larva, 51 blast cells divide and differentiate in a stereotypic manner during the four larval stages, giving rise to a fixed number of cells with determined fates. Proper temporal execution of cell fates is controlled by a set of heterochronic genes. Mutations in these genes can cause either a precocious phenotype, in which developmental events are skipped, or a retarded phenotype, in

which developmental events are repeated. For instance, loss-of-function in *lin-4* (*lineage variant-4)* causes reiteration of first larval stage cell fates during the second larval stage in various tissues, whereas mutations in *lin-14* cause a skipping of L1 cell fates (Moss 2007). Surprisingly, *lin-4* was found to code not for a protein, but for a small RNA, capable of triggering L2 fates by diminishing the protein levels of LIN-14 (Lee et al. 1993; Wightman et al. 1993) and LIN-28 (Moss et al. 1997) (Fig. 2.1). *lin-4* achieved repression of the *lin-14* and *lin-28* mRNAs by binding to complementary sequences in their 3′ untranslated regions (3′ UTRs) (Lee et al. 1993; Moss et al. 1997; Wightman et al. 1993).

Seven years later it was discovered that another heterochronic gene, *let-7* (*lethal-7*), also encoded for a small regulatory RNA that regulated temporal cell fates, in this case by promoting transition from L4 to adult cell fates through repression of *lin-41* (Reinhart et al. 2000; Slack et al. 2000). Due to their temporally regulated levels and their function as temporal switches for cell fates in *C. elegans*, *lin-4*

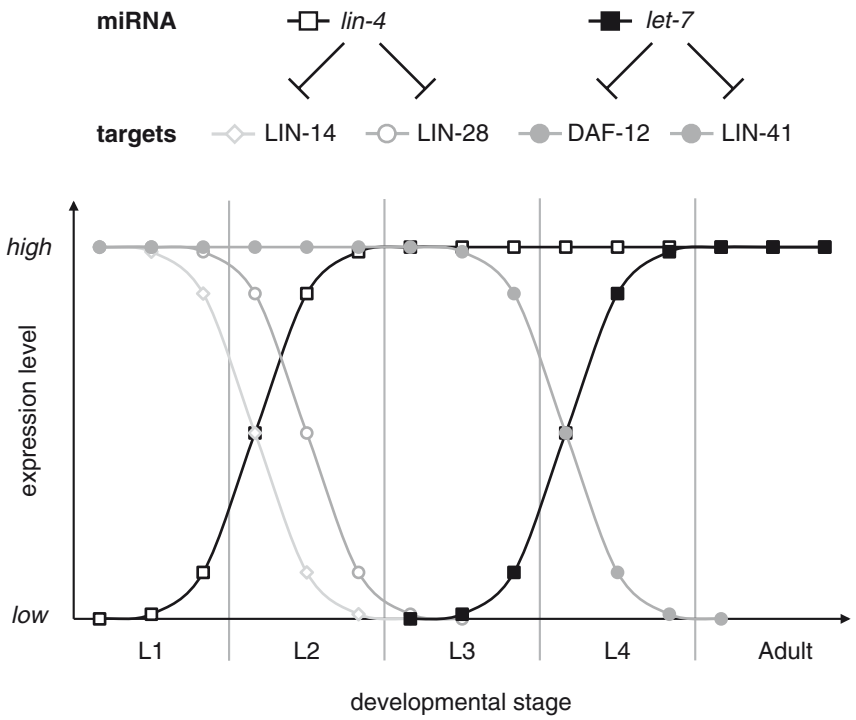

Fig. 2.1 Temporal expression of heterochronic genes in *C. elegans*. The postembryonic development in *C. elegans* proceeds through four larval stages (L1 to L4), each separated by a molt (*indicated by the vertical lines*), followed by the adult stage. *lin-4* starts to accumulate during L1 and represses *lin-14* starting mid-L1 and *lin-28* starting late L1/early L2, thereby promoting progression to developmental programs of L2 and L3, respectively. *let-7* starts to accumulate during L3 and represses *lin-41* and *daf-12* starting late L3/early L4, thereby promoting progression to adult cell-fates

and *let-7* were termed small temporal RNAs. Subsequently, homologues of *let-7* were identified in a variety of bilaterian species, including flies, zebrafish, and humans (Pasquinelli et al. 2000). It was this discovery that provided the starting point for the subsequent isolation of hundreds of miRNAs in various animals, including humans (reviewed in Groβhans and Slack 2002).

2.3 Polysome Profiling as an Assay to Assess the Translational State of mRNAs

The discovery that *lin-4* was partially complementary to sequences in the 3′ UTR of the *lin-14* mRNA and that these 3′ UTR sequences were required for regulation (Lee et al. 1993; Wightman et al. 1993) suggested that miRNAs regulate their targets through an antisense mechanism, possibly inducing mRNA degradation or translational repression. Although transcript degradation can be readily assessed by diverse techniques such as northern blotting, quantitative reverse transcription PCR (qRT-PCR), or microarrays, the appraisal of the translational state of a transcript is less straight-forward. Based on the observation that actively translated mRNAs are bound by many ribosomes, isolation of polyribosomes ("polysomes") can be used to copurify translated mRNAs. The prevalent method for the isolation of polysomes dates back to the early days of studies on protein translation (Wettstein et al. 1963). In its basic implementation, the transcripts in a cleared cell lysate (i.e., the postmitochondrial supernatant) are separated by ultracentrifugation through a sucrose density gradient. While the gradient is unloaded at a constant flow-rate, the UV-absorbance is recorded and fractions are collected. mRNAs that are associated with multiple ribosomes migrate to the denser fractions of the gradient, which can be observed on the UV-recording as a pattern of density peaks corresponding to multiples of 80S (Fig. 2.2). The 80S peak thus delimits the polysomal and the (sub)monosomal fractions. RNA can then be extracted from polysomal and (sub)monosomal fractions and analyzed by any quantitative assay, e.g., qRT-PCR and northern blotting. Different mRNAs will vary in their distributions across these fractions, reflecting for instance the fact that the number of ribosomes that can be loaded onto short transcripts is limited, but each transcript exhibits a characteristic, invariant distribution under constant experimental conditions. By contrast, if experimental conditions change to cause, for instance, activation of translation initiation, an increased accumulation in polysomal fractions results for the affected transcripts, whereas inhibition of translation initation will cause a shift to (sub)monosomal fractions. To "freeze" polysomes for the duration of the experiment, cells are typically treated with cycloheximide, which blocks elongation of the nascent polypeptide chain. A frequently used control is the application of puromycin, which induces premature termination of translation, and thus specifically disassembles actively translating polysomes, resulting in a shift of the associated mRNA.

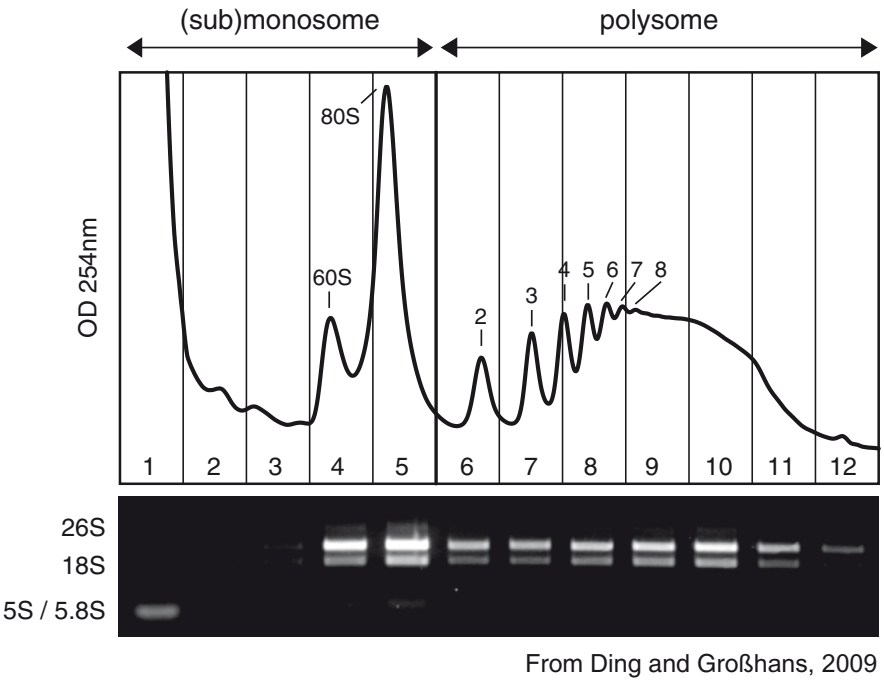

Fig. 2.2 A typical polysome profile. UV-recording at 254 nm of total worm lysate separated on a 15–60% (w/v) sucrose gradient. The major UV density peaks represent the 60S sub-monosomal, 80S monosomal, and a series of polysomal peaks (*from left to right*; the number of ribosomes is indicated). Total RNA of each fraction was isolated and separated on an agarose gel to visualize ribosomal RNAs. Adapted from (Ding and Großhans 2009)

2.4 MicroRNA-Mediated Gene Regulation in *C. elegans*: The Early View

Early work performed in *C. elegans* on *lin-4* and *let-7* established an antisense mechanism of interaction between miRNAs and target mRNAs. Gain-of-function mutations of *lin-14* yielded retarded phenotypes resembling those seen with *lin-4* loss-of-function and were caused by deletions in the 3′ UTR of *lin-14*. In both these mutant animals, LIN-14 protein persisted at a developmental stage, in which the protein was no longer detectable in wild-type animals (Olsen and Ambros 1999; Wightman et al. 1993). Reporter gene experiments then confirmed that the 3′ UTR of *lin-14* was sufficient for gene repression by *lin-4*, with mutations in the *lin-4* complementary regions compromising reporter gene regulation (Wightman et al. 1993). The mechanism of regulation however remained elusive. The massive fold decrease in LIN-14 protein between L1 and L2 was not adequately reflected by a decline in the transcript level, and the polyadenylation state of *lin-14* was not affected. Furthermore, *lin-14* was found to cosediment with actively transcribing polysomes in sucrose density gradients both before and after the onset of *lin-4*

expression (Olsen and Ambros 1999). Since *lin-14* did not exhibit a shift to the submonosomal fraction, a hallmark of repressed translation initiation, it was concluded that *lin-4* regulated *lin-14* downstream of translation initiation or even posttranslationally. Moreover, a subset of *lin-4* was found to comigrate with polysomes, a finding that was consistent with, although not necessarily diagnostic of, regulation after the initiation step (cf. Sect. 2.5.1).

Similar results were also obtained for another *lin-4* target, *lin-28* (Seggerson et al. 2002), which fostered the paradigm of miRNAs inhibiting translation at a step downstream of initiation, without substantially affecting mRNA stability.

However, more recent work provides evidence for miRNA-dependent target mRNA decay in *C. elegans* (Bagga et al. 2005), an observation that is consistent with a large body of work from other systems (Behm-Ansmant et al. 2006; Eulalio et al. 2007b; Giraldez et al. 2006; Wu and Belasco 2005). Northern blots of endogenous *C. elegans* mRNAs showed a more than fivefold decrease in the *lin-4* targets *lin-14* and *lin-28*, which was more than previously appreciated and *let-7* was similarly found to mediate degradation of its target *lin-41* (Bagga et al. 2005). To explain the discrepancy, it was speculated (Bagga et al. 2005) that previous studies with *C. elegans* (Olsen and Ambros 1999; Seggerson et al. 2002; Wightman et al. 1993), which were based on RNase protection experiments, were distorted by the detection of stable degradation products, but no such degradation intermediates have been demonstrated. We have recently shown transcript degradation for additional *C. elegans* miRNA targets and demonstrated that *C. elegans* miRNAs also block translation initiation (Ding and Großhans 2009) (see Sects. 2.6 and 2.7). Although some evidence suggests that degradation and translational repression are two distinct modes of miRNA target gene repression, it is still possible that degradation may indeed be a consequence of translational repression.

2.5 MicroRNA Mediated Gene Regulation in Other Model Organisms

Many in vivo and in vitro studies have been performed to elucidate the mechanism(s) of miRNA-mediated gene repression in different experimental systems. The resulting plethora of proposed mechanisms of action has sparked a lively debate that characterizes the field. We will shortly review some of the major findings (and conflicts among them), mostly obtained using cell-based assays and reporter genes, before we will discuss recent results on the mechanisms *C. elegans* miRNAs utilize to silence endogenous target genes in vivo, in a whole organism.

2.5.1 Evidence for Translational Repression After Initiation

Several cell-based (ex vivo) studies report translational repression after initiation, although they differ in their conclusion as to how this regulation takes place. In 293T cells, transfection of an artificial miRNA repressed its target reporter

mRNA, which remained associated with actively translating polysomes. (Petersen et al. 2006). Repression was not restricted to cap-dependent translation initiation, as both cap-dependent and IRES (internal ribosomal entry site)-dependent open reading frames of a bicistronic reporter gene were equally sensitive to the transfected miRNA. As pulse-labeling of nascent polypeptides indicated that repression occurred before completion of the synthesis of the full-length polypeptide chain, a ribosome drop-off model was proposed, in which miRNAs render ribosomes susceptible for premature translation termination.

Maroney and coworkers investigated the distribution of endogenous miRNAs and mRNAs in HeLa cells (Maroney et al. 2006). For instance, the KRAS mRNA, which is regulated by *let-7*, was found to be associated with translation competent ribosomes in the polysomal fractions. The finding that the KRAS mRNA remained in the polysomal fraction even under conditions known to interrupt translation initiation, argued against a ribosome drop-off and suggested a decelerating effect on the elongation rate.

However, a *let-7* mediated slow-down of the elongation rate in HeLa cells could not be observed for a reporter gene bearing the *C. elegans lin-41* 3′ UTR (Nottrott et al. 2006). Since the encoded protein remained undetectable, although reporter mRNA cosedimented with translation competent ribosomes, it was speculated that the nascent polypeptide was cotranslationally degraded. However, proteases involved in this process have not been identified, and in fact neither the inhibition of the proteasome nor the targeting of the reporter gene to the endoplasmic reticulum was found to restore protein accumulation in HeLa cells (Pillai et al. 2005). A model of cotranslational polypeptide degradation is thus based on negative evidence.

Cosedimentation of a considerable fraction of miRNAs or Argonaute proteins with polysomes was reported in many studies (Kim et al. 2004; Nelson et al. 2004; Nottrott et al. 2006; Olsen and Ambros 1999; Petersen et al. 2006). At first sight, this observation would argue against a mechanism that represses target gene translation initiation, as such a mechanism would deplete the miRNA target genes, and thus the miRNA and Argonaute, from the polysomal pool. However, a caveat to this interpretation is that efficient target gene repression might frequently require binding by several miRNAs (e.g., Doench et al. 2003; Vella et al. 2004). Thus, a substantial amount of miRNAs and Argonaute might be bound to polysomal mRNAs without greatly affecting translation.

2.5.2 Evidence for mRNA Deadenylation and Decay

Following a first report that showed that transfection of a miRNA into cultured cells resulted in reduced transcript levels for a number of apparently direct targets (Lim et al. 2005), nonendonucleolytic mRNA decay in response to miRNAs has been observed in *C. elegans* (Bagga et al. 2005) and many other systems. In zebrafish, *miR-430* was found to clear maternal mRNAs containing *miR-430* target sites at the onset of zygotic transcription (Giraldez et al. 2006). Depletion or ectopic expression of miRNAs alters the expression of validated miRNA targets or mRNAs containing

binding sites for these miRNAs (Krutzfeldt et al. 2005; Lim et al. 2005; Linsley et al. 2007). Similarly, transcript levels of miRNA targets were found to increase in cells depleted of Dicer or Argonaute proteins (Rehwinkel et al. 2006; Schmitter et al. 2006).

MicroRNAs deploy the general mRNA degradation machinery to clear target mRNAs. Decapping and accelerated mRNA deadenylation have been observed in zebrafish, and fruitfly and human cell lines (Behm-Ansmant et al. 2006; Eulalio et al. 2007b; Giraldez et al. 2006; Wu et al. 2006). Target destabilization was found to depend on Argonaute proteins, the CAF1–CCR4–NOT deadenylase complex, the decapping enzyme DCP2, and the P-body component GW182 (Behm-Ansmant et al. 2006; Eulalio et al. 2007b). Depletion of these components leads to the stabilization of many miRNA target mRNAs that are otherwise degraded. Furthermore, Argonaute proteins, miRNAs, and repressed mRNAs are often found to colocalize to P-bodies, discrete cytoplasmic foci that harbor mRNA-catabolizing enzymes (Eulalio et al. 2007a).

Intriguingly, targets of *let-7* are destabilized to different degrees in different mammalian cell lines (Schmitter et al. 2006), and reporter mRNAs in *D. melanogaster* S2 cells can be silenced exclusively by either degradation or nondegradation, presumably translational repression or by a combination of both mechanisms (Behm-Ansmant et al. 2006; Eulalio et al. 2007b), suggesting that differences in cellular factors as well as the architecture or environment of miRNA target sites can influence the extent of target degradation.

How miRNAs initiate degradation of their target transcripts is not known. Moreover, it is unclear whether degradation is an independent mechanism or consequence of translational repression, as current evidence cannot distinguish between these two possibilities (Eulalio et al. 2008a; Filipowicz et al. 2008).

2.5.3 *Evidence for Translational Repression at the Initiation Steps*

Recent studies that recapitulated miRNA mediated gene repression in cell-free systems concluded that miRNAs interfere with target gene expression at translation initiation (Mathonnet et al. 2007; Thermann and Hentze 2007; Wakiyama et al. 2007; Wang et al. 2006). These studies unanimously reported a shift of repressed reporter genes to the monosomal pool of mRNA, consistent with reduced ribosome loading. This repression of translation initiation was found to depend on an m^7Gp-ppN-cap, whereas cap independent association of ribosomes via different IRES or ApppN-capped mRNAs was refractory to translational regulation. Inhibition of translation initiation has also been reported in cell-based approaches (Bhattacharyya et al. 2006; Pillai et al. 2005), which includes the only study explicitly showing this mechanism for an endogenous mRNA (Bhattacharyya et al. 2006).

Nevertheless, there is little agreement on the mechanisms that repress translation initiation. Human AGO2 (Argonaute 2) binds to a methylated cap analog in vitro

via two tryptophan residues placed at an equivalent position in the initiation factor eIF4E (Kiriakidou et al. 2007). Thus, AGO2 miRNPs might compete with eIF4E for m^7G-cap binding and thereby abrogate the bridging between m^7G-cap and poly(A)-tail via eIF4G, which normally stimulates translation initiation. In line with disruption of mRNA circularization by eIF4F, whose subunits include eIF4E and eIF4G, eIF4F was found to be limiting for translational repression in mouse Krebs-2 cell extracts, and conversely, excess of eIF4F relieved translational repression (Mathonnet et al. 2007). Similarly, tethering of eIF4E and eIF4G to reporter constructs relieved translational repression in HeLa cells (Pillai et al. 2005). Nonetheless, recent work in fly cells suggests that cap-binding by AGO might not be sufficient to prevent translation initiation (Eulalio et al. 2008b).

If miRNAs repress translation initiation by interfering with mRNA circularization mediated by eIF4F, this would also imply a need for polyadenylation of the target transcript as a prerequisite for efficient circularization. However, the notion that a functional poly(A)-tail is necessary for translational regulation is controversial. Full miRNA mediated regulation of mRNA transfected into HeLa cells required a poly(A)-tail in one study (Humphreys et al. 2005), but not in another (Pillai et al. 2005). Moreover, in HEK293 cells, the poly(A) tail could be substituted by a histone stem-loop without eliminating repression (Eulalio et al. 2008b; Wu et al. 2006).

It has been suggested that translation initiation might be repressed by preventing 60S subunit joining, consistent with the finding that eIF6 was isolated in association with AGO2 and 60S ribosomes in HeLa cells (Chendrimada et al. 2007). eIF6 prevents premature assembly of the 60S and 40S ribosomal subunits by binding to 60S subunits. Recruitment of eIF6 by AGO2 could therefore interfere with translation initiation by preventing the recycling of ribosomal subunits. In *C. elegans*, RNAi against eIF6 led to an approximately twofold increase in LIN-14 and LIN-28 and their persistence at later time-points, when these proteins usually are not detected (Chendrimada et al. 2007). However, in our hands, depletion of eIF6 by RNAi induces slow growth, leaving it unclear whether the measured time-points indeed reflected two different developmental stages. Studies in mice, *D. melanogaster*, and *C. elegans* have indicated that eIF6 may not be generally required for miRNA function (Ding et al. 2008; Eulalio et al. 2007b, 2008b; Gandin et al. 2008) and it has been speculated that the involvement of eIF6 may be indirect, possibly reflecting a role in 60S subunit biogenesis (Filipowicz et al. 2008).

Although the precise mechanism and contributing factors remain unclear, various studies thus provide strong support for miRNA-mediated repression of translation initiation in vitro and ex vivo. Confusingly, however, this is precisely the mechanism that earlier studies in *C. elegans* appeared to rule out (Olsen and Ambros 1999; Seggerson et al. 2002). One possible conclusion is that miRNA functioned differently in *C. elegans* than in other organisms, or that indeed miRNAs studied in an intact organism, in vivo, behave differently from miRNAs studied in cultured cells or cell-free assays. The latter possibility is of particular concern given that almost all cell-based and cell-free studies have investigated transfected miRNA reporter genes, not endogenous target mRNAs, and both the modes of transfection (Lytle et al. 2007), and the promoter driving the reporter gene (Kong et al. 2008)

have been reported to affect the apparent mode of miRNA-mediated gene repression. However, as we will discuss later, we have now demonstrated that miRNAs do indeed also repress translation initiation of their endogenous target mRNAs in *C. elegans* (Ding and Großhans 2009).

2.6 The *let-7* miRNA Extensively Interacts with Translation Factors

With the aim to study the interaction between *let-7* and the translation machinery under physiological conditions, we recently performed a reverse genetic screen (Ding et al. 2008). A major strength of *C. elegans* as a model organism is the simplicity of RNAi mediated knock-down of individual genes by feeding libraries of bacteria producing double-stranded RNA (Fraser et al. 2000; Kamath et al. 2003). The temperature sensitive *let-7(n2853)* allele harbors a point mutation in the mature *let-7* miRNA that impairs target mRNA silencing (Reinhart et al. 2000; Vella et al. 2004). As a consequence, mutant animals die by bursting through the vulva at the larval to adult transition when grown at 20°C or above. The lethality phenotype can be partially rescued by RNAi mediated knock-down of individual *let-7* target genes (Abrahante et al. 2003; Groβhans et al. 2005; Lall et al. 2006; Lin et al. 2003; Slack et al. 2000). With the initial aim of identifying interaction partners of *let-7* in an unbiased approach, a library of 2,400 genes on chromosome I was screened for suppression of the *let-7* loss-of-function lethality phenotype. This initial screen identified 41 suppressors, including known and novel *let-7* target genes, as well as potential regulators of *let-7* expression, mediators of *let-7* activity and heterochronic genes (Ding et al. 2008). Twenty of these genes functioned in RNA or protein metabolism, among them several are putative subunits of eukaryotic translation initiation factors. When the screen was extended to include all translation factors with identifiable homologues in *C. elegans*, most of these, including initiation, elongation, and termination factors, partially suppressed the *let-7(n2853)* mutation.

Most *C. elegans* translation factors are thought to be essential, but RNAi typically achieves only partial depletion of targeted genes and animals were exposed to RNAi for only limited times. Larval development thus proceeded normally in most cases, although frequently slower than normal. To eliminate the possibility that this slow-growth contributed, indirectly, to suppression of *let-7(n2853)*-associated lethality, a subset of factors were depleted in wild-type animals, and shown to induce precocious differentiation of epidermal seam cells. This phenotype is consistent with a gain of *let-7* function, and suggests that suppression of *let-7* lethality is direct.

Unexpectedly, eIF6 was among the factors whose knock-down rescued *let-7(n2853)* animals and caused precocious seam cell differentiation in wild-type animals. In the light of the reported function of eIF6 as a mediator of *lin-4* function in *C. elegans* (Chendrimada et al. 2007), the opposite, *let-7* loss-of-function-like, retarded seam cell differentiation phenotype, would have been expected as a result

of its depletion. However, recent studies on *D. melanogaster* S2 cells question a general role of eIF6 in promoting miRNA function (Eulalio et al. 2008b), and this might be reflected by our results.

C. elegans has readily recognizable orthologues of most of the translation factors commonly found in higher eukaryotes (Rhoads et al. 2006). Except for the termination factor eRF1, subunits of all translation factors were found to significantly suppress *let-7(n2853)* lethality. In addition to eIF6, we also examined the consequences of depleting eIF3 on seam cell differentiation, and again observed precocious differentiation in animals expressing functional *let-7*. eIF3 is required for the Met-tRNA$_i$ binding to the 40S ribosomal subunit and later for the recruitment of mRNA to the 43S pre-initiation complex (PIC) to form the 48S complex (Rhoads et al. 2006). The opposing roles of the tumor suppressor gene *let-7* and the eIF3 protooncogenes (Dong and Zhang 2006) are intriguing and may well be conserved beyond *C. elegans*: In humans, increased amounts of eIF3 stimulate translation of genes involved in cell proliferation (Zhang et al. 2007), for instance MYC and cyclin D1, which are also target genes of *let-7* (Bussing et al. 2008).

The eIF4 complex recruits the 43S PIC to mRNA. Depletion of its eIF4A subunit resulted in potent suppression, whereas depletion of eIF4G led to developmental arrest. No suppression was observed with eIF4E depletion, which at first sight is surprising, as many studies highlight the importance of m^{7}G-cap-binding for miRNA mediated translational regulation (Mathonnet et al. 2007; Thermann and Hentze 2007; Wakiyama et al. 2007; Wang et al. 2006), and it could be assumed that depletion of the cap-binding factor would favor the recently postulated cap-binding by AGO2 (Kiriakidou et al. 2007). However, the lack of an observable interaction is likely due to redundancy, as five different loci in the *C. elegans* genome encode eIF4E isoforms.

Taken together, these results pointed to a high sensitivity of *let-7* function to altered translation levels. Considering the studies supporting miRNA mediated translational control to occur after initiation in *C. elegans*, the identification of many translation initiation factors was somewhat surprising and prompted us to examine translational control on the mRNA level.

2.7 Polysome Profiling Confirms Translational Repression at the Initiation Step in *C. elegans*

We have recently reported that *let-7* represses translation initiation in *C. elegans*, demonstrating this mode of action for the first time in an organism (Ding and Großhans 2009). To assess whether *let-7* regulates translation initiation in vivo, we examined the polysome association of the two endogenous *let-7* target genes *daf-12* and *lin-41* in wild-type and *let-7(n2853)* animals, by applying whole animal lysates to sucrose density gradient centrifugation. In agreement with a decrease in translation initiation, *daf-12* and *lin-41* were moderately, but consistently, depleted from the highly translated polysomal fractions in wild-type animals (Fig. 2.3). However,

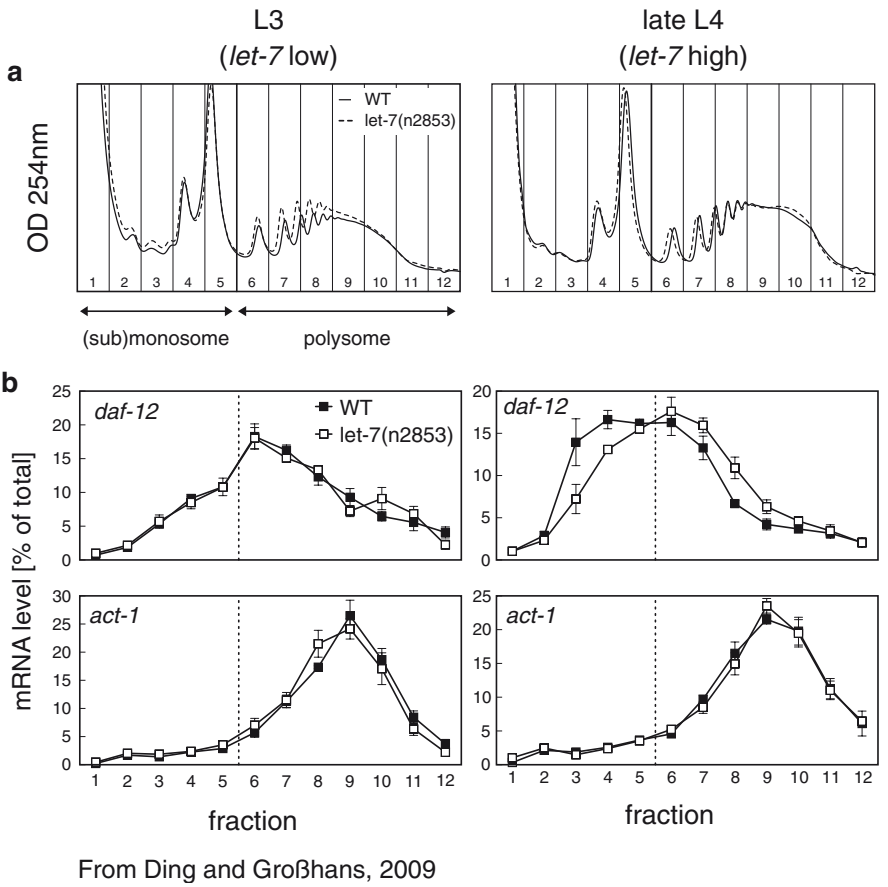

Fig. 2.3 *let-7* inhibits translation initiation of *daf-12* mRNA. (**a**) Polysome profiles of synchronized *wild-type* and *let-7(n2853)* animals at early L3, late L4. **(b)** Distribution of *daf-12* and *act-1* mRNA of across the fractions of the gradient. Before the onset of *let-7* expression in early L3, distribution of *daf-12* and *act-1* mRNA is essentially the same for wild-type and *let-7(n2853)* animals. In late L4, the distribution of the *let-7* target *daf-12* shifts to the (sub)-monosomal fractions in wild-type animals, whereas the distribution of *act-1*, which is not targeted by *let-7*, is not altered. Adapted from (Ding and Großhans 2009)

the limited degree of spatial and temporal coexpression of *let-7* miRNA and its targets limits the sensitivity of this assay. *let-7* is not universally expressed in *C. elegans* and as yet, regulation of target genes has been confirmed only in four different tissues, i.e., seam cells, ventral nerve cord, intestine, and head muscle (Abrahante et al. 2003; Groβhans et al. 2005; Lall et al. 2006; Lin et al. 2003; Slack et al. 2000).

Although the heterogeneity of a whole animal system complicates the analysis, such a model has the benefit of providing a true physiological context. Improved sensitivity can then be obtained through tissue specific expression of miRNA

target reporter genes. For instance, the apparent translational inhibition exerted by *let-7* considerably increased when a *lacZ* reporter gene carrying the *lin-41* 3′ UTR was directly expressed in epidermal seam cells, where *let-7* is also expressed (Fig. 2.4). Translational repression was specific, as translational repression of a *col-10::lacZ::lin-41* reporter gene relied on both wild-type *let-7* and the presence of previously described *let-7* binding sites (Vella et al. 2004).

Whereas previous reports on *lin-4* argued for translational repression downstream of initiation, the polysomal shifts observed in our experiments clearly demonstrated that *let-7* regulates two endogenous target genes by inhibiting translation at the initiation step. It thus appeared that two prominent miRNAs deployed two different modes of translational inhibition. To address this possibility, we examined the polysome association of transcripts in whole animal lysates of wild-type and *lin-4(e912)* mutant animals. In contrast to earlier studies (Olsen and Ambros 1999; Seggerson et al. 2002), we surprisingly discovered that *lin-4* also significantly inhibited translation initiation of its cognate target genes *lin-14* and

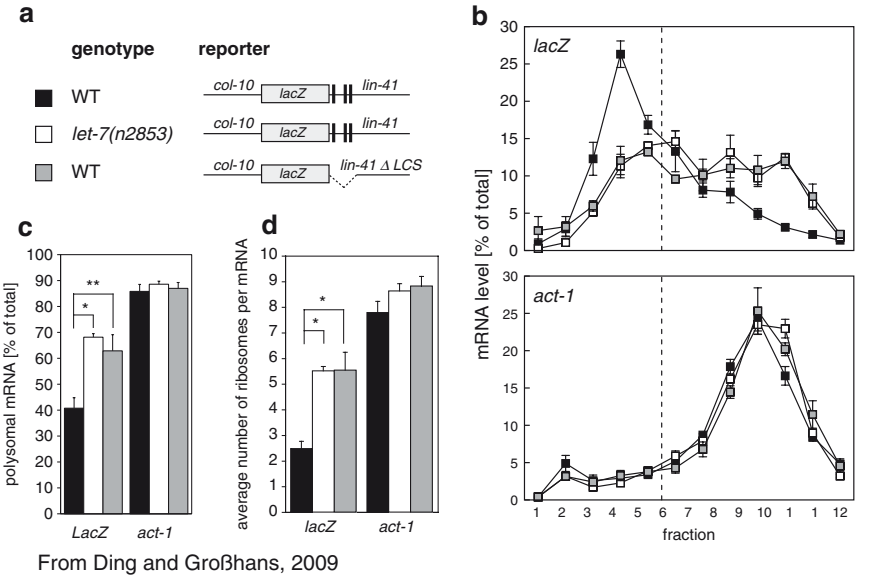

Fig. 2.4 Translational repression of *lin-41* is mediated by *let-7* and *let-7* binding sites. (**a**) Schematic representation of the reporter strains. The *lacZ* reporter genes were expressed in wild-type and *let-7(n2853)* animals under the control of the *col-10* promoter, which ensures constitutive expression in the seam cells, where *let-7* is also expressed. The vertical lines in the *lin-41* 3′ UTR represent *let-7* binding sites. In all experiments, synchronized late L4 animals were used. (**b**) Distribution of *lacZ* and *act-1* mRNA across the gradients. Only in the presence of both wild-type *let-7* and *let-7* binding sites, is the *lacZ* reporter gene translationally repressed. (**c**) Polysomal fraction of *lacZ*, endogenous *lin-41* and *act-1* as percentage of total RNA. (**d**) Average number of ribosomes on *lacZ* and *act-1* mRNA. (*, $p<0.05$; **, $p<0.01$; one-sided Student's *t*-test). Adapted from (Ding and Großhans 2009)

lin-28, indicating that *lin-4* and *let-7* function through the same mechanism. A cause for the discrepancy with the earlier data may be the fact that in earlier studies *lin-4* loss-of-function was approximated by comparing wild-type L1 animals to wild-type L2 animals as mature *lin-4* starts to accumulate at late L1 (Fig. 2.1). Thus, regulatory events occurring during *C. elegans* development, independently of *lin-4*, may have affected translational profiles of *lin-14* or *lin-28*.

In addition to translational repression, we also observed increased transcript levels of endogenous *daf-12* and *lin-41* mRNA in *let-7* mutant relative to wild-type animals (Ding and Großhans 2009), as previously observed with *lin-41* (Bagga et al. 2005). Transcript degradation might thus either provide an alternate mechanism for repression of miRNA target genes, or be a consequence of translational repression.

2.8 Inhibition of Translation Initiation and Transcript Degradation Both Depend on the GW182 Proteins AIN-1 and AIN-2

The *C. elegans* GW182 homolog AIN-1 (Argonaute interacting protein 1) has been identified through its function in developmental timing (Ding et al. 2005). The retarded heterochronic seam cell phenotype caused by *ain-1* loss-of-function mutations closely resembled the combined loss-of-function in the three *let-7* "sister" miRNAs *mir-48*, *mir-84*, and *mir-241*, which are related in sequence to *let-7* and function partially redundantly with it (Abbott et al. 2005; Lau et al. 2001; Lim et al. 2003). Genetic analysis of a reduction-of-function allele suggested that *ain-1* and its homolog *ain-2* function partially redundantly in post-transcriptional gene repression in *C. elegans* (Zhang et al. 2007). AIN-1 and AIN-2 were found to coimmunoprecipitate with DCR-1 (Dicer), mature miRNAs, and the Argonaute proteins ALG-1 and ALG-2, establishing GW182 proteins as bona fide components of the miRNA-induced silencing complex in *C. elegans* (Zhang et al. 2007). Complexes of GW182 proteins with Argonautes have also been identified in a variety of other organisms, including the human homologues TRNC6A-C (Behm-Ansmant et al. 2006; Eulalio et al. 2008b; Landthaler et al. 2008; Liu et al. 2005; Meister et al. 2005). Depletion of fly AGO1 or GW182 prevents the regulation of the same set of miRNA target genes, indicating that GW182 acts in the same pathway (Behm-Ansmant et al. 2006; Eulalio et al. 2007b). However, reporter genes mainly regulated at the translational level appeared less susceptible to GW182 depletion (Behm-Ansmant et al. 2006; Eulalio et al. 2007b), consistent with the proposed role of GW182 in directing miRNA targets to P-bodies for subsequent degradation (Ding et al. 2005). Nonetheless, the fact that miRNA target mRNAs could be coimmunoprecipitated with AIN-1/2 (Zhang et al. 2007) suggests that these mRNAs are at least partially stable under these conditions.

We attempted to uncouple translational repression and degradation by depleting the GW182 family members AIN-1 and AIN-2. To this end, we analyzed total

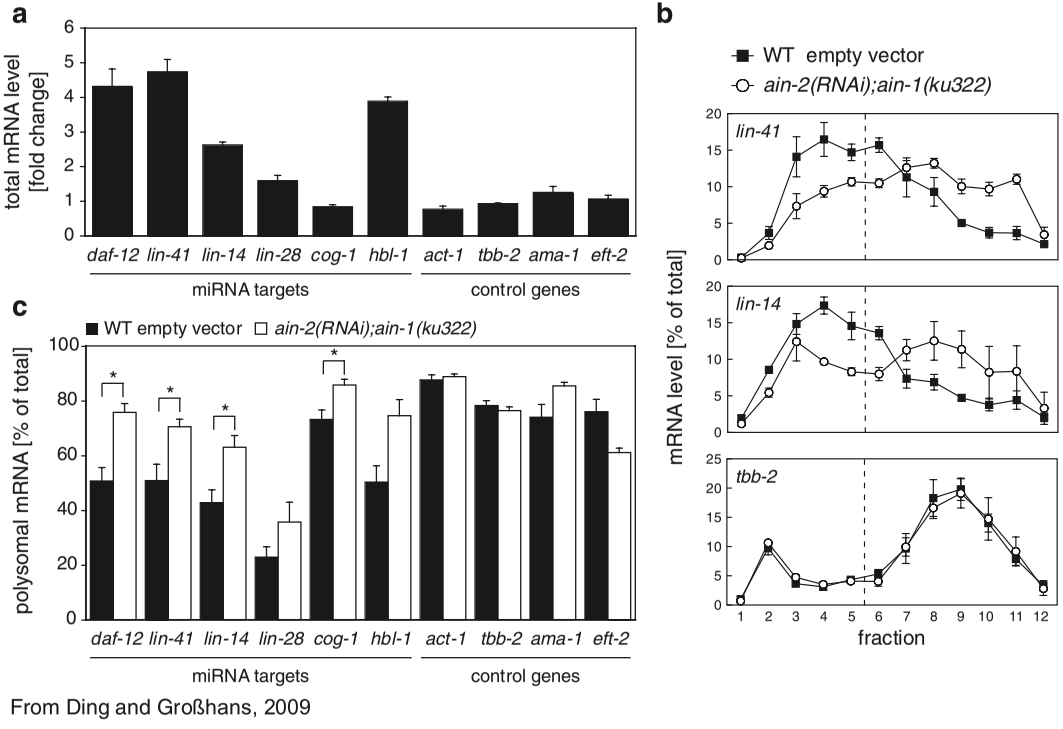

Fig. 2.5 The GW182 proteins AIN-1 and AIN-2 mediate translational repression and mRNA degradation. (**a**) Fold-change in mRNA levels between synchronized wild-type (empty vector RNAi control) animals and *ain-2(RNAi)*; *ain-1(ku322)* animals at late L4 stage. mRNA levels were analyzed by quantitative reverse-transcription PCR and normalized to the average of the control genes *act-1, tbb-2, ama-1,* and *eft-2*. (**b**) Distribution of the *let-7* target *lin-41*, the *lin-4* target *lin-14* and, *tbb-2*, not known to be a miRNA target, across the gradient. (**c**) Polysomal fractions of miRNA target genes and control genes as percentage of the total mRNA. Synchronized late L4 wild-type (empty vector RNAi control) and *ain-2(RNAi)*; *ain-1(ku322)* animals. (*, $p<0.05$, *lin-28*: $p=0.053$; *hbl-1*: $p=0.056$; one-sided Student's *t*-test). Adapted from (Ding and Großhans 2009)

transcript levels and polysome profiles of wild-type and *ain-2(RNAi); ain-1(ku322)* double mutant animals. As anticipated, the combined depletion of AIN-1/2 resulted in a substantial increase in total *daf-12* and *lin-41* transcripts. To our surprise, however, the mutations also abrogated translational repression. In fact, the relief of translational repression caused by AIN-1/2 depletion exceeded that seen with the *let-7(n2853)* mutation, possibly reflecting residual *let-7* activity in *let-7(n2853)* animals and/or a redundant activity of the *let-7* family members *mir-48*, *mir-84,* and *mir-241*. We tested four additional miRNA target mRNAs (Fig. 2.5): *cog-1*, which is targeted by *lsy-6* in the ASEL head neuron (Johnston and Hobert 2003); *hbl-1*, which is targeted by *mir-48*, *mir-84*, *mir-241*, *let-7*, and *lin-4* (Abbott et al. 2005; Abrahante et al. 2003; Lin et al. 2003); and the *lin-4* targets *lin-14* and *lin-28* (Moss et al. 1997; Wightman et al. 1993). All of these showed the characteristic polysomal shifts in the *ain-2(RNAi); ain-1(ku322)* mutant relative to wild-type animals, confirming their translational repression by an AIN-1/-2-dependent mechanism. Of note, the total *cog-1* mRNA level remained unchanged, indicating that repression could also occur independently of target mRNA degradation. Consistent with our findings, a degradation independent, repressive function of GW182 has recently also been shown with miRNA target reporter genes in Drosophila cells (Eulalio et al. 2008b). Taken together, our results demonstrate that repression of translation initiation by miRNAs is wide-spread in *C. elegans* and requires AIN-1/2.

2.9 Conclusions and Future Perspectives

Experiments on miRNA modes of action in vitro, ex vivo, and in vivo have previously yielded disparate results. The first two approaches predominantly, although not exclusively, supported repression of translation initiation and transcript degradation. By contrast, in vivo studies yielded conflicting results on the relevance of degradation and appeared to rule out repression of translation initiation. It was possible that these disparities reflected true mechanistic differences in different organisms, consistent with the fact that the in vivo work largely relied on *C. elegans*, whereas the other two approaches utilized human and Drosophila cells. More disconcertingly, ex vivo and in vitro studies had almost exclusively relied on transfected miRNA target reporter genes and two studies raised concerns that the transfection procedures and the promoters used to express these reporter genes influenced the apparent mode of miRNA activity. Our recent work now demonstrates that repression of translation initiation by miRNAs also occurs in vivo, in *C. elegans*, and on endogenous mRNAs targeted by three different miRNAs. Thus, miRNAs have now been shown to mediate repression of translation initiation in vivo, ex vivo, and in vitro, on both endogenous targets and reporter mRNAs, making a particularly compelling case for this mode of repression.

Loss-of-function of the GW182 homologues AIN-1 and AIN-2 relieves miRNA-mediated gene repression, supporting the notion that these proteins are essential miRNA effectors in *C. elegans*, consistent with the developmental defects observed

in earlier studies. Although AIN-1/-2 are required for both translational repression and transcript degradation, it is unclear whether these two constitute independent mechanisms or whether target degradation is a consequence of translational repression. However, at least for the *lsy-6* target *cog-1*, translational repression is not accompanied by target degradation, and we do not observe a correlation between the extent of translational repression and target gene degradation for various other miRNA:target pairs that we tested, which may hint at two distinct mechanisms. AIN-1 and AIN-2 may then coordinate translational repression and target degradation, possibly by interacting with distinct mediators or effectors. Future work directed towards the identification of these mediators and effectors may solve the question whether translational control and target degradation are a result of functionally distinct silencing complexes, and therefore, may be uncoupled. Now that both mechanisms have been demonstrated in *C. elegans*, its powerful genetic tools can be brought to bear on the issue. Detailed dissection of the genetic interaction partners of *let-7* that we recently uncovered might provide an avenue into identifying the factors involved.

Acknowledgments X.D. was supported by a PhD student fellowship from the Boehringer Ingelheim Foundation. Research in H.G.'s lab is funded by the Novartis Research Foundation and the Swiss National Science Foundation.

References

Abbott AL, Alvarez-Saavedra E, Miska EA, Lau NC, Bartel DP, Horvitz HR, Ambros V (2005) The let-7 MicroRNA family members mir-48, mir-84, and mir-241 function together to regulate developmental timing in Caenorhabditis elegans. Dev Cell 9:403–414

Abrahante JE, Daul AL, Li M, Volk ML, Tennessen JM, Miller EA, Rougvie AE (2003) The Caenorhabditis elegans hunchback-like gene lin-57/hbl-1 controls developmental time and is regulated by microRNAs. Dev Cell 4:625–637

Bagga S, Bracht J, Hunter S, Massirer K, Holtz J, Eachus R, Pasquinelli AE (2005) Regulation by let-7 and lin-4 miRNAs results in target mRNA degradation. Cell 122:553–563

Behm-Ansmant I, Rehwinkel J, Doerks T, Stark A, Bork P, Izaurralde E (2006) mRNA degradation by miRNAs and GW182 requires both CCR4:NOT deadenylase and DCP1:DCP2 decapping complexes. Genes Dev 20:1885–1898

Bhattacharyya SN, Habermacher R, Martine U, Closs EI, Filipowicz W (2006) Relief of microRNA-mediated translational repression in human cells subjected to stress. Cell 125:1111–1124

Bussing I, Slack FJ, Groβhans H (2008) let-7 microRNAs in development, stem cells and cancer. Trends Mol Med 14:400–409

Chalfie M, Horvitz HR, Sulston JE (1981) Mutations that lead to reiterations in the cell lineages of C. elegans. Cell 24:59–69

Chendrimada TP, Finn KJ, Ji X, Baillat D, Gregory RI, Liebhaber SA, Pasquinelli AE, Shiekhattar R (2007) MicroRNA silencing through RISC recruitment of eIF6. Nature 447:823–828

Denli AM, Tops BB, Plasterk RH, Ketting RF, Hannon GJ (2004) Processing of primary microRNAs by the Microprocessor complex. Nature 432:231–235

Ding XC, Großhans H (2009) Repression of C. elegans microRNA targets at the initiation level of translation requires GW182 proteins. EMBO J 28:213–222

Ding L, Spencer A, Morita K, Han M (2005) The developmental timing regulator AIN-1 interacts with miRISCs and may target the argonaute protein ALG-1 to cytoplasmic P bodies in C. elegans. Mol Cell 19:437–447

Ding XC, Slack FJ, Großhans H (2008) The let-7 microRNA interfaces extensively with the translation machinery to regulate cell differentiation. Cell Cycle 7:3083–3090

Doench JG, Petersen CP, Sharp PA (2003) siRNAs can function as miRNAs. Genes Dev 17:438–442

Dong Z, Zhang JT (2006) Initiation factor eIF3 and regulation of mRNA translation, cell growth, and cancer. Crit Rev Oncol Hematol 59:169–180

Eulalio A, Behm-Ansmant I, Izaurralde E (2007a) P bodies: at the crossroads of post-transcriptional pathways. Nat Rev Mol Cell Biol 8:9–22

Eulalio A, Rehwinkel J, Stricker M, Huntzinger E, Yang SF, Doerks T, Dorner S, Bork P, Boutros M, Izaurralde E (2007b) Target-specific requirements for enhancers of decapping in miRNA-mediated gene silencing. Genes Dev 21:2558–2570

Eulalio A, Huntzinger E, Izaurralde E (2008a) Getting to the root of miRNA-mediated gene silencing. Cell 132:9–14

Eulalio A, Huntzinger E, Izaurralde E (2008b) GW182 interaction with Argonaute is essential for miRNA-mediated translational repression and mRNA decay. Nat Struct Mol Biol 15:346–353

Filipowicz W, Bhattacharyya SN, Sonenberg N (2008) Mechanisms of post-transcriptional regulation by microRNAs: are the answers in sight? Nat Rev Genet 9:102–114

Fraser AG, Kamath RS, Zipperlen P, Martinez-Campos M, Sohrmann M, Ahringer J (2000) Functional genomic analysis of C. elegans chromosome I by systematic RNA interference. Nature 408:325–330

Gandin V, Miluzio A, Barbieri AM, Beugnet A, Kiyokawa H, Marchisio PC, Biffo S (2008) Eukaryotic initiation factor 6 is rate-limiting in translation, growth and transformation. Nature 455:684–688

Giraldez AJ, Mishima Y, Rihel J, Grocock RJ, Van Dongen S, Inoue K, Enright AJ, Schier AF (2006) Zebrafish MiR-430 promotes deadenylation and clearance of maternal mRNAs. Science 312:75–79

Grishok A, Pasquinelli AE, Conte D, Li N, Parrish S, Ha I, Baillie DL, Fire A, Ruvkun G, Mello CC (2001) Genes and mechanisms related to RNA interference regulate expression of the small temporal RNAs that control C. elegans developmental timing. Cell 106:23–34

Groβhans H, Slack FJ (2002) Micro-RNAs: small is plentiful. J Cell Biol 156:17–21

Groβhans H, Johnson T, Reinert KL, Gerstein M, Slack FJ (2005) The temporal patterning microRNA let-7 regulates several transcription factors at the larval to adult transition in C. elegans. Dev Cell 8:321–330

Horvitz HR, Sulston JE (1980) Isolation and genetic characterization of cell-lineage mutants of the nematode Caenorhabditis elegans. Genetics 96:435–454

Humphreys DT, Westman BJ, Martin DI, Preiss T (2005) MicroRNAs control translation initiation by inhibiting eukaryotic initiation factor 4E/cap and poly(A) tail function. Proc Natl Acad Sci U S A 102:16961–16966

Johnston RJ, Hobert O (2003) A microRNA controlling left/right neuronal asymmetry in Caenorhabditis elegans. Nature 426:845–849

Kamath RS, Fraser AG, Dong Y, Poulin G, Durbin R, Gotta M, Kanapin A, Le Bot N, Moreno S, Sohrmann M et al (2003) Systematic functional analysis of the Caenorhabditis elegans genome using RNAi. Nature 421:231–237

Ketting RF, Fischer SE, Bernstein E, Sijen T, Hannon GJ, Plasterk RH (2001) Dicer functions in RNA interference and in synthesis of small RNA involved in developmental timing in C. elegans. Genes Dev 15:2654–2659

Kim J, Krichevsky A, Grad Y, Hayes GD, Kosik KS, Church GM, Ruvkun G (2004) Identification of many microRNAs that copurify with polyribosomes in mammalian neurons. Proc Natl Acad Sci U S A 101:360–365

Kiriakidou M, Tan GS, Lamprinaki S, De Planell-Saguer M, Nelson PT, Mourelatos Z (2007) An mRNA m(7)G cap binding-like motif within human Ago2 represses translation. Cell 129:1141–1151

Knight SW, Bass BL (2001) A role for the RNase III enzyme DCR-1 in RNA interference and germ line development in Caenorhabditis elegans. Science 293:2269–2271

Kong YW, Cannell IG, de Moor CH, Hill K, Garside PG, Hamilton TL, Meijer HA, Dobbyn HC, Stoneley M, Spriggs KA et al (2008) The mechanism of micro-RNA-mediated translation repression is determined by the promoter of the target gene. Proc Natl Acad Sci U S A 105:8866–8871

Krutzfeldt J, Rajewsky N, Braich R, Rajeev KG, Tuschl T, Manoharan M, Stoffel M (2005) Silencing of microRNAs in vivo with 'antagomirs'. Nature 438:685–689

Lall S, Grun D, Krek A, Chen K, Wang YL, Dewey CN, Sood P, Colombo T, Bray N, Macmenamin P et al (2006) A genome-wide map of conserved microRNA targets in C. elegans. Curr Biol 16:460–471

Landthaler M, Gaidatzis D, Rothballer A, Chen PY, Soll SJ, Dinic L, Ojo T, Hafner M, Zavolan M, Tuschl T (2008) Molecular characterization of human Argonaute-containing ribonucleoprotein complexes and their bound target mRNAs. RNA 14:2580–2596

Lau NC, Lim LP, Weinstein EG, Bartel DP (2001) An abundant class of tiny RNAs with probable regulatory roles in Caenorhabditis elegans. Science 294:858–862

Lee RC, Feinbaum RL, Ambros V (1993) The C. elegans heterochronic gene lin-4 encodes small RNAs with antisense complementarity to lin-14. Cell 75:843–854

Lim LP, Lau NC, Weinstein EG, Abdelhakim A, Yekta S, Rhoades MW, Burge CB, Bartel DP (2003) The microRNAs of Caenorhabditis elegans. Genes Dev 17:991–1008

Lim LP, Lau NC, Garrett-Engele P, Grimson A, Schelter JM, Castle J, Bartel DP, Linsley PS, Johnson JM (2005) Microarray analysis shows that some microRNAs downregulate large numbers of target mRNAs. Nature 433:769–773

Lin SY, Johnson SM, Abraham M, Vella MC, Pasquinelli A, Gamberi C, Gottlieb E, Slack FJ (2003) The C elegans hunchback homolog, hbl-1, controls temporal patterning and is a probable microRNA target. Dev Cell 4:639–650

Linsley PS, Schelter J, Burchard J, Kibukawa M, Martin MM, Bartz SR, Johnson JM, Cummins JM, Raymond CK, Dai H et al (2007) Transcripts targeted by the microRNA-16 family cooperatively regulate cell cycle progression. Mol Cell Biol 27:2240–2252

Liu J, Valencia-Sanchez MA, Hannon GJ, Parker R (2005) MicroRNA-dependent localization of targeted mRNAs to mammalian P-bodies. Nat Cell Biol 7:719–723

Lytle JR, Yario TA, Steitz JA (2007) Target mRNAs are repressed as efficiently by microRNA-binding sites in the 5' UTR as in the 3' UTR. Proc Natl Acad Sci U S A 104:9667–9672

Maroney PA, Yu Y, Fisher J, Nilsen TW (2006) Evidence that microRNAs are associated with translating messenger RNAs in human cells. Nat Struct Mol Biol 13:1102–1107

Mathonnet G, Fabian MR, Svitkin YV, Parsyan A, Huck L, Murata T, Biffo S, Merrick WC, Darzynkiewicz E, Pillai RS et al (2007) MicroRNA inhibition of translation initiation in vitro by targeting the cap-binding complex eIF4F. Science 317:1764–1767

Meister G, Landthaler M, Peters L, Chen PY, Urlaub H, Luhrmann R, Tuschl T (2005) Identification of novel argonaute-associated proteins. Curr Biol 15:2149–2155

Moss EG (2007) Heterochronic genes and the nature of developmental time. Curr Biol 17:R425–R434

Moss EG, Lee RC, Ambros V (1997) The cold shock domain protein LIN-28 controls developmental timing in C. elegans and is regulated by the lin-4 RNA. Cell 88:637–646

Nelson PT, Hatzigeorgiou AG, Mourelatos Z (2004) miRNP:mRNA association in polyribosomes in a human neuronal cell line. RNA 10:387–394

Nottrott S, Simard MJ, Richter JD (2006) Human let-7a miRNA blocks protein production on actively translating polyribosomes. Nat Struct Mol Biol 13:1108–1114

Olsen PH, Ambros V (1999) The lin-4 regulatory RNA controls developmental timing in Caenorhabditis elegans by blocking LIN-14 protein synthesis after the initiation of translation. Dev Biol 216:671–680

Pasquinelli AE, Reinhart BJ, Slack F, Martindale MQ, Kuroda MI, Maller B, Hayward DC, Ball EE, Degnan B, Muller P et al (2000) Conservation of the sequence and temporal expression of let-7 heterochronic regulatory RNA. Nature 408:86–89

Petersen CP, Bordeleau ME, Pelletier J, Sharp PA (2006) Short RNAs repress translation after initiation in mammalian cells. Mol Cell 21:533–542

Pillai RS, Bhattacharyya SN, Artus CG, Zoller T, Cougot N, Basyuk E, Bertrand E, Filipowicz W (2005) Inhibition of translational initiation by Let-7 MicroRNA in human cells. Science 309:1573–1576

Rehwinkel J, Natalin P, Stark A, Brennecke J, Cohen SM, Izaurralde E (2006) Genome-wide analysis of mRNAs regulated by Drosha and Argonaute proteins in Drosophila melanogaster. Mol Cell Biol 26:2965–2975

Reinhart BJ, Slack FJ, Basson M, Pasquinelli AE, Bettinger JC, Rougvie AE, Horvitz HR, Ruvkun G (2000) The 21-nucleotide let-7 RNA regulates developmental timing in Caenorhabditis elegans. Nature 403:901–906

Rhoads RE, Dinkova TD, Korneeva NL (2006) Mechanism and regulation of translation in C. elegans. WormBook 1–18

Schmitter D, Filkowski J, Sewer A, Pillai RS, Oakeley EJ, Zavolan M, Svoboda P, Filipowicz W (2006) Effects of Dicer and Argonaute down-regulation on mRNA levels in human HEK293 cells. Nucl Acids Res 34:4801–4815

Seggerson K, Tang L, Moss EG (2002) Two genetic circuits repress the Caenorhabditis elegans heterochronic gene lin-28 after translation initiation. Dev Biol 243:215–225

Slack FJ, Basson M, Liu Z, Ambros V, Horvitz HR, Ruvkun G (2000) The lin-41 RBCC gene acts in the C. elegans heterochronic pathway between the let-7 regulatory RNA and the LIN-29 transcription factor. Mol Cell 5:659–669

Thermann R, Hentze MW (2007) Drosophila miR2 induces pseudo-polysomes and inhibits translation initiation. Nature 447:875–878

Vella MC, Choi EY, Lin SY, Reinert K, Slack FJ (2004) The C. elegans microRNA let-7 binds to imperfect let-7 complementary sites from the lin-41 3'UTR. Genes Dev 18:132–137

Wakiyama M, Takimoto K, Ohara O, Yokoyama S (2007) Let-7 microRNA-mediated mRNA deadenylation and translational repression in a mammalian cell-free system. Genes Dev 21:1857–1862

Wang B, Love TM, Call ME, Doench JG, Novina CD (2006) Recapitulation of short RNA-directed translational gene silencing in vitro. Mol Cell 22:553–560

Wettstein FO, Staehelin T, Noll H (1963) Ribosomal aggregate engaged in protein synthesis: characterization of the ergosome. Nature 197:430–435

Wightman B, Ha I, Ruvkun G (1993) Posttranscriptional regulation of the heterochronic gene lin-14 by lin-4 mediates temporal pattern formation in C. elegans. Cell 75:855–862

Wu L, Belasco JG (2005) Micro-RNA regulation of the mammalian lin-28 gene during neuronal differentiation of embryonal carcinoma cells. Mol Cell Biol 25:9198–9208

Wu L, Fan J, Belasco JG (2006) MicroRNAs direct rapid deadenylation of mRNA. Proc Natl Acad Sci U S A 103:4034–4039

Zhang L, Ding L, Cheung TH, Dong MQ, Chen J, Sewell AK, Liu X, Yates JR 3rd, Han M (2007) Systematic identification of C. elegans miRISC proteins, miRNAs, and mRNA targets by their interactions with GW182 proteins AIN-1 and AIN-2. Mol Cell 28:598–613

2.9 GW182 proteins are essential components of animal miRISC

The GW182 protein family is named after the glycine-tryptophane repeats found in their N-terminal portion and the molecular mass of one of their human paralogs, Trinucleotide Repeat Containing 6 protein A (TNRC6A), the first GW182 protein to be identified (Eystathioy et al., 2002). There are three GW182 proteins in vertebrates named TNRC6A, TNRC6B and TNRC6C, and one in drosophila called dGW182 or Gawky (Eulalio et al., 2009d). *C. elegans* encodes two GW182 proteins, the Argonaute Interacting proteins AIN-1 and AIN-2 (Ding et al., 2005; Zhang et al., 2007).

Several lines of evidence show that GW182 proteins are essential components of animal miRISC acting downstream of Argonaute proteins. GW182 proteins physically interact with Argonaute proteins (Behm-Ansmant et al., 2006; Ding et al., 2005; Eulalio et al., 2008; Landthaler et al., 2008; Liu et al., 2005; Meister et al., 2005; Zhang et al., 2007). Depletion of dGW182 abrogates miRNA-mediated gene regulation in drosophila (Behm-Ansmant et al., 2006; Eulalio et al., 2009a; Eulalio et al., 2008; Rehwinkel et al., 2006) and depletion of either TNRC6A, B, or C leads to a partial defect in miRNA-mediated gene silencing in human cells (Jakymiw et al., 2005; Landthaler et al., 2008; Li et al., 2008; Liu et al., 2005; Meister et al., 2005; Zipprich et al., 2009). Combined depletion of AIN-1 and AIN-2 abrogates miRNA-mediated gene regulation in *C. elegans* (Ding and Grosshans, 2009; Zhang et al., 2007). Disruption of the direct interaction between GW182 and Argonaute proteins by point mutations or a peptide that competes with GW182 for Argonaute binding prevents miRNA-mediated gene silencing (Eulalio et al., 2008; Till et al., 2007). Conversely, tethering of GW182 to a reporter mRNA bypasses the requirement of Argonaute proteins to induce translational repression and degradation of the reporter mRNA in drosophila (Behm-Ansmant et al., 2006; Chekulaeva et al., 2009; Eulalio et al., 2009a) or human cells (Li et al., 2008; Zipprich et al., 2009).

Depletion experiments conducted in drosophila cells (Behm-Ansmant et al., 2006; Eulalio et al., 2009b; Eulalio et al., 2007) and *in vitro* experiments using mouse Krebs-2 ascites extract (Fabian et al., 2009) have shown that GW182-mediated

mRNA deadenylation and degradation requires the CAF1:CCR4:NOT1 deadenylase complex. Deadenylation is then followed by decapping of the mRNA by the DCP1:DCP2 decapping complex and degradation by the 5' to 3' exonuclease XRN1 (Behm-Ansmant et al., 2006; Eulalio et al., 2009b; Eulalio et al., 2007; Fabian et al., 2009).

Mammalian TNRC6A, TNRC6B and TNRC6C and drosophila dGW182 share a similar domain organization (Figure 2.2). The N-terminal portion is characterized by numerous GW, WG or GWG motifs, followed by a ubiquitin-associated (UBA) domain, a glutamine-rich (Q-rich) domain and a C-terminal RNA recognition motif (RRM) (Eulalio et al., 2009d). The RRM likely does not bind RNA ((Eulalio et al., 2009c) and H. Matys, personal communication). These domains are embedded in protein sequences that are predicted to be unstructured (Behm-Ansmant et al., 2006; Ding and Han, 2007; Eulalio et al., 2009d). The C-terminal region between the Q-rich domain and the carboxy terminus have been annotated as a bipartite silencing domain (SD), consisting of a mid domain and a C-terminal domain separated by the RRM (Tritschler et al., 2010). However, this domain assignment is not shared by others (Fabian et al., 2010).

C. elegans AIN-1 and AIN-2 are highly divergent from their fly or mammalian homologs. AIN-1 and AIN-2 contain only few GW repeats (seven in AIN-1 and four in AIN-2), and lack a defined Q-rich domain, the RRM and the bipartite silencing domain. Furthermore, the protein sequences of AIN-1 and AIN-2 show only little similarity with each other (Zhang et al., 2007). However, a likely homolog of AIN-1/2 in the nematode *Brugia malayi* includes a small part of the silencing domain found in mammals and flies (Zipprich et al., 2009), which includes a PAM2 motif (discussed below). Thus, the *B. malayi* protein "may represent an evolutionary link between TNRC6 and AIN proteins" (Zipprich et al., 2009).

The contribution of individual domains of GW182 proteins to silencing has been extensively studied in drosophila and human cells, indicating that the N-terminus binds Argonaute, whereas the C-terminus mediates silencing. The N-terminal region of dGW182 is necessary and sufficient for interaction with drosophila AGO1 (Behm-

Ansmant et al., 2006) and GW repeats are responsible for the interaction with Argonaute proteins (Behm-Ansmant et al., 2006; Eulalio et al., 2009a; Jakymiw et al., 2005; Till et al., 2007). For drosophila dGW182, tethering of the glutamine-rich domain or a C-terminal domain including the RRM to a reporter mRNA can repress protein expression from that reporter (Chekulaeva et al., 2009; Eulalio et al., 2009a). Similar fragments have been found to mediate silencing in human cells (Baillat and Shiekhattar, 2009; Lazzaretti et al., 2009; Zipprich et al., 2009). The RRM contributes to, but is not required for, silencing of reporter mRNAs (Eulalio et al., 2009a; Eulalio et al., 2009c; Zipprich et al., 2009). A direct contribution of the N-terminal domain to silencing is controversial. In drosophila, an N-terminal fragment was found to mediate silencing when tethered to an mRNA reporter gene (Chekulaeva et al., 2009; Chekulaeva et al., 2010), and silencing was found to be independent of the Argonaute binding capacity (Chekulaeva et al., 2010), whereas two other studies came to a different conclusion (Eulalio et al., 2009a; Eulalio et al., 2009c).

Recent studies focused on the region annotated as bipartite silencing domain. These studies propose that GW182 proteins act as PABPC1 interacting proteins (PAIP) in drosophila and human cells by a direct interaction of the silencing domains with PABPC1 (Fabian et al., 2009; Huntzinger et al., 2010; Zekri et al., 2009). PABPC1 contains four N-terminal RNA recognition motifs (RRM1-4), a proline-rich linker, and a C-terminal domain termed PABC or MLLE (mademoiselle) (Kozlov et al., 2010a). The MLLE domain recognizes a conserved motif termed PABP interacting motif 2 (PAM2), which was first identified in PABPC1 interacting proteins PAIP1 and PAIP2 (Roy et al., 2002). Similar to the PAM2 motif found on PAIP1 and PAIP2, the PAM2 motif in TNRC6A-C directly interacts with the PABPC1 MLLE domain (Fabian et al., 2009; Huntzinger et al., 2010; Jinek et al., 2010; Kozlov et al., 2010b). In drosophila, two sites on dGW182 have been shown to interact with PABPC1: a PAM2 motif which directly binds MLLE on PABPC1 (Huntzinger et al., 2010; Zekri et al., 2009) and M2 and C-terminal regions that interact with the N-terminal RRM on PABPC1 (Huntzinger et al., 2010). A single amino acid substitution in the PAM2 motif of TNRC6B was found to abolish the ability of human TNRC6B to rescue silencing in drosophila cells depleted of endogenous dGW182 (Huntzinger et al.,

2010). However, it is not clear whether TNRC6B recapitulates all aspects of dGW182 in gene silencing in drosophila.

It is not known how the interaction between PABPC1 and GW182 mediates translational repression and mRNA degradation. A possible mechanism would be that GW182 proteins compete with eIF4G for binding PABPC1 and thus impair translation initiation by preventing the closed loop configuration of mRNAs. This idea is so far supported by the observation that the silencing domain of dGW182 competes with eIF4G in cell lysates (Zekri et al., 2009). Furthermore, competition could favor an open conformation which might render the 5' cap and poly(A) tail more accessible to mRNA degradation. Alternatively, a GW182-PABPC1 complex might provide a binding platform for additional interaction partners, for instance, it could help to recruit the CAF1:CCR4:NOT1 complex. In line with this, PABPC1 is required for accelerated deadenylation of miRNA targets *in vitro* (Fabian et al., 2009). The binding platform model may also apply for the interaction between GW182 proteins and the hyperplastic disc protein EED in mouse embryonic stem cells. Like PABPC1, EED contains a PABC domain which interacts with GW182. Thus, EED may act in parallel to PABPC1 in recruiting the CAF1:CCR4:NOT1 complex (Su et al., 2011).

However, *C. elegans* AIN-1 and AIN-2 lack most of the C-terminal domains found in mammals and flies, including the bipartite silencing domain. Conversely, the *C. elegans* orthologs of PABPC1, PAB-1 and PAB-2, do not have an MLLE domain. Nevertheless, PAB-1, PAB-2 and eIF4G were found to coimmunoprecipitate with AIN-2 (Zhang et al., 2007) and RNAi-mediated depletion of PAB-2 aggravated heterochronic defects in an *ain-1* mutant allele (X. C. Ding, unpublished). It is unclear whether *C. elegans* AIN-1 and AIN-2 mediate translational repression and mRNA degradation by a mechanism that is divergent from drosophila or human GW182 or whether AIN-1 and AIN-2 interact with PAB-1 and PAB-2 by alternative means.

Figure 2.2

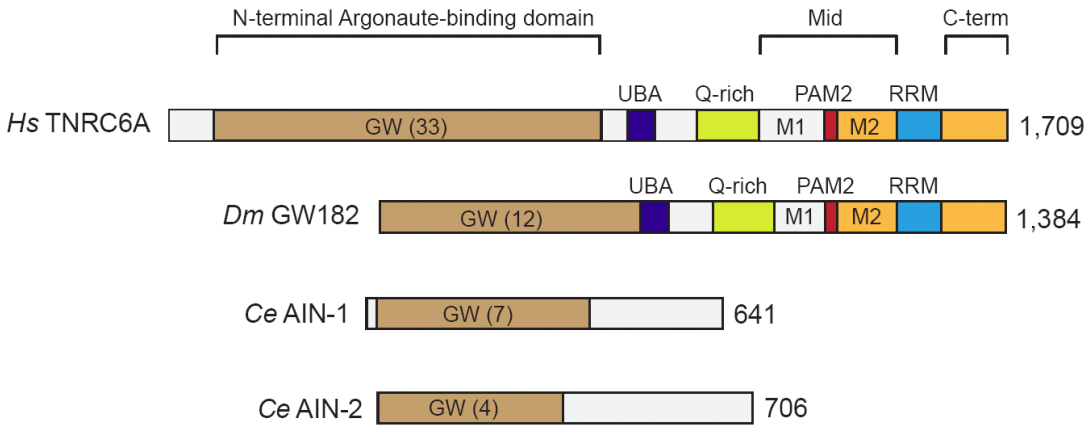

Figure 2.2 The domain organization of GW182 proteins. Comparison of the short isoform of human TNRC6A, drosophila GW182, and *C. elegans* AIN-1 and AIN-2. UBA: ubiquitin-associated domain, Q-rich: glutamine-rich domain, RRM: RNA recognition motif. The N-terminal Argonaute-binding domain is indicated and the number of glycine-tryptophane (GW) motifs present in the domain are indicated in the brackets. The mid- and the C-terminal domain of the bipartite silencing domain are indicated. The mid-domain consists of regions M1 and M2 and the poly(A)-binding protein interacting motif 2 (PAM2). Adapted from Tritschler et al., 2010.

3. The type II poly(A)-binding protein PABP-2 is a downstream target of the *let-7* miRNA in the heterochronic pathway of *Caenorhabditis. elegans*

3.1 Published manuscript

Published online 16 March 2011

Nucleic Acids Research, 2011, Vol. 39, No. 13 ***5647–5657***
doi:10.1093/nar/gkr145

The type II poly(A)-binding protein PABP-2 genetically interacts with the *let-7* miRNA and elicits heterochronic phenotypes in *Caenorhabditis elegans*

Benjamin A. Hurschler[1], David T. Harris[2] and Helge Großhans[1,*]

[1]Friedrich Miescher Institute for Biomedical Research (FMI), Maulbeerstrasse 66, WRO-1066.1.38, CH-4002 Basel, Switzerland and [2]Howard Hughes Medical Institute, Department of Biology, Massachusetts Institute of Technology, Cambridge, MA, USA

Received July 12, 2010; Revised January 31, 2011; Accepted February 27, 2011

ABSTRACT

The type II poly(A)-binding protein PABP2/PABPN1 functions in general mRNA metabolism by promoting poly(A) tail formation in mammals and flies. It also participates in poly(A) tail shortening of specific mRNAs in flies, and snoRNA biogenesis in yeast. We have identified *Caenorhabditis elegans pabp-2* as a genetic interaction partner of the *let-7* miRNA, a widely conserved regulator of animal stem cell fates. Depletion of PABP-2 by RNAi suppresses loss of *let-7* activity, and, in *let-7* wild-type animals, leads to precocious differentiation of seam cells. This is not due to an effect on *let-7* biogenesis and activity, which remain unaltered. Rather, PABP-2 levels are developmentally regulated in a *let-7*-dependent manner. Moreover, using RNAi PABP-2 can be depleted by >80% without significantly impairing larval viability, mRNA levels or global translation. Thus, it unexpectedly appears that the bulk of PABP-2 is dispensable for general mRNA metabolism in the larva and may instead have more restricted, developmental functions. This observation may be relevant to our understanding of why the phenotypes associated with human PABP2 mutation in oculopharyngeal muscular dystrophy (OPMD) seem to selectively affect only muscle cells.

INTRODUCTION

MicroRNAs (miRNAs) are small, non-coding RNAs that post-transcriptionally regulate gene expression in animals, plants and protozoa. Incorporated into a multi-subunit miRNA-induced silencing complex (miRISC), miRNAs serve as guide molecules to provide the specificity in target mRNA recognition by an antisense mechanism. Binding of miRISC ultimately prevents protein accumulation by target mRNA destabilization and/or translational repression, which may involve target mRNA deadenylation [reviewed by (1)].

The *let-7* miRNA is phylogenetically conserved in bilaterian animals, with a remarkable 100% sequence identity of the mature miRNA in *Caenorhabditis elegans* and humans (2,3). *let-7* was originally identified as a heterochronic gene in *C. elegans* (4). The genes of the heterochronic pathway (Figure 1A) control temporal patterning during post-embryonic development, i.e. they direct the developmental stage-specific execution of cell fates (5). Thus, loss of *let-7* function causes a defect in the larval-to-adult (L/A) transition such that cells reiterate larval stage four (L4) cell fates in adult animals, ultimately leading to lethality by vulval bursting (4). For instance, the stem cell-like seam cells would normally exit the cell cycle and terminally differentiate at the L/A transition but continue to divide and fail to differentiate in *let-7* mutant animals. In contrast to this retarded heterochronic phenotype, over-expression of *let-7* or depletion of some of its targets such as *lin-41*, leads to the opposite, precocious phenotype, where seam cells differentiate prematurely at the L3-to-L4 molt (referred to as 'L3 molt' hereafter) (4,6). These functions of *C. elegans let-7* in regulating temporal cell fates by controlling cell proliferation and differentiation are mirrored by mammalian *let-7*, which acts as a tumour suppressor and regulator of stem cells by repressing stem cell self-renewal and promoting differentiation (7).

We previously identified *pabp-2*, the *C. elegans* orthologue of the type II poly(A)-binding protein PABP2/PABPN1, in a reverse genetic screen for suppressors of *let-7* loss-of-function lethality (8). Despite their shared name, type II or nuclear poly(A)-binding proteins are structurally and functionally unrelated to type I or

*To whom correspondence should be addressed. Tel: +41 61 6976675; Fax: +41 61 6973976; Email: helge.grosshans@fmi.ch

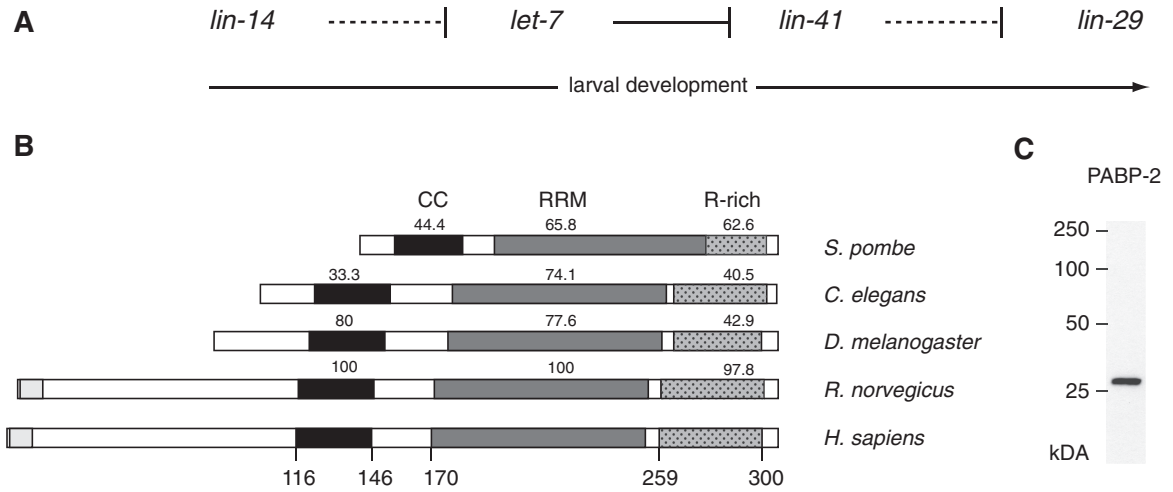

Figure 1. Conservation of eukaryotic PABP2. (**A**) Schematic depiction of the heterochronic pathway, which temporally regulates seam cell division and differentiation. For clarity, only those heterochronic genes investigated in this study are depicted. Solid lines represent direct repression of downstream genes, dashed lines indicate genetic interactions for which repression has not been shown to be direct (regulation of *lin-29* by *lin-41*) or is assumed to be indirect (*lin-14* versus *let-7*). (**B**) schematic representation of PABP2 protein in different species. The predicted coiled-coil (CC; black) region, RNA recognition motif (RRM; grey) and arginine-rich region (R-rich; dotted) are indicated. Human and rat proteins bear N-terminal extensions that contain poly-alanine tracts (light grey) that are expanded in disease. Numbers above domains indicate the degree of identity of the amino acid sequence to the corresponding human domains, numbers below the human sequence correspond to the amino acid positions. (B) Western blot using a polyclonal rat antibody reveals PABP-2 as a single band at ~27 kDa.

cytoplasmic poly(A)-binding proteins, which have recently been reported to interact with miRISC (9–11). Mammalian PABP2 was initially identified as an enhancer of nuclear polyadenylation (12). *In vitro*, the poly(A) polymerase (PAP), the cleavage and polyadenylation specificity factor (CPSF) and PABP2 are both necessary and sufficient for faithful and efficient pre-mRNA polyadenylation (12,13). As poly(A) tail-length determines both the stability and the translation efficiency of an mRNA (14–16), PABP2 is thus likely to be of major importance to general mRNA metabolism.

CPSF and PABP2 cooperatively stimulate PAP in a process that involves CPSF binding to the polyadenylation signal AAUAAA, positioned ~20 nt upstream of the cleavage site and PABP2 covering the growing poly(A) tail (13,17,18). Formation of a tight, spherical PABP2 particle is thought to fold back the growing poly(A) tail to maintain the contact between CPSF and PAP. Once the poly(A) tail has reached a critical length, no further PABP2 can be accommodated, and processivity of poly(A) tail synthesis is disrupted. Thus, PABP2 not only promotes polyadenylation, but also appears to act as a molecular ruler that defines the ultimate poly(A) tail length (17).

Consistent with the function assigned to PABP2 *in vitro*, depletion of PABP2 in cultured mouse myoblasts led to a shortening of mRNA poly(A) tails (19). In *Drosophila*, PABP2 was shown to be essential for viability, and a transgene bearing a point mutation that prevents PAP stimulation was unable to rescue the lethality of a null allele (20). In contrast, deletion of *pabp2* in *Schizosaccharomyces pombe* was tolerated and, unexpectedly, caused hyperadenylation of bulk mRNA (21). Moreover, fission yeast Pab2 was found to participate in the processing of 3′-extended small nucleolar (sno)RNAs (22). Finally, despite a nuclear steady-state localization, PABP2 shuttles between nucleus and cytoplasm, consistent with additional cytoplasmic roles (23). Indeed, cytoplasmic PABP2 functions to shorten the poly(A) tails of oscar and cyclinB mRNAs in *Droshophila* embryos, establishing an essential developmental function (20). Taken together, although strong evidence supports an important role of PABP2 in general mRNA metabolism, these functions might not be generally conserved across eukaryotes, and PABP2 might have been recruited for additional or alternative functions in different organisms.

Little is known about *C. elegans* PABP-2. Like its mammalian counterpart, PABP-2 contains a putative coiled-coil region, a single RNA recognition motif (RRM), and a C-terminal arginine-rich domain (Figure 1B). However, like its *Drosophila* and *S. pombe* orthologues, *C. elegans* PABP-2 lacks a region of homology to the N-terminus of mammalian PABP2. In human PABP2, this region includes a polyalanine tract, the expansion of which causes oculopharyngeal muscular dystrophy (OPMD), a late-onset, progressive disease (24).

Here, we demonstrate that in *C. elegans*, depletion of PABP-2 not only rescues loss of *let-7* function, but also causes precocious seam cell differentiation. Surprisingly, efficient depletion of PABP-2 leaves global translation and mRNA levels largely unaffected, while causing accumulation of the LIN-29 transcription factor, the most downstream effector gene known in the heterochronic pathway. Moreover, PABP-2 concentration decreases during animal development in a *let-7*-dependent manner, although PABP-2 is unlikely to be a direct *let-7* target. Our results support the idea that the bulk of PABP-2 in *C. elegans* larvae is not required for general mRNA metabolism but

may play more specialized roles in development. Given the tissue-specificity of phenotypes seen upon PAPB2 mutation in human OMPD, such non-canonical functions of PABP2 may deserve more detailed study also in other animals, including humans.

MATERIALS AND METHODS

Caenorhabditis elegans strains and handling

Strains were maintained and cultured as described (25). Wild-type N2, MT7626: *let-7(n2853)* and VT516 *lin-29(n546)/mnC1 dpy-10(e128) unc-52(e444)II* strains were provided by CGC. *him-5; [ajm-1::gfp/MH27::GFP; rol-6]* (26) was used to visualize seam cells. MT19756: *nIs408[lin-29b::mCherry]* contains an integrated array (nEx1681) formed by the injection of PCR product (50 ng/µl) containing the *lin-29B* locus (LG II sequence 11 917 298–11 927 996), which has mCherry inserted in place of the stop codon, and a plasmid carrying *ttx-3::gfp* (40 ng/µl). The *lin-29b::mCherry* reporter rescues the Pvl, alae, molting and seam cell division defects of the putative null allele *lin-29(n836)* (David T. Harris and H. Robert Horvitz, unpublished data). *maIs105[col-19::gfp]; let-7(n2853)* was provided by Frank Slack and Ryusuke Niwa. HW761: *lin-29(n546)/mnC1 dpy-10(e128) unc-52(e444)II; him-5; [ajm-1::gfp/MH27::GFP; rol-6]* was used to visualize seam cells in a *lin-29(lf)* background and was established by crossing VT516 with *him-5; [ajm-1::gfp/MH27::GFP; rol-6]* males. HW758 *nIs408[lin-29b/mCherry] I; him-5; [ajm-1::gfp/MH27::GFP; rol-6]*, used to visualize *lin-29b* expression and seam cell fusion in the same animals, was established by crossing MT19756 with *him-5; [ajm-1::gfp/MH27::GFP; rol-6]* males.

RNAi by feeding synchronized L1 larvae on RNAi plates at 25°C was performed as described (27). Unless indicated otherwise, animals for molecular studies were harvested at the L4 stage, when *let-7* levels are high (4). RNAi feeding constructs from published RNAi libraries (28,29) were used against *daf-12*, *hbl-1*, *lin-41*, *lin-14*, *pab-1, eif-3.e* and *pabp-2*.

To assess brood sizes, wild-type animals were grown at 25°C on L4440 (*mock(RNAi)*) control or *pabp-2(RNAi)* feeding plates. Gravid adults were singled and transferred onto OP50 plates for further growth at 25°C. The number of progeny was counted 24 and 72 h after transfer to OP50 plates. Since egg laying in control animals was essentially complete by 24 h, with animals producing fewer than seven progeny within the following 48 h, the analysis was restricted to the first 24 h.

lin-29 epistasis

lin-29 epistasis was tested using HW761 *lin-29(n546)/mnC1 dpy-10(e128) unc-52(e444)II; him-5; [ajm-1::gfp/MH27::GFP; rol-6)* animals. *mnC1* homozygotes arrest in late larval development and eventually die. Hence, young adults segregate into 1/3 *lin-29(n546)* homozygotes and 2/3 *lin-29(n546)/mnC1* heterozygotes, which was confirmed by the frequency of *lin-29(lf)* phenotypes including protruding vulva and sterility. Synchronized HW761 L1 larvae were grown on RNAi feeding plates at 25°C until young adult stage. Failure of terminal seam cell differentiation was assessed by fluorescence microscopy. The reverse epistasis experiment, the suppression of *pabp-2(RNAi)* phenotypes in *lin-29(lf)* animals could not be tested. At the L3 molt, when we examined precocious cell fusion, *lin-29(n546)* homozygous, *lin-29(n546)/mnC1* heterozygous and *mnC1* homozygous animals were all indistinguishable, so that only one-fourth of the animals would have the desired *lin-29(n546)* genotype. Thus, the maximum possible reduction of precocious seam cell fusion falls within the variability of our results.

Polyribosome preparation and analysis

Polyribosome preparations were performed by sucrose density gradient ultracentrifugation as described (30). For each gradient fraction, 400 ng of RNA was reverse transcribed using the ImProm-II Reverse Transcription System (Promega) according to the manufacturer's recommendations. Random hexamer primers were used to avoid a bias against short poly(A) tails, which may occur as a consequence of miRNA action (1) or PABP-2 depletion.

Quantitative PCR reactions were performed in technical duplicate using the ABsolute^{TM} QPCR SYBRs Green ROX Mix (Thermo Fisher Scientific) on an ABI Prism 7000 real-time thermal cycler. Relative transcript levels were calculated using the $2[-\Delta\Delta C(T)]$ method (31). (For primer pairs see Supplementary Data.) The relative transcript levels were corrected for the total amount of RNA extracted from each fraction and mapped as percentage of the sum of all fractions. Reverse transcription of total RNA was performed on aliquots of the same samples that were used for polysome profiling using unequal duplicates of 400 and 800 ng of RNA input. Repetition of one experiment using oligo(dT)-priming of reverse transcription instead of random hexamers did not change the results. The fold-change in transcript levels between *pabp-2* and *mock(RNAi)* derived from total RNA or from the sum of all fractions also yielded comparable results, confirming the robustness of the assay.

Northern blotting

RNA samples were separated on TBE Urea PAGE gels and transferred to Hybond Nx membrane (GE Healthcare). Chemical cross-linking with EDC was performed according to the method described in (32). Antisense DNA oligonucleotides were 5′-labelled using T4 polynucleotide kinase (PNK) and [y-^{32}P]ATP. (See Supplementary Data for oligonucleotide sequences). Radioactive signals were detected using a Storage Phosphor Screen and a Typhoon 9400 scanner and quantified with Imagequant TL software (all GE Healthcare).

Antibodies and western blotting

SDS–PAGE and western blotting was performed according to standard protocols (33). To obtain an antibody against PABP-2, recombinant GST-PABP-2 was expressed in *Escherichia coli*, purified on glutathione sepharose 4B (GE Healthcare), released by thrombin

cleavage and gel extracted. Polyclonal antibodies against PABP-2 were raised in rats by Charles River Laboratories (Kisslegg, Germany) and unprocessed immune serum was used 1:500 to detect PABP-2 as a single band. Actin was detected by monoclonal mouse anti-actin MAB1501 (Millipore, 1:1000 dilution). Horseradish peroxidase-conjugated anti-mouse (NA931V, GE Healthcare) or anti-rat (112-035-003, Jackson Labs) secondary antibodies were used for signal detection by ECL (GE healthcare); bands were quantified in ImageJ (34).

Nomarski and fluorescent imaging

Microscopy images were acquired using an Axioplan microscope (axio imager Z1, Zeiss) equipped with a CCD camera (AxioCam Mrm, Zeiss). Adobe Photoshop software was used to crop images or to adjust levels, leaving gamma unaltered.

RESULTS

RNAi-mediated knockdown of *pabp-2* suppresses *let-7(n2853)* lethality

The temperature sensitive *let-7(n2853)* allele harbours a point mutation in the seed region of the mature *let-7* miRNA that impairs target mRNA silencing (4,35). As a consequence, mutant animals die by bursting through the vulva at the L/A transition when grown at 20°C or above (Figure 2A and C). To identify *let-7* interaction partners, we previously screened an RNAi-by-feeding library of approximately 2400 genes on *C. elegans* chromosome I for suppression of *let-7*-associated lethality (8). In the course of this screen, we identified *pabp-2*, encoding the type II poly(A)-binding protein PABP-2, as a potent suppressor. Almost 60% of synchronized *let-7(n2853)* L1 larvae reach the adult stage when grown on bacteria expressing a double-stranded RNA against the genomic region of *pabp-2* at 25°C (Figure 2B and C). In *let-7* wild-type animals, RNAi-mediated knockdown of *pabp-2* led to a >10-fold reduction in brood size and fully penetrant early larval arrest of viable progeny (Figure 2D). Double mutant *let-7(n2853); pabp-2(RNAi)* animals similarly often bore dead embryos and rare viable progeny underwent early larval arrest (Figure 2B and E).

RNAi-mediated depletion of PABP-2 was mirrored in homozygous *pabp-2(ok1121)* mutant progeny, deleted for *pabp-2*, which similarly died *in utero* of their heterozygous (balanced) mothers or underwent early larval arrest (data not shown). Further reflecting specificity, three additional RNAi constructs against exons 2 and 3 as well as the entire coding region of *pabp-2*, also suppressed *let-7* lethality, albeit to variable extents (data not shown).

To verify PABP-2 depletion directly and to examine the extent of knockdown, we generated a rat polyclonal antibody against PABP-2 recombinantly expressed in *E. coli*. When tested on whole animal lysates, this antibody recognized a single band of an apparent size of ~27 kDa (Figure 1C), slightly above the predicted size but consistent with the migration pattern observed for the recombinant protein (data not shown). When examined in mid-L4 stage animals, we found that *pabp-2(RNAi)* reduced PABP-2 protein levels by >80% relative to animals exposed to mock RNAi (Figure 2F).

Depletion of PABP-2 causes precocious seam cell fusion

To ascertain that the suppression of the *let-7(n2853)* lethality reflected a heterochronic function of PABP-2, we examined seam cell differentiation. Terminal differentiation of seam cells at the L/A transition in wild-type animals involves their fusion into a syncytium. In *let-7(n2853)* animals, seam cells fail to terminally differentiate at the L/A transition whereas overexpression of *let-7*, or depletion of some of its targets such as *lin-41* or *hbl-1*, causes seam cells to fuse precociously, at the L3 molt (4,6,42,43) (Figure 3C). Whereas only 4% of wild-type animals exposed to mock RNAi displayed seam cell fusion at this stage, this number was increased to 47% of animals on *pabp-2* RNAi (Figure 3). Thus *pabp-2(RNAi)* causes heterochronic defects opposite to *let-7(n2853)*.

pabp-2(RNAi) promotes LIN-29 activity

To situate *pabp-2* more clearly in the heterochronic pathway, we examined its relation to *lin-29*, the most downstream heterochronic gene known to regulate seam cell differentiation (5). In wild-type animals, this zinc finger transcription factor is upregulated during the L4 stage to drive transcription of direct targets such as the adult cuticular collagen *col-19* (36,37).

Using a functional *lin-29b::mCherry* fusion gene (see 'Materials and Methods' section), LIN-29 first becomes visible in wild-type seam cells in L4 stage animals, prior to seam cell fusion (Figure 4A). As reported for endogenous LIN-29 (36), accumulation of LIN-29/mCherry occurs precociously at the L3 molt upon RNAi-mediated depletion of the early acting heterochronic gene *lin-14* (53% of animals) or the late acting *lin-41* (52% of animals) (Figure 4B–E). RNAi against *pabp-2* caused a similar precocious LIN-29B/mCherry accumulation (50%; Figure 4B and F). Knockdown of all three genes also caused comparable levels of precocious seam cell fusion (Figure 4B).

To examine whether altered LIN-29 accumulation was functionally relevant and able to explain the rescue of *let-7* mutant animals, we examined activation of the LIN-29 target *col-19* (37) using a *col-19::gfp* reporter (38). This cuticular collagen is expressed in adults but not in larvae (39), and fails to be activated in *let-7(n2853)* mutant adults, where LIN-29 levels remain low (4). Consistent with restored function of LIN-29, *let-7(n2853); pabp-2(RNAi)* animals displayed highly penetrant (90%) expression of *col-19::gfp*, similar to what was observed with control *let-7(n2853); lin-41(RNAi)* animals (Figure 5). This effect is specific and not an indirect consequence of restored animal viability, since escaping *let-7(n2853)* adults on *mock(RNAi)* failed to activate *col-19* expression, as did *let-7(n2853)* animals exposed to *eif-3.e(RNAi)*, a potent suppressor of *let-7(n2853)* vulval bursting [Figure 5; M. Rausch and M. Ecsedi, unpublished data; (8)].

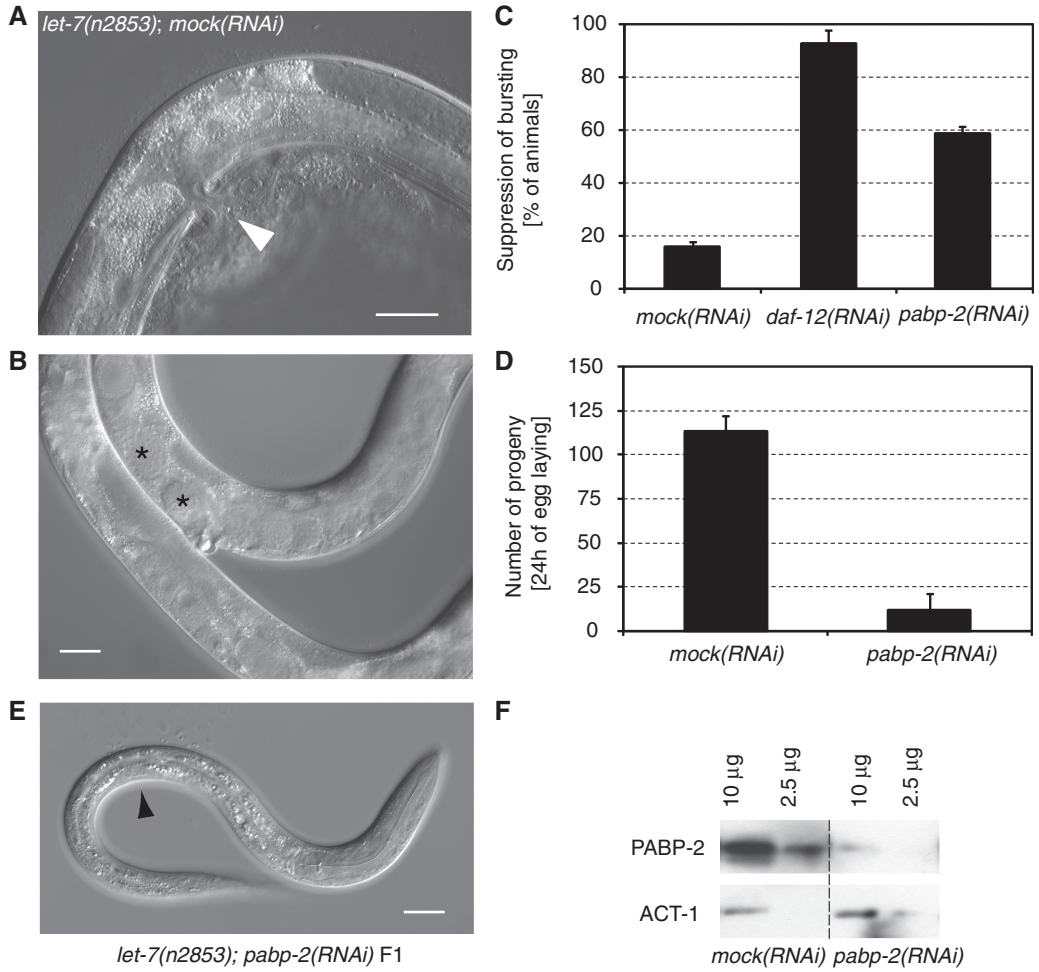

Figure 2. RNAi-mediated knockdown of *pabp-2* suppresses *let-7(n2853)* lethality. (**A**) *let-7(n2853)* animals die at the L/A transition by bursting through the vulva (white arrowhead) when grown at 25°C, (**B**) *let-7(n2853); pabp-2(RNAi)* animals survive into adulthood as indicated by the presence of embryos (asterisks), although most embryos die *in utero*, (**C**) Suppression of *let-7(n2853)*-mediated vulval bursting upon *pabp-2(RNAi)* or *daf-12(RNAi)*, which served as a positive control. In this and subsequent figures, '*mock(RNAi)*' denotes control animals that were fed bacteria carrying the insertless L4440 RNAi vector. $n \geq 4$ independent trials with ≥70 animals each, (**D**) Number of viable progeny during the first 24 h of egg laying at 25°C; $n = 10$ animals each. (**E**) Arrested F1 progeny of a *let-7(n2853); pabp-2(RNAi)* mother. The number of cells in the gonad (black arrowhead) indicates that progeny arrest at late L1/early L2 stage. (**F**) At late L4, PABP-2 protein levels were reduced by >80% in *pabp-2(RNAi)* relative to *mock(RNAi)* animals. Non-adjacent lanes of the same blot are shown. Error bars denote SEM. Scale bars are 20 µm.

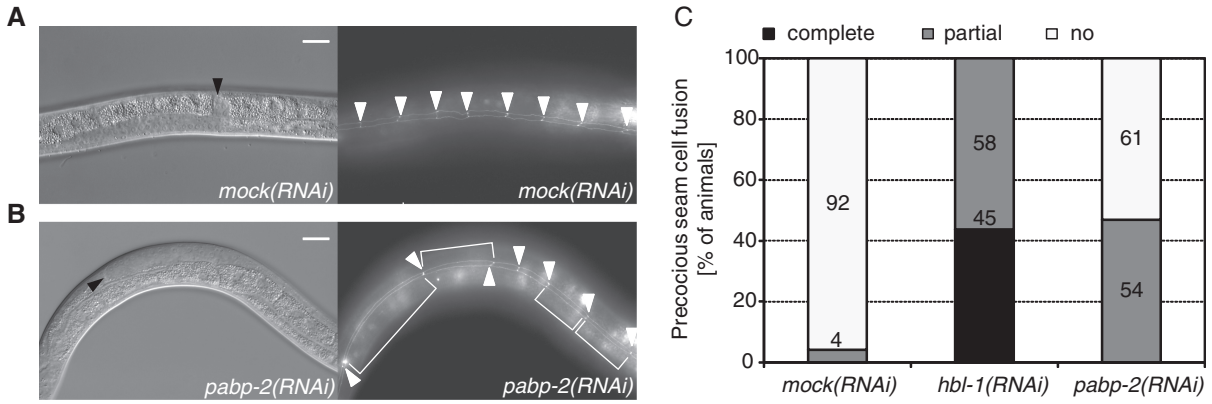

Figure 3. Depletion of PABP-2 causes precocious seam cell fusion. Synchronized *him-5; [ajm-1::gfp/MH27::GFP; rol-6]* L1-stage larvae were exposed to RNAi as indicated and examined for precocious seam cell fusion upon reaching L4 stage. (**A** and **B**) Photomicrographs of animals grown on *mock* and *pabp-2(RNAi)*, respectively. Arrowheads in the Nomarski micrographs (left panels) point to the distal tips of the gonads. Arrowheads in the GFP micrographs (right panels) indicate the cell–cell junctions between seam cells in absence of cell fusion visualized by the expression of AJM-1::GFP. (**C**) The penetrance of precocious seam cell fusion from three independent experiments. The numbers on the bars indicate the absolute number of animals assigned to the respective category. Scale bars are 20 µm.

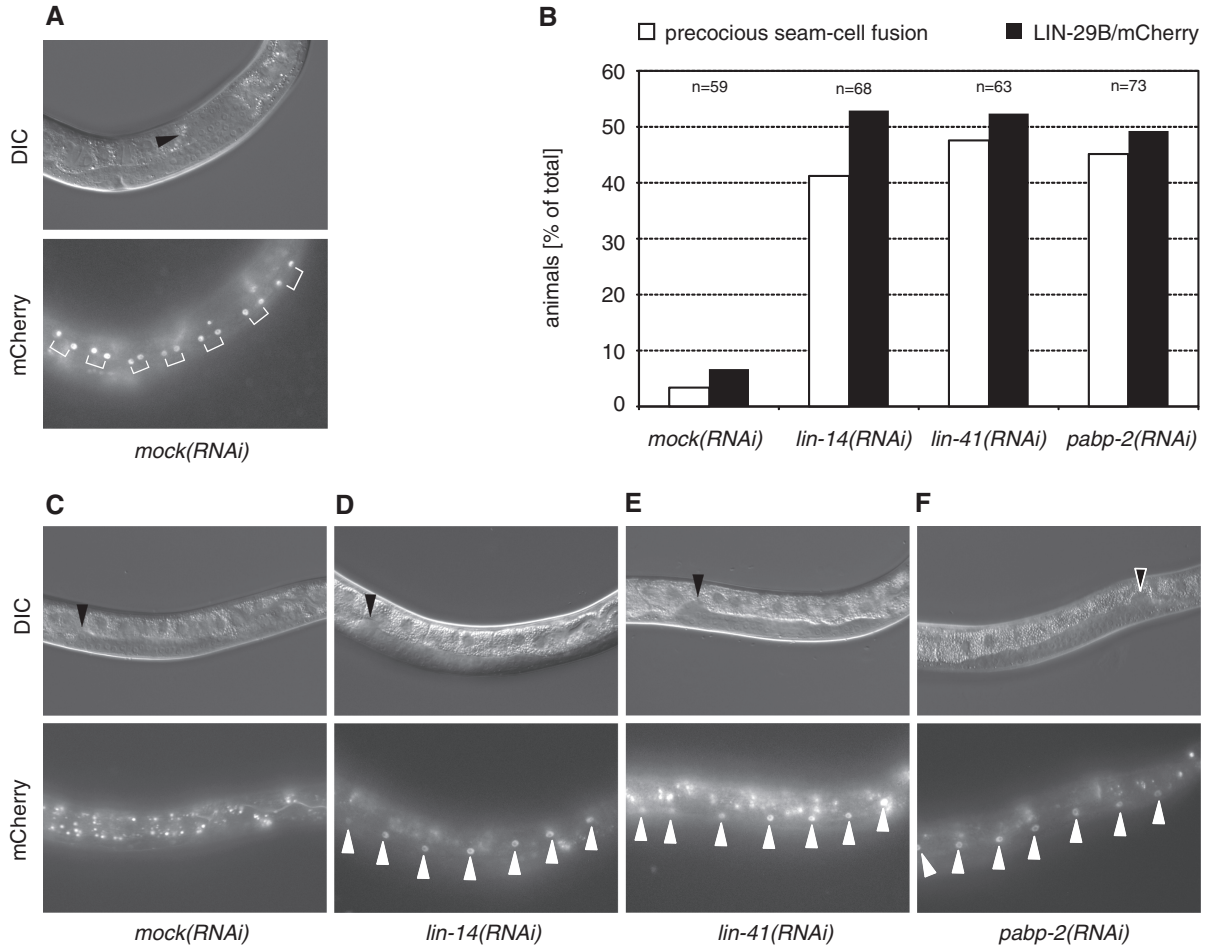

Figure 4. LIN-29/mCherry accumulates precociously in *pabp-2(RNAi)* animals. Strain HW761 expressing *lin-29b/mCherry* was exposed to RNAi by feeding as synchronized L1-stage larvae. (**A** and **C–F**) Photomicrographs of animals grown on the indicated RNAi. Upper panels show Nomarski micrographs and lower panels show fluorescence micrographs. Arrowheads in the Nomarski micrographs point to the distal tip of the gonad, white arrowheads in the fluorescence micrographs point to seam cell nuclei. (A) Mock-treated L4 animal accumulating LIN-29B at mid L4. The brackets indicate the nuclei of the daughter cells of the final seam cell division. (**B**) Percentage of animals exhibiting precocious seam cell fusion (white bars) and LIN-29B accumulation in seam cell nuclei at late L3. The number of animals examined is indicated above the bars. (**C**–F) Late L3 stage animals exposed to (C) mock RNAi, (D) *lin-14(RNAi)*, (E) *lin-41(RNAi)* and (F) *pabp-2(RNAi)*.

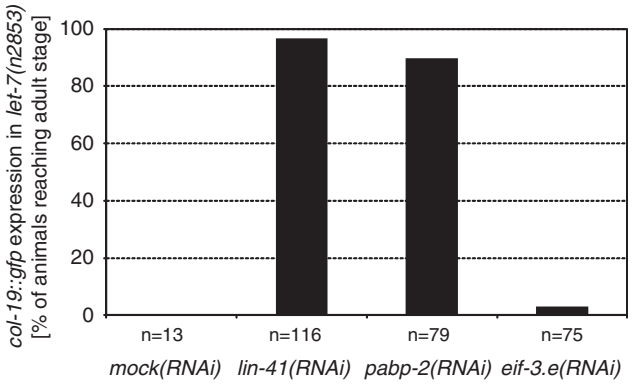

Figure 5. *pabp-2(RNAi)* restores expression of the LIN-29 target *col-19* in *let-7(n2853)* animals. Expression of *col-19::gfp* in *let-7(n2853)* adults. Note that only animals that bypassed *let-7(n2853)* lethality at the L/A transition could be scored. (Survival of *let-7(n2853)* animals in this assay: *mock(RNAi)*: 5%; *lin-41(RNAi)*: 94%; *pabp-2(RNAi)*: 55%; *eif-3.e(RNAi)*: 76%). The total number of animals examined in three biological replicates is indicated.

Finally, we wished to examine how *lin-29* and *pabp-2* interact genetically. Since technical reasons prevented us from examining whether loss of *lin-29* suppressed the precocious seam cell phenotype of *pabp-2(RNAi)* (see 'Materials and Methods' section), we investigated whether the retarded seam cell fusion phenotype seen in *lin-29(n546)* null mutant animals (37) was suppressed by *pabp-2(RNAi)*. As expected (see 'Material and Methods' section), approximately one-third (31%) of adult animals derived from balanced *lin-29(n546)/mnC1* heterozygous hermaphrodites displayed unfused seam cells on mock RNAi. This number remained unchanged when the two control genes *lin-14* and *lin-41* were depleted by RNAi, consistent with their function upstream of *lin-29* in the heterochronic pathway (5) (Figure 1A). Similarly, *pabp-2(RNAi)* was unable to suppress the seam cell fusion defect in *lin-29(n546)* mutant animals. Thus, taken together, the expression and genetic interaction data support a model where *papb-2* functions upstream of, and at least in part through, *lin-29*.

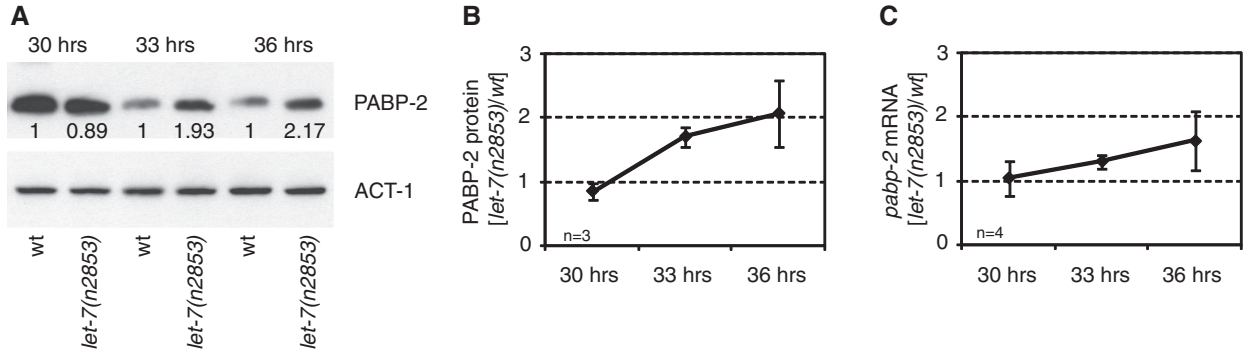

Figure 6. *pabp-2* is over-expressed in *let-7(n2853)* starting late L4. (**A–C**) Expression of PABP-2 protein and *pabp-2* mRNA in wild-type and *let-7(n2853)* animals at 30, 33 and 36 h of postembryonic development (corresponding to mid-L4 to late L4/young adult stage). Numbers below the PABP-2 bands in (A) indicate PABP-2 signal by western blotting normalized to actin signal, with wild-type signal set to one for each time point. (B) Protein quantification normalized to PABP-2 signal in wild-type animals for each time-point; shown is the average of three independent trials. Note that in wild-type animals, PABP-2 signal declines ~5-fold over the time course. (C) mRNA quantification by RT–qPCR.

PABP-2 protein is overexpressed in late L4-stage *let-7(n2853)* animals

The genetic interaction between *pabp-2* and *let-7* might be explained by repression of *pabp-2* expression by *let-7*. However, sequence analysis using RNAhybrid (40) revealed that the entire *pabp-2* locus was devoid of sequences enabling *let-7*:*pabp-2* mRNA duplex formation. Still, to examine whether *let-7* might indirectly regulate PABP-2 levels, we assessed its levels by western blotting. In contrast to the apparent house-keeping function of PABP2 in mRNA metabolism, but consistent with a function in temporal patterning, we found a substantial decline of PAPB-2 protein levels in wild-type animals during the L4 stage such that we observed an ~5-fold signal decrease between 30 and 33 h after initiating growth of synchronized L1 larvae at 25°C (Figure 6A). Moreover, PABP-2 levels were comparable in wild-type and *let-7(n2853)* mutant animals at 30 h, but ~2-fold elevated in *let-7(n2853)* at 33 and 36 h (Figure 6A and B). A similar trend was observed when examining *pabp-2* mRNA levels (Figure 6C), suggesting that loss of *let-7* activity affects PABP-2 levels through increased transcription or stability of the *papb-2* mRNA, Thus, PAPB-2 levels are not only developmentally regulated, but this regulation is also mediated, in part, by *let-7*.

let-7 biogenesis occurs normally in PABP-2 depleted animals

MicroRNAs of the *let-7* family are components of several double negative regulatory loops, where factors that are repressed by the miRNAs themselves repress *let-7* biogenesis [reviewed in (7)]. The fact that depletion of *pabp-2* mirrored *let-7* overexpression together with the known RNA-binding activity of PABP2 proteins and their role in the biogenesis of different RNA species thus prompted us to ask whether PABP-2 might also normally inhibit *let-7* function, perhaps by interfering with its biogenesis. Hence, we used northern blotting to study whether *pabp-2(RNAi)* enhanced *let-7* biogenesis. Consistent with a previous report (4), levels of mature *let-7* were ~3-fold reduced in *let-7(n2853)* animals relative to wild-type animals, whereas pre-*let-7* levels were largely unaffected or only modestly increased (Figure 7A). However, depletion of PABP-2 affected neither pre-*let-7* nor mature *let-7* levels regardless of whether wild-type or *let-7(n2853)* mutant animals were investigated (Figure 7). Thus, PABP2 does not play a significant role in *let-7* biogenesis.

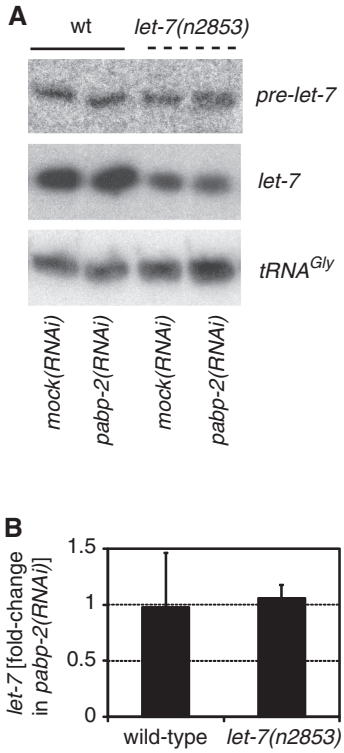

Figure 7. *let-7* biogenesis occurs normally in PABP-2-depleted animals. (**A**) Northern blots using total RNA from synchronized late L4 animals grown on *mock* or *pabp-2(RNAi)*. Oligonucleotides specific for pre-*let-7*, *let-7* or $tRNA^{Gly(TCC)}$ were used. The experiment was performed on biological triplicates, a representative example is shown. (**B**) Relative fold-change of mature *let-7* levels in *pabp-2(RNAi)* versus *mock(RNAi)* in wild-type and *let-7(n2853)* animals. $n = 3$, error bars represent SEM.

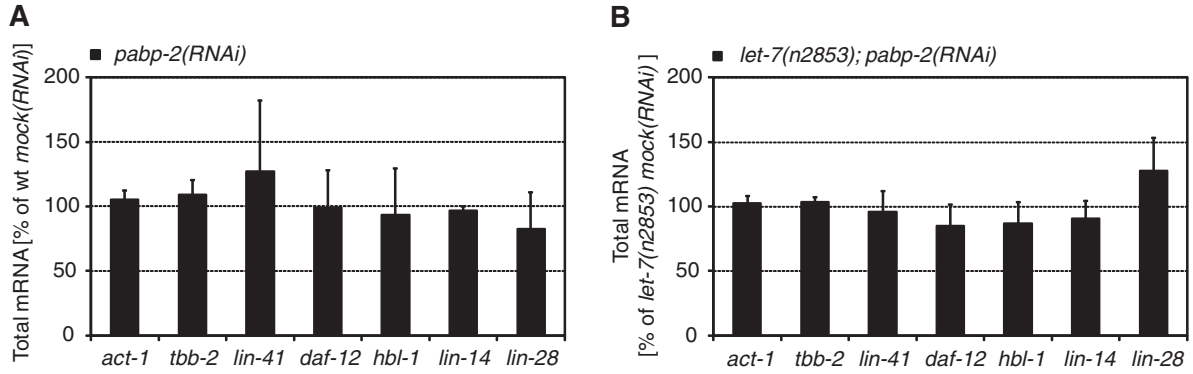

Figure 8. Depletion of PABP-2 does not affect *let-7* target mRNA stability. (**A** and **B**) Analysis of total mRNA levels in wild-type or *let-7(n2853)* mutant animals by qRT-PCR. mRNA levels in animals exposed to *pabp-2(RNAi)* are given as percentage of the mRNA levels observed in *mock(RNAi)* animals.

Depletion of PABP-2 does not affect *let-7* target mRNA stability

Caenorhabditis elegans miRNAs regulate their cognate targets by target mRNA destabilization (30,41) and/or translational repression at the initiation step (30). To test whether depletion of PABP-2 affected *let-7* target gene silencing, we first determined the mRNA levels of the *let-7* target genes *daf-12*, *lin-41* and *hbl-1*, all three of which function in seam cell temporal patterning (4,6,27,42,43). We further included *lin-14* and *lin-28*, two targets of the *lin-4* miRNA (44,45), to examine potentially more general roles of *pabp-2* in miRNA function, as well as *act-1* and *tbb-1* as non-miRNA regulated reference genes.

We extracted total RNA of L4-stage wild-type and *let-7(n2853)* animals grown on *pabp-2(RNAi)* or *mock(RNAi)*. As the expression levels of *let-7* target genes are typically low at this stage, we used quantitative reverse transcription–PCR (qRT–PCR) to detect transcripts. The expression levels of *act-1* (actin) and *tbb-2* (β-tubulin) were comparable in *pabp-2(RNAi)* and *mock(RNAi)*, suggesting that the depletion of PABP-2 did not substantially affect overall mRNA levels. Moreover, the levels of the miRNA target genes *lin-41, daf-12, hbl-1, lin-14* and *lin-28* did not show any statistically significant changes, regardless of whether *pabp-2(RNAi)* was performed on wild-type or *let-7(n2853)* mutant animals (Figure 8). We conclude that PABP-2 depletion does not affect *let-7*-mediated mRNA degradation.

Depletion of PABP-2 has only minor effects on translation efficiency

Since miRNA-mediated mRNA degradation and translational repression may be independent mechanisms of target mRNA silencing, we next performed polysome profiling on animals exposed to *pabp-2(RNAi)* to establish the translation initiation efficiency of miRNA targets. To this end, we used sucrose-density gradient ultracentrifugation to fractionate whole animal lysates from L4-stage wild-type and *let-7(n2853)* animals grown on either *pabp-2(RNAi)* or *mock(RNAi)* feeding plates. We then performed qRT–PCR to analyse the distribution of transcripts across the fractions.

Surprisingly, given the importance of poly(A) length in controlling mRNA translation and the suspected role of PABP-2 in determining polyadenylation globally, the UV-absorbance gradient profiles of lysates of *pabp-2(RNAi)* and *mock(RNAi)* were essentially the same (Figure 9A). A small increase was only seen in the 80S peak, which represents mRNAs bound by one ribosome and, possibly, also free ribosomes, but the relative amount of RNA recovered from polysomal fractions did not change significantly (Supplementary Figure S1A). In contrast, when we knocked down *pab-1*, one of two *C. elegans* orthologues of the type I poly(A)-binding protein, a considerable depletion in polyribosomes resulted (Figure 9B). Thus, unlike *pab-1*, knockdown of *pabp-2* does not appear to have a general effect on translation.

When we specifically examined the miRNA target genes *lin-41*, *daf-12*, *hbl-1*, *lin-14* and *lin-28* from the polysomal fractions in wild-type and *let-7(n2853)* animals, we found them to be consistently, though modestly, depleted from polysomes upon PABP-2 knockdown. However, the control genes *act-1* and *tbb-2* were depleted as well, albeit to a lower extent (Figure 9C and D). Although we cannot exclude that this moderate inhibition of translation in *pabp-2(RNAi)* animals may account for the rescue of *let-7(n2853)* lethality, it thus appears that PABP-2 has no major and specific function in miRNA-mediated translational repression.

DISCUSSION

PABP2 functions as a general mRNA metabolic factor in mammals, but also plays specific developmental roles in fly embryogenesis. We have revealed a heterochronic function of *C. elegans* PAPB-2 by demonstrating its genetic interaction with the heterochronic *let-7* miRNA, its temporally regulated expression, its responsiveness to *let-7* levels and its role in the prevention of precocious seam cell fusion. The genetic interaction between *let-7* and *pabp-2* and the fact that *pabp-2* lacks obvious

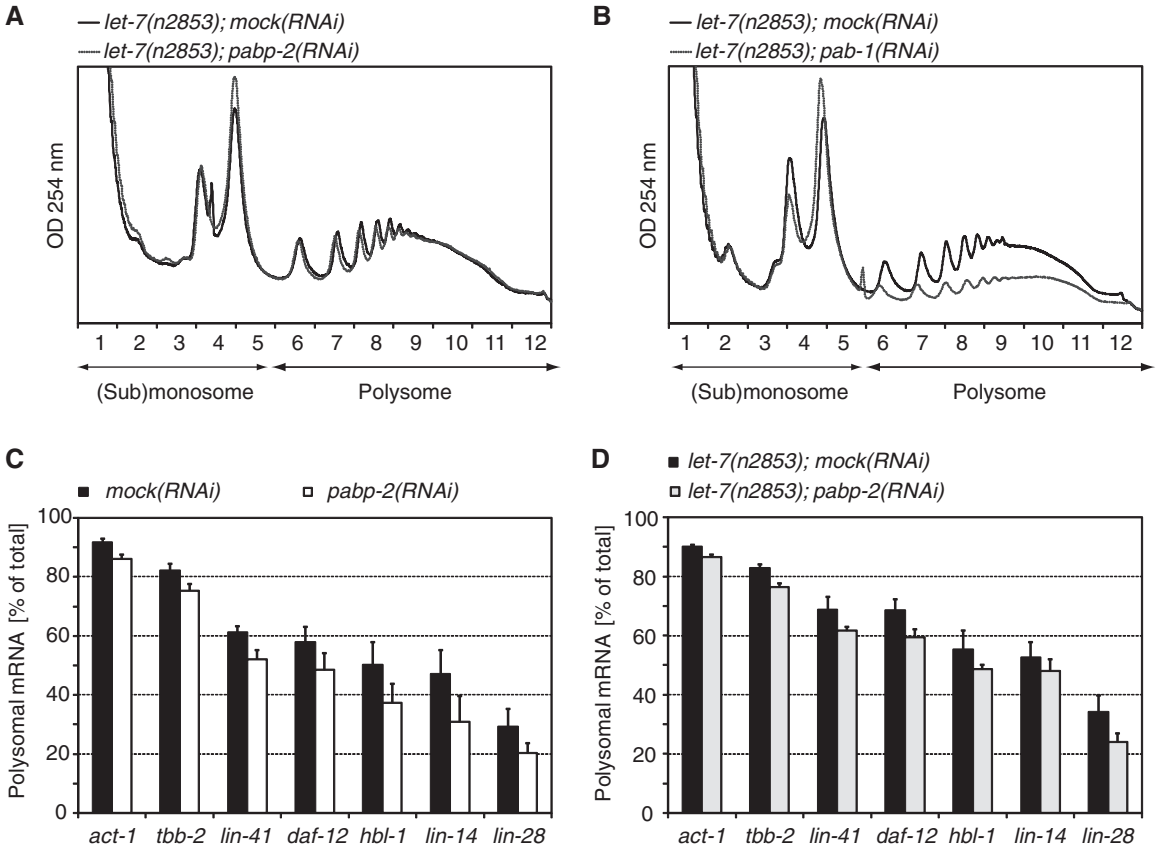

Figure 9. Depletion of PABP-2 has only minor effects on translation efficiency. (**A**) Typical polysome profiles of *let-7(n2853)* animals grown on *mock(RNAi)* or *pabp-2(RNAi)*. Fractions 1–5 comprise the (sub)-monosome, fractions 6–12 the polysomes. (**B**) RNAi against *pab-1*, the *C. elegans* orthologue of the human or yeast cytoplasmic (type I) poly(A)-binding protein restrains translation. (**C** and **D**) Polysomal fractions of mRNAs are plotted as percentage of the total (=monosomal+polysomal fractions) in late L4 wild-type (**C**) and *let-7(n2853)* (**D**) animals grown on either *mock(RNAi)* or *pabp-2(RNAi)*. Numbers are the averages of ≥3 independent experiments. Error bars represent SEM.

miRNA binding sites suggested that *pabp-2* is either a negative regulator of *let-7* biogenesis or *let-7* activity; or that *pabp-2* antagonizes the developmental role of *let-7* in seam cell and vulva development without a direct molecular interaction. The first two scenarios appeared particularly appealing considering that PAPB-2 is an RNA binding protein involved in polyadenylation, because the *let-7* primary miRNA is polyadenylated (46), and because mRNA deadenylation is considered to be one of the mechanisms through which miRNAs silence their target mRNAs (1).

However, the data we present here argue against a specific function of PAPB-2 in either process, as *let-7* levels were unaffected by PAPB-2 depletion, as were the levels of *let-7* target mRNAs. In contrast, we observed a mild depletion of *let-7* target mRNAs from polysomes upon *pabp-2(RNAi)*, but this effect was also observed for control genes and thus non-specific. Formally, we cannot rule out that such a general translational repression rescues *let-7(n2853)* lethality by sufficiently reducing translation of the key *let-7* targets *daf-12* and *lin-41*. However, we consider this unlikely because the extent of translational repression observed across four independent experiments was variable, whereas the suppression of *let-7(n2853)* lethality was not, i.e. there was little correlation between these two read-outs. Therefore, we consider it more likely that PABP-2 functions downstream of, or in parallel to, *let-7* in the heterochronic pathway. Given that PABP-2 accumulates to inappropriate levels in the *let-7(n2853)* mutant, we favour the former possibility. An attractive possibility that remains to be explored is that PAPB-2 functions together with LIN-41.

Restoration of expression of the LIN-29 target gene *col-19* in *let-7(n2853); pabp-2(RNAi)* double mutant animals, precocious LIN-29/mCherry accumulation in *pabp-2(RNAi)* single mutant animals and failure to suppress the retarded seam cell phenotype of the *lin-29(n546)* mutation further suggests that *papb-2* acts upstream of *lin-29*. With regard to LIN-29/mCherry accumulation we note with interest that we failed to observe good correlation of precocious LIN-29/mCherry accumulation and precocious seam cell fusion at the L3 molt, i.e. we observed fused seam cells without detectable LIN-29/mCherry accumulation, as well as unfused seam cells displaying strong LIN-29/mCherry signal (data not shown). In contrast, in wild-type seam cells, fusion during the L4 stage was preceded by LIN-29/mCherry accumulation. Although we cannot rule out that our reporter might not fully capture all the details of endogenous LIN-29 accumulation, it will be interesting to examine whether

LIN-29 activity is subject to regulation, e.g. through post-translational modification or the requirement of co-factors that are themselves subject to regulation. In accord with the notion of additional layers of regulation, precocious accumulation of LIN-29 was previously found to be insufficient to drive seam cell differentiation in early *lin-41(RNAi)* larvae (6).

In vitro, mammalian PABP2 is required for pre-mRNA polyadenylation (12), supporting an important function of PAPB2 in general mRNA metabolism *in vivo*. Consistent with this notion, PABP2 is essential for embryonic viability in flies (20) and *C. elegans* (this study). Surprisingly however, we could deplete PABP-2 by >80% from *C. elegans* larvae without affecting their viability or mRNA stability, and with little if any effect on global translation, indicating that, in this situation, the bulk of PABP-2 is dispensable for general mRNA metabolism. Although unexpected in view of the above findings, we note that this mirrors, in an animal, the situation in yeast where *pab2* can be deleted in *S. pombe* and does not exist in *Saccharomyces cerevisiae*. Moreover, siRNA-mediated depletion of mouse PABP2 from murine primary myoblasts resulted in a decrease of particularly long poly(A) tracts (~300 nt), but seemed to have little effect on shorter poly(A) tracts (~100 nt) (19). Finally, a polyalanine tract expansion in the N-terminus of human PAPB2 leads to OPMD, an adult-onset, progressive disease characterized by selective phenotypes restricted to a subset of muscle cells. Although redundant activities, residual PABP2 function, or, in the case of OPMD, toxicity of the accumulating mutant PABP2 may explain some of these phenomena, we would like to propose that functions of PABP2 that affect only selected mRNAs (20) may deserve equal consideration to general mRNA metabolic roles in future studies on PABP2 function. Clearly, the fact that *C. elegans* PABP-2 levels are developmentally regulated, in a *let-7*-dependent manner, supports functions beyond mere housekeeping activity.

SUPPLEMENTARY DATA

Supplementary Data are available at NAR Online.

ACKNOWLEDGEMENT

The authors thank Dr. David Baillie, Dr. Ryusuke Niwa, Dr. Frank Slack and the Caenorhabditis Genetics Center (CGC) for strains used in this work, Magdalene Rausch and Matyas Ecsedi for sharing unpublished data and Dr. Rafal Ciosk and Dr. Witold Filipowicz for critical reading of this manuscript.

FUNDING

Novartis Research Foundation through the Friedrich Miescher Institute; the Swiss National Science Foundation (grant number 3100A0-114001); and the European Research Council (ERC Starting Independent Investigator Grant number 241985—'miRTurn'). Howard Hughes Medical Institute to the laboratory of Dr. H. Robert Horvitz (to D.H.). Funding for open access charge: ERC.

Conflict of interest statement. None declared.

REFERENCES

1. Fabian,M.R., Sonenberg,N. and Filipowicz,W. (2010) Regulation of mRNA translation and stability by microRNAs. *Annu. Rev. Biochem.*, **79**, 351–379.
2. Lagos-Quintana,M., Rauhut,R., Lendeckel,W. and Tuschl,T. (2001) Identification of novel genes coding for small expressed RNAs. *Science*, **294**, 853–858.
3. Pasquinelli,A.E., Reinhart,B.J., Slack,F., Martindale,M.Q., Kuroda,M.I., Maller,B., Hayward,D.C., Ball,E.E., Degnan,B., Muller,P. *et al.* (2000) Conservation of the sequence and temporal expression of let-7 heterochronic regulatory RNA. *Nature*, **408**, 86–89.
4. Reinhart,B.J., Slack,F.J., Basson,M., Pasquinelli,A.E., Bettinger,J.C., Rougvie,A.E., Horvitz,H.R. and Ruvkun,G. (2000) The 21-nucleotide let-7 RNA regulates developmental timing in Caenorhabditis elegans. *Nature*, **403**, 901–906.
5. Rougvie,A.E. (2005) Intrinsic and extrinsic regulators of developmental timing: from miRNAs to nutritional cues. *Development*, **132**, 3787–3798.
6. Slack,F.J., Basson,M., Liu,Z., Ambros,V., Horvitz,H.R. and Ruvkun,G. (2000) The lin-41 RBCC gene acts in the C. elegans heterochronic pathway between the let-7 regulatory RNA and the LIN-29 transcription factor. *Mol. Cell*, **5**, 659–669.
7. Büssing,I., Slack,F.J. and Großhans,H. (2008) let-7 microRNAs in development, stem cells and cancer. *Trends Mol. Med.*, **14**, 400–409.
8. Ding,X.C., Slack,F.J. and Großhans,H. (2008) The let-7 microRNA interfaces extensively with the translation machinery to regulate cell differentiation. *Cell Cycle*, **7**, 3083–3090.
9. Fabian,M.R., Mathonnet,G., Sundermeier,T., Mathys,H., Zipprich,J.T., Svitkin,Y.V., Rivas,F., Jinek,M., Wohlschlegel,J., Doudna,J.A. *et al.* (2009) Mammalian miRNA RISC recruits CAF1 and PABP to affect PABP-dependent deadenylation. *Mol. Cell*, **35**, 868–880.
10. Zekri,L., Huntzinger,E., Heimstädt,S. and Izaurralde,E. (2009) The silencing domain of GW182 interacts with PABPC1 to promote translational repression and degradation of microRNA targets and is required for target release. *Mol. Cell. Biol.*, **29**, 6220–6231.
11. Walters,R.W., Bradrick,S.S. and Gromeier,M. (2010) Poly(A)-binding protein modulates mRNA susceptibility to cap-dependent miRNA-mediated repression. *RNA*, **16**, 239–250.
12. Wahle,E. (1991) A novel poly(A)-binding protein acts as a specificity factor in the second phase of messenger RNA polyadenylation. *Cell*, **66**, 759–768.
13. Bienroth,S., Keller,W. and Wahle,E. (1993) Assembly of a processive messenger RNA polyadenylation complex. *EMBO J.*, **12**, 585–594.
14. Beilharz,T.H. and Preiss,T. (2007) Widespread use of poly(A) tail length control to accentuate expression of the yeast transcriptome. *RNA*, **13**, 982–997.
15. Millevoi,S. and Vagner,S. (2009) Molecular mechanisms of eukaryotic pre-mRNA 3′ end processing regulation. *Nucleic Acids Res.*, **38**, 2757–2774.
16. Parker,R. and Song,H. (2004) The enzymes and control of eukaryotic mRNA turnover. *Nat. Struct. Mol. Biol.*, **11**, 121–127.
17. Kuhn,U., Gundel,M., Knoth,A., Kerwitz,Y., Rudel,S. and Wahle,E. (2009) Poly(A) tail length is controlled by the nuclear poly(A)-binding protein regulating the interaction between poly(A) polymerase and the cleavage and polyadenylation specificity factor. *J. Biol. Chem.*, **284**, 22803–22814.
18. Wahle,E. (1995) Poly(A) tail length control is caused by termination of processive synthesis. *J. Biol. Chem.*, **270**, 2800–2808.
19. Apponi,L.H., Leung,S.W., Williams,K.R., Valentini,S.R., Corbett,A.H. and Pavlath,G.K. (2010) Loss of nuclear

poly(A)-binding protein 1 causes defects in myogenesis and mRNA biogenesis. *Hum. Mol. Genet.*, **19**, 1058–1065.
20. Benoit,B., Mitou,G., Chartier,A., Temme,C., Zaessinger,S., Wahle,E., Busseau,I. and Simonelig,M. (2005) An essential cytoplasmic function for the nuclear poly(A) binding protein, PABP2, in poly(A) tail length control and early development in Drosophila. *Dev. Cell*, **9**, 511–522.
21. Perreault,A., Lemieux,C. and Bachand,F. (2007) Regulation of the nuclear poly(A)-binding protein by arginine methylation in fission yeast. *J. Biol. Chem.*, **282**, 7552–7562.
22. Lemay,J.F., D'Amours,A., Lemieux,C., Lackner,D.H., St-Sauveur,V.G., Bahler,J. and Bachand,F. (2010) The nuclear poly(A)-binding protein interacts with the exosome to promote synthesis of noncoding small nucleolar RNAs. *Mol. Cell*, **37**, 34–45.
23. Lemay,J.F., Lemieux,C., St-Andre,O. and Bachand,F. (2010) Crossing the borders: Poly(A)-binding proteins working on both sides of the fence. *RNA Biol.*, **7**, 291–295.
24. Brais,B., Bouchard,J.P., Xie,Y.G., Rochefort,D.L., Chretien,N., Tome,F.M., Lafreniere,R.G., Rommens,J.M., Uyama,E., Nohira,O. *et al.* (1998) Short GCG expansions in the PABP2 gene cause oculopharyngeal muscular dystrophy. *Nat. Genet.*, **18**, 164–167.
25. Brenner,S. (1974) The genetics of Caenorhabditis elegans. *Genetics*, **77**, 71–94.
26. Mohler,W.A., Simske,J.S., Williams-Masson,E.M., Hardin,J.D. and White,J.G. (1998) Dynamics and ultrastructure of developmental cell fusions in the Caenorhabditis elegans hypodermis. *Curr. Biol.*, **8**, 1087–1090.
27. Großhans,H., Johnson,T., Reinert,K.L., Gerstein,M. and Slack,F.J. (2005) The temporal patterning microRNA let-7 regulates several transcription factors at the larval to adult transition in C. elegans. *Dev. Cell*, **8**, 321–330.
28. Kamath,R.S., Fraser,A.G., Dong,Y., Poulin,G., Durbin,R., Gotta,M., Kanapin,A., Le Bot,N., Moreno,S., Sohrmann,M. *et al.* (2003) Systematic functional analysis of the Caenorhabditis elegans genome using RNAi. *Nature*, **421**, 231–237.
29. Rual,J.F., Ceron,J., Koreth,J., Hao,T., Nicot,A.S., Hirozane-Kishikawa,T., Vandenhaute,J., Orkin,S.H., Hill,D.E., van den Heuvel,S. *et al.* (2004) Toward improving Caenorhabditis elegans phenome mapping with an ORFeome-based RNAi library. *Genome Res.*, **14**, 2162–2168.
30. Ding,X.C. and Großhans,H. (2009) Repression of C. elegans microRNA targets at the initiation level of translation requires GW182 proteins. *EMBO J.*, **28**, 213–222.
31. Livak,K.J. and Schmittgen,T.D. (2001) Analysis of relative gene expression data using real-time quantitative PCR and the 2(-Delta Delta C(T)) Method. *Methods*, **25**, 402–408.
32. Pall,G.S. and Hamilton,A.J. (2008) Improved northern blot method for enhanced detection of small RNA. *Nat. Protoc.*, **3**, 1077–1084.
33. Schagger,H. (2006) Tricine-SDS-PAGE. *Nat. Protoc.*, **1**, 16–22.
34. Abramoff,M., Magelhaes,P. and Ram,S. (2004) Image Processing with ImageJ. *Biophotonics Int.*, **11**, 36–42.
35. Vella,M.C., Choi,E.Y., Lin,S.Y., Reinert,K. and Slack,F.J. (2004) The C. elegans microRNA let-7 binds to imperfect let-7 complementary sites from the lin-41 3′UTR. *Genes Dev.*, **18**, 132–137.
36. Bettinger,J.C., Lee,K. and Rougvie,A.E. (1996) Stage-specific accumulation of the terminal differentiation factor LIN-29 during Caenorhabditis elegans development. *Development*, **122**, 2517–2527.
37. Rougvie,A.E. and Ambros,V. (1995) The heterochronic gene lin-29 encodes a zinc finger protein that controls a terminal differentiation event in Caenorhabditis elegans. *Development*, **121**, 2491–2500.
38. Abbott,A.L., Alvarez-Saavedra,E., Miska,E.A., Lau,N.C., Bartel,D.P., Horvitz,H.R. and Ambros,V. (2005) The let-7 MicroRNA family members mir-48, mir-84, and mir-241 function together to regulate developmental timing in Caenorhabditis elegans. *Dev. Cell*, **9**, 403–414.
39. Liu,Z., Kirch,S. and Ambros,V. (1995) The Caenorhabditis elegans heterochronic gene pathway controls stage-specific transcription of collagen genes. *Development*, **121**, 2471–2478.
40. Rehmsmeier,M., Steffen,P., Hochsmann,M. and Giegerich,R. (2004) Fast and effective prediction of microRNA/target duplexes. *RNA*, **10**, 1507–1517.
41. Bagga,S., Bracht,J., Hunter,S., Massirer,K., Holtz,J., Eachus,R. and Pasquinelli,A.E. (2005) Regulation by let-7 and lin-4 miRNAs results in target mRNA degradation. *Cell*, **122**, 553–563.
42. Abrahante,J.E., Daul,A.L., Li,M., Volk,M.L., Tennessen,J.M., Miller,E.A. and Rougvie,A.E. (2003) The Caenorhabditis elegans hunchback-like gene lin-57/hbl-1 controls developmental time and is regulated by microRNAs. *Dev. Cell*, **4**, 625–637.
43. Lin,S.Y., Johnson,S.M., Abraham,M., Vella,M.C., Pasquinelli,A., Gamberi,C., Gottlieb,E. and Slack,F.J. (2003) The C elegans hunchback homolog, hbl-1, controls temporal patterning and is a probable microRNA target. *Dev. Cell*, **4**, 639–650.
44. Moss,E.G., Lee,R.C. and Ambros,V. (1997) The cold shock domain protein LIN-28 controls developmental timing in C. elegans and is regulated by the lin-4 RNA. *Cell*, **88**, 637–646.
45. Wightman,B., Ha,I. and Ruvkun,G. (1993) Posttranscriptional regulation of the heterochronic gene lin-14 by lin-4 mediates temporal pattern formation in C. elegans. *Cell*, **75**, 855–862.
46. Bracht,J., Hunter,S., Eachus,R., Weeks,P. and Pasquinelli,A.E. (2004) Trans-splicing and polyadenylation of let-7 microRNA primary transcripts. *RNA*, **10**, 1586–1594.

Supplementary material and methods

qPCR primer sequences

qPCR primer pairs were designed based on (1). For all primer pairs, amplification efficiencies were determined to be equal or superior to 1.8.

Primer	5' to 3' sequence
qPCR *act-1* F1	GTTGCCCAGAGGCTATGTTC
qPCR *act-1* R1	CAAGAGCGGTGATTTCCTTC
qPCR *daf-12* F2	GATCCTCCGATGAACGAAAA
qPCR *daf-12* R2	CTCTTCGGCTTCACCAGAAC
qPCR *lin-41* F1	GGATTGTTCGACACCAACG
qPCR *lin-41* R1	ACCATGATGTCAAACTGCTGTC
qPCR *tbb-2* F1	CAAATTCTGGGAGGTCATCTC
qPCR *tbb-2* R1	CATACTTTCCGTTGTTGGCT
qPCR *hbl-1* F1	ACTGCACATATGCCACCAAA
qPCR *hbl-1* R1	TGATGTAACCGGCTCAACTG
qPCR *lin-14* F2	GGATTCAATGCGACAGGATT
qPCR *lin-14* R2	CGATGCTGGTTTCAATGATG
qPCR *lin-28* F1	ATTCAAGAGCGATCGAATGG
qPCR *lin-28* R1	CACACTTTTGCATCGGTTTTT
qPCR *pabp-2* F1	GAAGGAATGCAAAACGCACT
qPCR *pabp-2* R1	GACCTCTTGGACGAAATCCA
qPCR *pabp-2* F2	CCGCCCATTATTCAAAAACT
qPCR *pabp-2* R2	CGATCGGAAAAACGAGAGAC

Antisense DNA oligonucleotides for northern blotting

Oligo probe	5' to 3' sequence
let-7(n2853)	AACTATACAACCTACTATCTCA
pre-let-7	CACCGGTGGTAATATTCCAAACTATACAAC
tRNA^{Gly}	GCTTGGAAGGCATCCATGCTGACCATT

Supplementary References

1. Andreas Untergasser, Harm Nijveen, Xiangyu Rao, Ton Bisseling, René Geurts, and Jack A.M. Leunissen: Primer3Plus, an enhanced web interface to Primer3 Nucleic Acids Research 2007 35: W71-W74; doi:10.1093/nar/gkm306

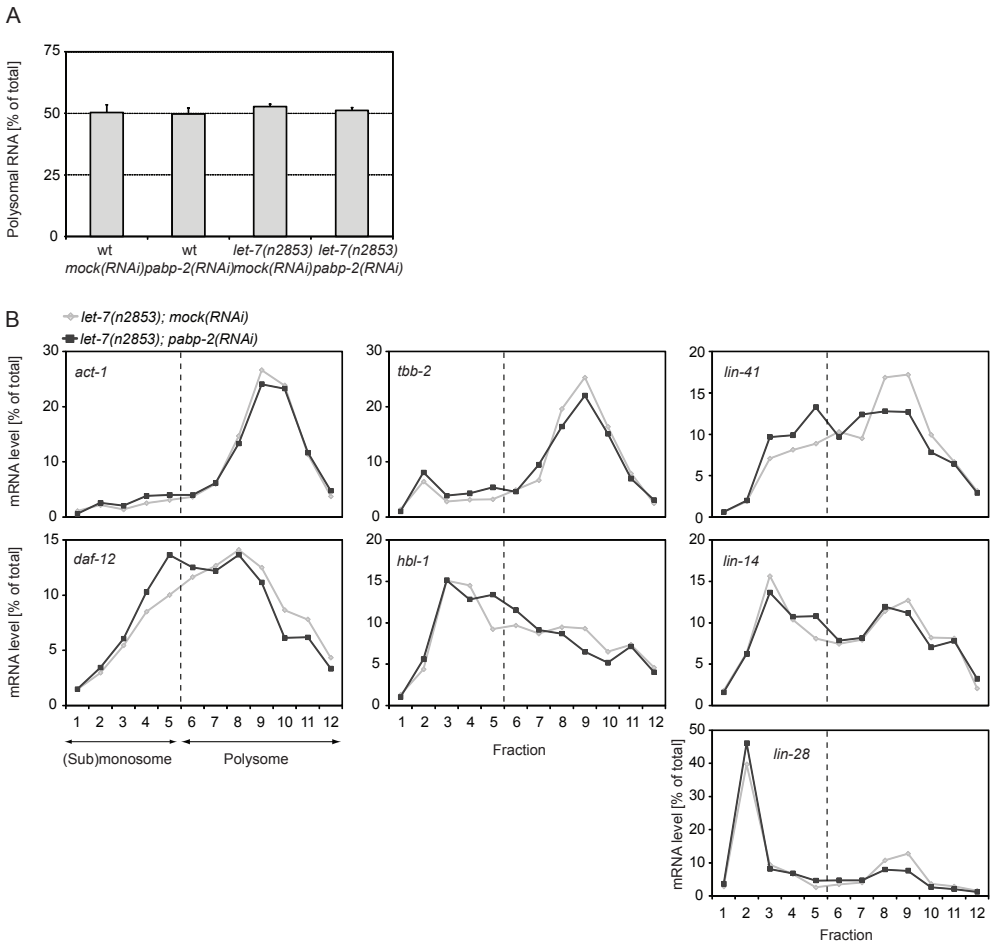

Supplementary Figure S1

(A) Polysomal RNA recovery from wild-type and *let-7(n2853)* animals exposed to either *pabp-2* or *mock(RNAi)*. Error bars represent s.e.m. (B) Distribution of mRNAs across polysome profiles from synchronized *let-7(n2853)* mutants exposed to either *pabp-2* or *mock(RNAi)*.

3.2 Additional Results

pabp-2 is predominantly expressed in intestine and neural tissues in L4 larvae and young adults

The results presented in the published manuscript above (Figure 6) show that PABP-2 protein is over-expressed in late L4-stage *let-7(n2853)* animals and that this over-expression correlates with an increased *pabp-2* mRNA level at the same developmental time-points. A time-course following PABP-2 protein levels throughout larval development is further provided in Figure 3.1, showing that PABP-2 levels sharply decline during late developmental stages in wild-type animals. To address the possibility that loss of *let-7* activity affects PABP-2 levels through increased transcription, we analyzed the expression pattern of a GFP reporter driven from the 3 kb long genomic sequence found directly upstream of the *pabp-2* open reading frame (ORF). The *pabp-2::gfp* transcriptional fusion was expressed from an extrachromosomal array in both wild-type and *let-7(n2853)* animals. While the *pabp-2* promoter was constitutively active in the embryo, GFP expression during larval stages and in young adults appeared to be largely restricted to the intestine and neural tissues (Figure 3.2). Older adults completely lacked a detectable GFP signal (not shown). At the late L4 stage, *pabp-2* promoter activity was observed in the intestine and neural tissues including the ventral cord, tissues in which *let-7* activity had previously been confirmed by regulation of *let-7* target reporter genes (Abrahante et al., 2003; Grosshans et al., 2005; Lin et al., 2003) and *let-7* transcriptional reporter genes (Johnson et al., 2003). Thus, an indirect regulation of PABP-2 by *let-7*, for instance by a transcription factor, potentially occurs in the tissues with the highest promoter activity in L4. However, we could not detect any difference in *pabp-2* promoter driven GFP expression in respect of tissue specificity or signal intensity in wild-type compared to *let-7(n2853)* animals.

PABP-2 may associate with polysomal mRNAs

Unlike the type I poly(A)-binding protein PAB-1, knock-down of PABP-2 did not appear to have a general effect on translation (published manuscript, Figure 9). However, an association of Pab2 with polysomes was previously reported in *S. pombe*

(Lemieux and Bachand, 2009). We thus addressed the question whether PABP-2 associates with translationally active mRNAs in *C. elegans*. To this end, we analyzed the fractions of our polysome gradients for the presence of PAB-1 and PABP-2 by western blotting. We observed that a considerable fraction of PABP-2 migrated into the high-polysomal fractions (Figure 3.3 A). Similar to PAB-1, PABP-2 is largely absent from the 60S submonsomal and 80S monosomal fractions, whereas the high polysomal fractions were enriched for both PAB-1 and PABP-2. The migration into the denser fractions of the sucrose gradient was RNA dependent since micrococcal nuclease treatment restricted PABP-2 as well as PAB-1 recovery to the lighter fractions (Figure 3.3 B). Addition of 1 mM EDTA to dissolve ribosomes likewise prevented migration of poly(A)-binding proteins into the denser fractions (Figure 3.3C). We thus conclude that PABP-2 can efficiently bind to poly(A) tails of mRNAs.

Independently transcribed snoRNAs accumulate in *let-7(n2853); pabp-2(RNAi)* double, but not in *pabp-2(RNAi)* single mutant animals

Small nucleolar RNAs (snoRNAs) are a major class of nuclear RNAs that guide 2'-O-ribose methylation and pseudouridylation of ribosomal RNAs (rRNAs), small nuclear RNAs (snRNAs) and other RNA targets (Kiss et al., 2006). Recently, the type II poly(A)-binding protein was found to be involved in the synthesis of snoRNAs in *Schizosaccharomyces pombe*, most likely by recruiting the exosome component Rrp6 to polyadenylated snoRNA precursors for final processing (Lemay et al., 2010). Independently transcribed H/ACA and C/D box snoRNAs accumulated in *pab2Δ* cells, whereas the levels of many mature snoRNAs decreased. Accumulation of polyadenylated snoRNA precursors has also been shown in *D. melanogaster* (Nakamura et al., 2008), where, however, a possible role of *pabp2* was not addressed, and in *S. cerevisiae* (Grzechnik and Kufel, 2008), where no readily identifiable orthologue of PAPB2 exists in the first place.

The *C. elegans* genome codes for an estimated ~150 different snoRNAs (Wang and Ruvinsky, 2010). We investigated whether *pabp-2(RNAi)* impaired pre-snoRNA processing by assessing the levels and size distribution of independently transcribed

H/ACA box and C/D box snoRNAs by northern blotting. In *pabp-2(RNAi)* animals, the H/ACA box snoRNAs K02C4.8, W01C9.6 and the C/D box snoRNAs H09I01.2, C16D9.10 were detected as one single band, arguing against a substantial accumulation of extensively polyadenylated snoRNA precursors (Figure 3.4). Furthermore, in three biological replicates of the experiment, there was no deficiency in snoRNA processing relative to wild-type animals. The levels of those snoRNAs were also comparable in *let-7(n2853)* single mutant animals. Surprisingly, however, we observed a moderate but reproducible increase in the expression levels of three out of four snoRNAs in *let-7(n2853); pabp-2(RNAi)* relative to the *let-7(n2853)* single mutant animals (Figure 3.4). Thus, although the *let-7* mutation itself does not affect snoRNA levels, it does so synergistically with depletion of PABP-2. At this point, it is not clear whether this upregulation contributes to the rescue of *let-7(n2853)* by depletion of PABP-2.

3.3 Additional discussion

The finding that *pabp-2* is mainly expressed in tissues with known *let-7* activity in L4 and young adult animals is in agreement with a proposed indirect (or direct) regulation of PABP-2 levels by *let-7*. However, we did not observe any difference in the expression of a GFP reporter under the control of the *pabp-2* promoter. It is not clear whether the GFP expression from a multi-copy extrachromsomal array predominates transcriptional control or whether the supposed *pabp-2* promoter, a 3 kb segment of upstream genomic sequence, fails to capture all regulatory elements. Alternatively, regulation of *pabp-2* expression is predominantly post-transcriptional. To discriminate between these scenarios, it would be essential to establish single copy integrated reporter genes to test 5' or 3' regulatory elements. Ideally, a PABP-2/GFP translational fusion would serve as a reporter and/or rescue construct, however, given the equal size of GFP and PABP-2, the rescue approach is likely to fail. A further short-fall of our GFP expression study is that we failed to detect GFP expression in seam-cells, the cell lineage affected by the observed heterochronic phenotype. Possibly, the forced nuclear localization of e.g. a GFP/H2B reporter may overcome this limitation as it would increase the local concentration of the reporter gene.

The observation of polysome-associated PABP-2 is in contrast to the prevalent view that type II poly(A)-binding proteins are not associated with general translation. However, from the data presented here it is not clear, whether PABP-2 resides on poly(A)-tails of cytoplasmic mRNAs *in vivo* or whether nuclear PABP-2 displaced PAB-1 in the whole animal extracts. However, in a previous study conducted in *S. pombe*, cells were treated with formaldehyde prior to lysis and polysome profiling (Lemieux and Bachand, 2009), showing that Pab2 was present on polysomal mRNAs before the rupture of the nuclear membrane. Although a large fraction of cellular PABP-2 may reside on polysomal mRNAs in *C. elegans*, our finding that depletion of >80% of PABP-2 caused little if any effect on global translation argues against an essential function of polysome associated PABP-2 in translation. Although we cannot rule out the possibility that PABP-2 regulates translation of a subset of massages, the physiological role of polysome associated PABP-2 needs yet to be explored.

Interestingly, we found that PAPB-2 depletion caused elevated levels of some snoRNAs in *let-7(n2853)* mutant but not wild-type animals, pointing to a joint function in keeping snoRNA levels low. At this point, we do not know whether snoRNA upregulation contributes to suppression of *let-7(n2853)* lethality by PABP-2 depletion, but we note that in *Drosophila* snoRNAs have been implicated in the control of the proliferation vs. differentiation decision: deletion of *wicked*, a homologue of the U3 snoRNP component UTP18, induced premature differentiation of germline stem cells and reduced proliferation and growth of neural stem cells (Fichelson et al., 2009). Moreover, we have previously identified the snoRNP components Nop58/Nop5p (*C.e.* W01B11.3), Nop14p (*C. e.* Y48G1A.4) and Nop56p (*C.e.* K07C5.4) as strong suppressors of *let-7(n2853)* lethality (Ding et al., 2008). Furthermore, in a genome-wide reverse genetic screen for suppression of *let-7(n2853)* lethality, genes that hosted an intronic snoRNA were overrepresented in the list of suppressor genes ($p < 10^{-7}$, hypergeometric test; my interpretation of M. Ecsedi, M. Rausch, unpublished data). Thus, it will be interesting to determine in future work if snoRNPs generally contribute to temporal cell fate regulation in *C. elegans*.

3.4 Additional Figures

Figure 3.1

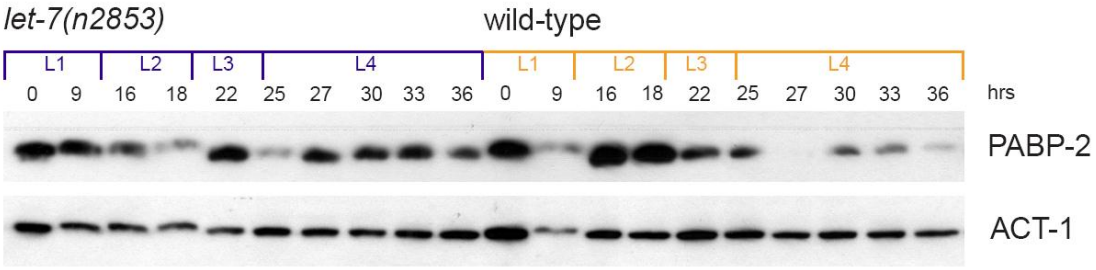

Figure 3.1 Time course of PABP-2 protein levels during postembryonic development. *let-7(n2853)* and wild-type animals were grown at 25° C and samples were collected after the indicated hours of postembryonic development. In *let-7(n2853)* animals, PABP-2 levels are visibly increased in late larval development. Under the investigated conditions, *let-7(n2853)* animals die by bursting at the vulva starting 36-38 hours of larval development, thus no adult animals could be compared. The larval stages are roughly indicated.

Figure 3.2

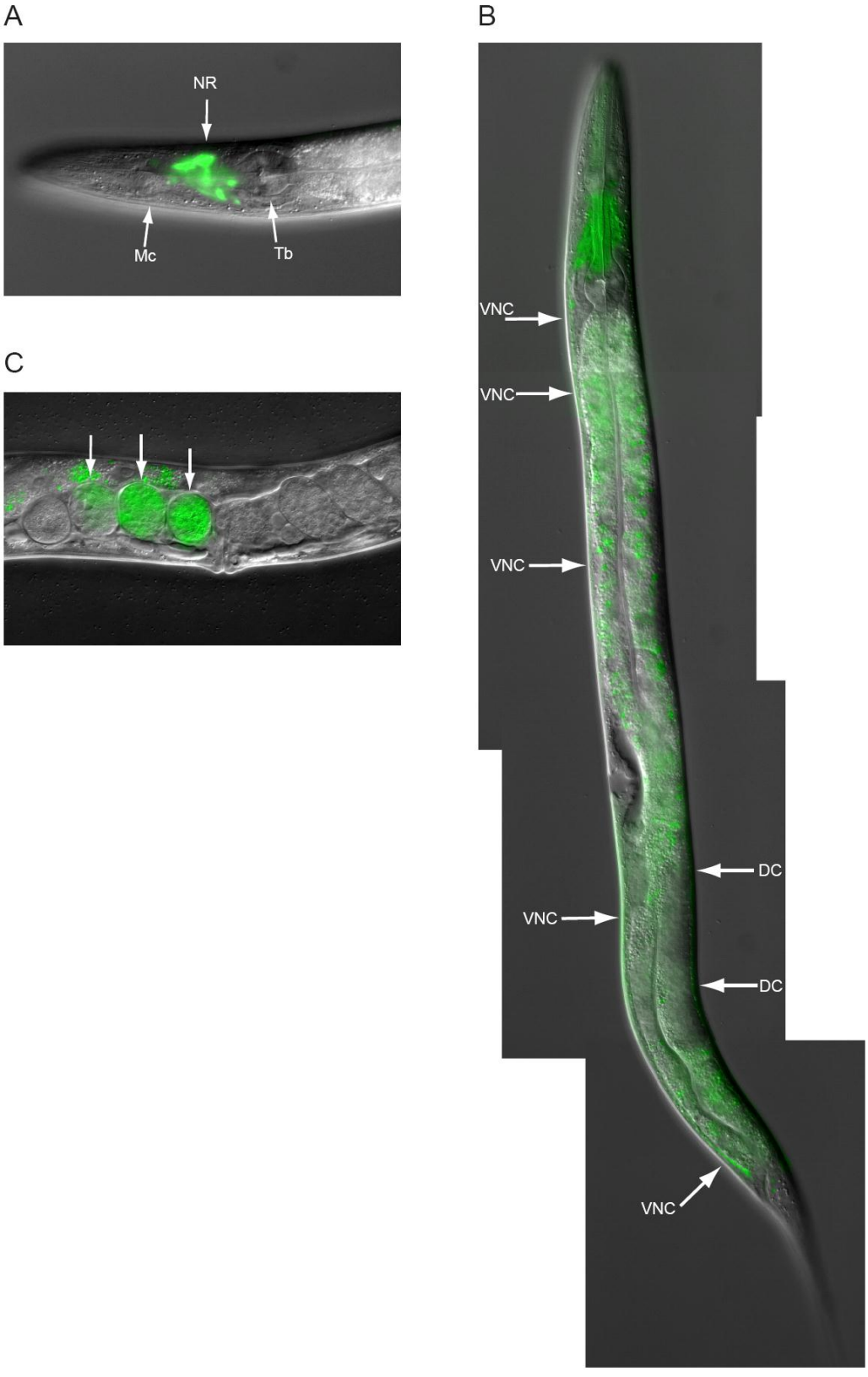

Figure 3.2 *papbp-2* promoter activity is predominantly observed in intestine and neural tissues in L4 larvae and young adults. A transcriptional *pabp-2::gfp* fusion was expressed from an extrachromosomal array. All animals shown are wild-type. (A) Head of a young adult animal. GFP accumulates in the neurons of the nerve ring (NR) located between the metacarpus (Mc) and the terminal bulb (Tb) of the pharynx. (B) Lateral view of a late L4 larva. The arrowheads indicate the ventral nerve cord (VNC) and the dorsal cord (DC). (C) The *pabp-2::gfp* array is transmitted at a low frequency, so that less than half of the animals inherit it. In animals carrying the array, high expression of *pabp-2::gfp* was observed throughout embryonic development. Animals expressing the *pabp-2::gfp* array often displayed a miss-shaped gonad or delayed egg-laying reminiscent of *pabp-2(RNAi)* (see posterior gonad of (C)). Merged DIC and epifluorescent images, pseudo-colored.

Figure 3.3

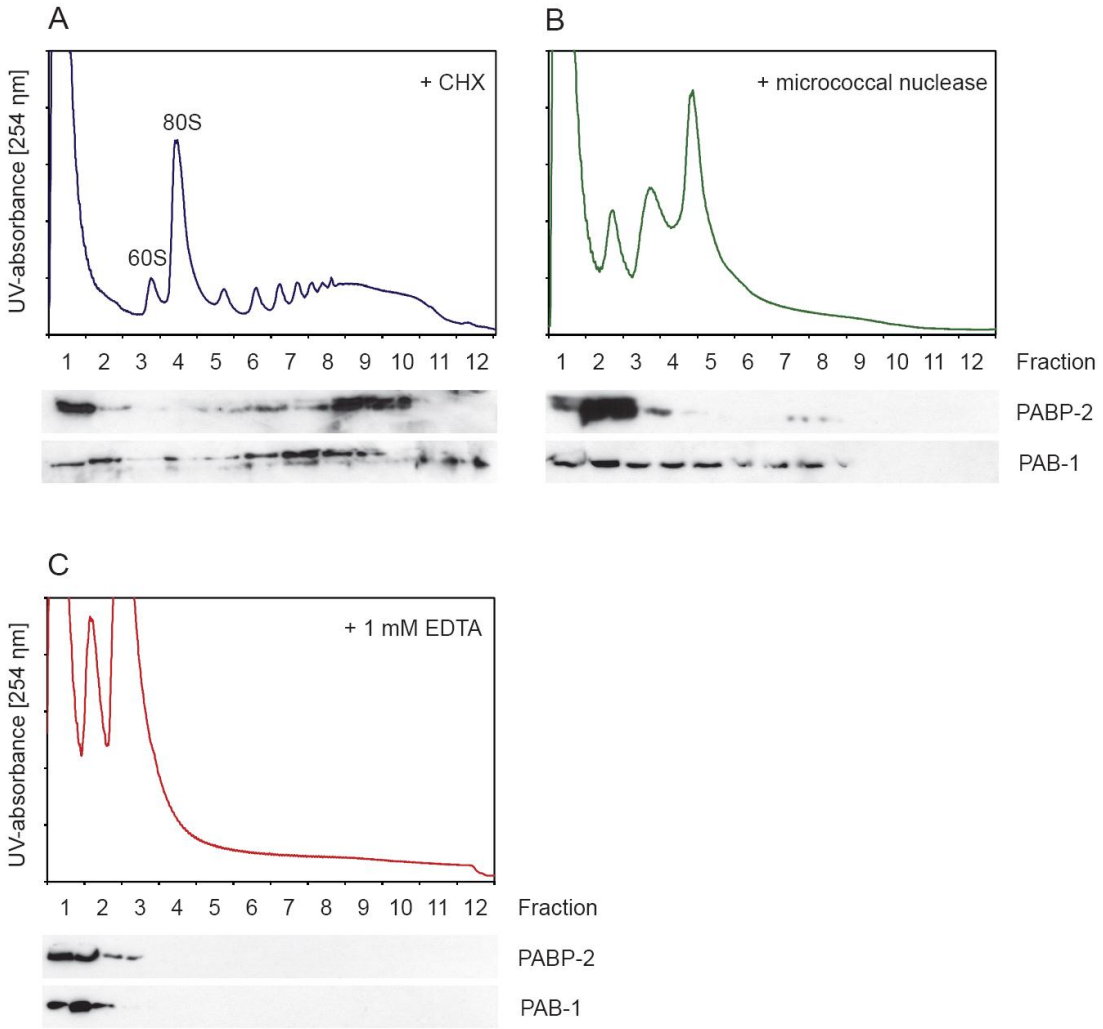

Figure 3.3 PABP-2 migrates with the high polysomal fractions in sucrose density centrifugation. Gradients of whole animal lysates treated with cycloheximide (CHX) to preserve polysomes (A), micrococcal nuclease to digest mRNAs (B), and 1 mM EDTA to disrupt polysomes (C) are shown. Similar to the type I poly(A)-binding protein PAB-1, PABP-2 is predominantly found in the high polysomal fractions in an RNA dependent manner.

Figure 3.4

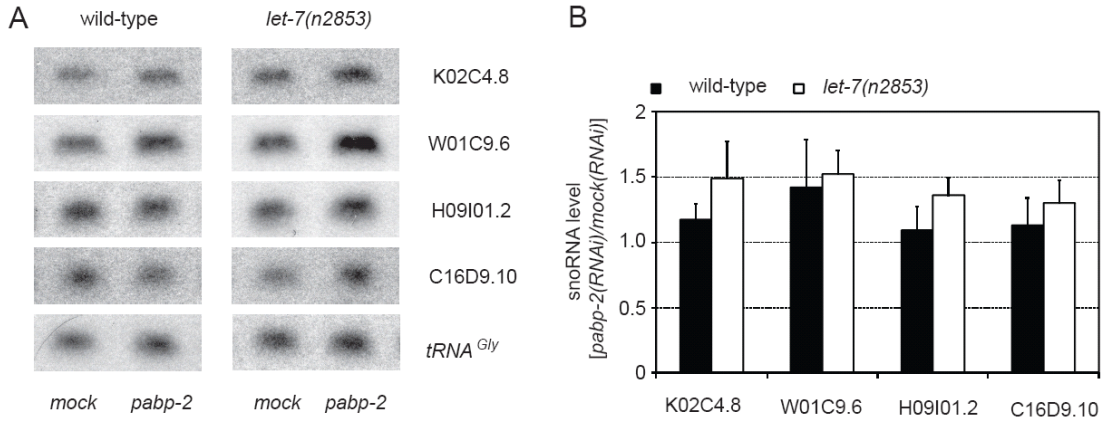

Figure 3.4 Independently transcribed snoRNAs accumulate in *let-7(n2853)*; *pabp-2(RNAi)* animals. (A) Northern blot of total RNA from synchronized late L4 wild-type and *let-7(n2853)* animals exposed to the indicated RNAi. Oligonucleotides complementary to the H/ACA class snoRNAs K02C4.8, W01C9.6 and the C/D class snoRNAs H09I01.2 and C16D9.10 were used to detect snoRNA. tRNAGly(TCC) served as loading control. (B) Quantifications of mature snoRNA levels of three independent experiments. Error bars represent s.e.m.

3.5 Additional methods:

Nomarski and fluorescent imaging of promoter *pabp-2::gfp* expression

BC17993 *dpy-5(e907) I; sEx17993[rCesC17E4.5::GFP;pCeh361]* expressing GFP from the *pabp-2* promoter was provided by David Baillie. BC17993 was crossed with MT7626 *let-7(n2853)* to study GFP expression in *let-7(n2853)* background. For unknown reasons, BC17993 (like the original BC10478, D. Baillie, personal communication) cannot recover from frozen stocks.

Detection of PABP-2 and PAB-1 in polysome gradients.

Polysome preparation and western blotting were performed as described in (Hurschler et al., 2011). Micrococcal nuclease (NEB) was added to a final concentration of 4000 gel units/ml to the standard lysis buffer used in our polysome profiling protocol. After lysis of the worms, the sample was incubated 15 minutes at room temperature. PAB-1 was detected using monoclonal mouse anti PAB-1 24L1 (gift of Rafal Ciosk) at a concentration of 1:500 and horseradish peroxidase-conjugated anti-mouse (NA931V, GE Healthcare) was used for signal detection by ECL.

Northern blotting

To detect snoRNAs, total RNA was separated on an 8% TBE Urea PAGE gel, transferred to Zeta probe gt membrane (BioRad) and crosslinked with one UV auto-crosslinking cycle (120 mJ) by using a UV Stratalinker 1800 (Stratagene). Antisense DNA oligonucleotides were 5'-labelled using T4 polynucleotide kinase (PNK) and [y-32P]ATP. Radioactive signals were detected using a Storage Phosphor Screen and a Typhoon 9400 scanner and quantified with Imagequant TL software (all GE Healthcare).

Oligo probes:	5’ to 3’ sequence
C16D9.10 (sn2841)	GTCATAGTAGGTAAGAGTTGATCGTCACCGC
H09I01.2 (sn2429)	CAGTCACTCATTGAGATTCCTACACAGAAGG
K02C4.8	CGGTATTGCGTGGTTAATGACAGC
W01C9.6	GCTCATATTGCACTACACTTTAGCCACA

4. Mechanism of miRNA-mediated gene silencing in *C. elegans*

4.1 Introduction

We have previously reported that *lin-4* and *let-7* regulate their endogenous target genes by translational repression and target degradation in *C. elegans*. Both, translational repression and target gene degradation required the presence of AIN-1 and AIN-2, the *C. elegans* orthologs of the GW182 protein family (Ding and Grosshans, 2009). Although translational repression frequently coincided with target gene degradation, there was no strong correlation between these two mechanisms. For instance, the *lsy-6* target *cog-1* was found to be translationally repressed, however, its transcript levels remained unchanged (Ding and Grosshans, 2009).

Based on our published data, we are confident that *C. elegans* miRNAs repress their cognate target genes by repression of translation initiation and target degradation *in vivo*. However, the fundamental question remains as to whether translational repression and mRNA degradation are two sequential events, where translational repression is prerequisite for mRNA degradation or whether translational repression and mRNA degradation are two parallel, independently occurring mechanisms. Provided that translational repression and mRNA degradation are indeed parallel mechanisms, the repressive mechanism must be either determined by the repressive complex or by additional cues on the miRNA target itself. We reasoned that if translational repression and mRNA degradation were parallel events, it should be possible to uncouple them. As an entry point to our study, we decided to investigate a possible role of miRISC core components in determining translational repression or mRNA degradation.

4.2 Results

AIN-1 and AIN-2 single mutant analysis suggests different requirements of GW182 proteins for translational repression and mRNA degradation

Proteins of the Argonaute family are the core components of miRISC and recruit both the miRNA and GW182 proteins. *C. elegans* encodes 27 Argonaute genes, however, only ALG-1 and ALG-2 are known to function in the miRNA pathway (Peters and Meister, 2007). We thus analyzed the requirement of ALG-1 and ALG-2 in translational repression and mRNA degradation. Analysis of polysome profiles and total mRNA levels of miRNA target genes showed that *alg-1(gk214)* or *alg-1(RNAi)* abolished translational repression and target degradation to a similar extent as observed in *ain-1(ku322); ain-2(RNAi)* animals, whereas *alg-2(ok304)* did not lead to a detectable effect (X.C. Ding, personal communication). These observations are in line with the described phenotypes of these two mutations: the *alg-1(gk214)* allele leads to phenotypes associated with severe loss in miRNA function including alae defects, retarded developmental timing and bursting at the vulva. *alg-2(ok304)* has no phenotype on its own, however, it was found to be synthetic lethal with *alg-1(gk214)* (Grishok et al., 2001). Thus, *alg-1* plays the major role in miRNA function in *C. elegans*. Since both translational repression and mRNA degradation depend on the expression of ALG-1, the identity of the Argonaute protein in miRISC is unlikely to determine the repressive mechanism in *C. elegans*. ALG-1 and ALG-2 equally associate with both AIN-1 and AIN-2 (Zhang et al., 2007), the most down-stream essential effector genes for *C. elegans* miRNA function known to date. We therefore decided to analyze the requirement of the GW182 proteins AIN-1 and AIN-2 for translational repression and target mRNA degradation.

To this end, we analyzed mRNA levels and polysome association of miRNA target genes in *ain-1(ku322)* and *ain-2(tm1863)* single mutant animals (Figure 4.1, X.C. Ding, unpublished). *ain-1(ku322)* encodes a premature stop codon (Zhang et al., 2007), however, trace levels of full length AIN-1 could still be detected (Zhang et al., 2007) (also see Figure 4.6). *ain-2(tm1863)* contains a 689 bp deletion, affecting exons 3 and 4 (Figure 4.2). *ain-2(tm1863); ain-1(ku322)* double mutant animals were

severely sick and could not be grown as synchronized cultures. Therefore, we approximated the double mutant situation by culturing *ain-1(ku322)* on *ain-2(RNAi)* plates.

In *ain-1(ku322)* single mutant animals, translational repression was relieved to a similar extent as in *ain-1(ku322)*; *ain-2(RNAi)* double mutant animals. In contrast, translational repression occurred to the same extent in *ain-2(tm1863)* as in wild-type animals (Figure 4.1 A). Thus, expression of AIN-1 was sufficient to mediate the full scale of translational repression observed in wild-type animals, whereas AIN-2 was apparently dispensible.

A different situation was found at the total mRNA level. In the *ain-1(ku322); ain-2(RNAi)* double mutant situation, we observed a 4- to 5-fold increase in the transcript levels of the *let-7* target genes *daf-12* and *lin-41*, respectively. Similarly, the *lin-4* target genes *lin-14* and *lin-28* increased by 2- to 3-fold, respectively (Figure 4.1B). Although *ain-1(ku322)* virtually abolished translational repression, it could not prevent degradation of *daf-12* and could only partially prevent degradation of *lin-41* and *lin-14*. Thus, at least for some target genes, regulation at the mRNA level still occurs even when translational repression is lost. Whereas loss of AIN-2 in presence of AIN-1 did not lead to a detectable effect, AIN-2 was capable to mediate substantial degradation of *daf-12, lin-41* and *lin-14* in the absence of AIN-1.

Additional expression of AIN-2 rescues *ain-1(ku322)* specific developmental defects

Thus far, our data supported a working model in which translational repression is specifically mediated by AIN-1, whereas both AIN-1 and AIN-2 can mediate mRNA degradation. To study the degree of redundancy of AIN-1 and AIN-2 more directly, we aimed to rescue *ain-1(ku322)* specific developmental defects by additional expression of AIN-2 from its endogenous promoter. *ain-1(ku322)* animals display several development defects, including retarded seam cell fusion and breaks in the alae structure (Ding et al., 2005), whereas no such phenotypes are observed in *ain-2(tm1863)* (Zhang et al., 2007). We thus established *ain-1(ku322)* rescue lines by injecting fosmid DNA containing the full coding sequence of either *ain-1* or *ain-2*

together with a *Pmyo-2::mCherry* coinjection marker into the gonads of *ain-1(ku322)* animals. For simplicity, we will refer to the strains as *IK23, IK24 ain-1(ku322); Ex[ain-1]* and *IK25, IK26 ain-1(ku322); Ex[ain-2]*. A concise description of the genotypes is provided in the method section.

Progeny testing of these animals confirmed transmission of the established extrachromosmal arrays at a frequency of roughly 50 %, as judged by the expression of pharyngeal mCherry. Both, *IK23* and *IK24 ain-1(ku322); Ex[ain-1]* lines rescued *ain-1(ku322)* specific developmental defects such as vulval bursting or alae defects, proving the principle that *ain-1(ku322)* can be rescued by the expression of AIN-1 from an extrachromosomal array (not shown).

We next analyzed *IK25* and *IK26 ain-1(ku322); Ex[ain-2]* animals. More than 30% of the animals of the parent strain, i.e. animals that lost expression of pharyngeal mCherry, displayed defects in the alae structure. Additional expression of AIN-2 in mCherry positive *IK25* or *IK26* rescued the *ain-1(ku322)* phenotype so that less than 2% of tested animals showed defects in the alae structure (Figure 4.3). To ensure that rescue was indeed due to the expression of AIN-2 and not to an unrelated sequence present on the fosmid DNA, the same animals were grown on *ain-2(RNAi)*. Both *ain-1(ku322)* parent strain and *IK25* and *IK26 ain-1(ku322); Ex[ain-2]* rescue strains displayed fully penetrant alae defects when grown on *ain-2(RNAi)* (Figure 4.3), confirming that rescue depended on AIN-2. Thus, additional expression of AIN-2 can rescue *ain-1(ku322)* specific cell differentiation defects. We conclude that AIN-1 and AIN-2 are, at least partially, redundant with regard to their developmental functions.

Overexpression of AIN-2 restores translational repression of miRNA target genes in *ain-1(ku322)* animals

The finding that additional expression of AIN-2 rescued *ain-1(ku322)* associated developmental defects raised the question on how this rescue was occurring at the level of miRNA target gene regulation. Conceivably, additional expression of AIN-2 either restored translational repression, or increased target mRNA degradation, or accomplished both. To solve this, we performed polysome profiling on pharyngeal mCherry positive *IK24 ain-1(ku322); Ex[ain-1]* and *IK25 ain-1(ku322); Ex[ain-1]*

animals. Compared to wild-type animals, translational repression of the miRNA target genes *daf-12*, *lin-41*, *hbl-1*, *lin-14*, and *lin-28* was relieved in *ain-1(ku322)* animals (Figure 4.4 A). Contrary to *ain-1(ku322)* animals, *ain-1(ku322); Ex[ain-1]* and *ain-1(ku322); Ex[ain-2]* showed wild-type translational repression of miRNA target genes (Figure 4.4 A). Thus, translational repression is not unique to AIN-1. Although additional expression of AIN-1 or AIN-2 restored translational repression in this experiment, it did not fully restore the low transcript levels found in wild-type animals (Figure 4.4B).

Endogenous levels of both AIN-1 and AIN-2 are required for substantial miRNA target regulation at the protein level

Thus far, our analysis was restricted to the analysis of polysome profiles and total mRNA levels. To study the contribution of AIN-1 and AIN-2 in reducing protein production, we established wild-type and *ain-1(ku322)* lines expressing a single-copy integrated *Pwrt-2::gfp(pest)/h2b* reporter gene under the control of the *unc-54*, *lin-41*, and *daf-12* 3' UTRs (M. Ecsedi, unpublished). The *wrt-2* promoter was chosen to drive reporter expression in seam-cells. We have previously shown *let-7* specific regulation of a *lin-41* 3' UTR reporter gene in seam cells to be mediated by translational repression and target degradation (Ding and Grosshans, 2009). The *wrt-2::gfp(pest)/h2b* reporter genes localized to the nuclei of seam cells and, even more distinct, to the nuclei of the hyp-7 syncytium. The *lin-41* and *daf-12* 3' UTR reporters were silenced in seam cell nuclei, and to a lesser extent, also in hyp-7 nuclei of L4 wild-type animals, consistent with repression by *let-7*. The *unc-54* 3' UTR reporter, included as a control, was refractory to miRNA mediated silencing. (Figure 4.5, 1st row).

In *ain-1(ku322); ain-2(RNAi)* animals, we observed a severe loss of miRNA function as evidenced by the increased number of seam cells (Figure 4.5, bottom row). There was no visible difference between GFP expression from *unc-54* or *lin-41* and *daf-12* 3' UTR reporter genes, which further confirmed an almost complete loss of miRNA function. In the case of *ain-1(ku322)* animals, the GFP signal from *lin-41* and *daf-12* 3' UTR reporter genes was clearly detectable in seam cells, albeit less intense than the signal from the *unc-54* 3' UTR control gene (Figure 4.5, 3rd row). In contrast,

depletion of AIN-2 by RNAi did not visibly increase GFP expression from the *lin-41* 3' UTR reporter and only showed a moderate effect on the expression of the *daf-12* 3' UTR reporter in seam cells.

To compare the read out of the reporter gene assay with the regulation of endogenous target genes, we analyzed the same reporter lines by western blotting. *ain-1(ku322)* single mutation had no or only a mild effect on endogenous LIN-41 or LIN-28 (Figure 4.6). Expression of LIN-41 was also similar in *ain-1(tm3681)*, a newly available *ain-1* deletion mutant. Endogenous LIN-41, LIN-28 and reporter GFP clearly accumulated in *ain-1(ku322); ain-2(RNAi)* animals and appeared unaffected in wild-type *ain-2(RNAi)* animals, which is in agreement with the previous analysis of polysome profiles, transcript levels and reporter gene assays (Figure 4.6). It is not clear whether the weak increase of protein levels in *ain-1* single mutants is a threshold effect of western-blotting, since wild-type levels of LIN-41 and LIN-28 are at the limit of detection in late L4 animals. Nevertheless, the data support a synergistic effect of a combined loss of AIN-1 and AIN-2 on the protein level.

4.3 Discussion

The work presented here shows that AIN-1 and AIN-2 are partially redundant with regard to their developmental function and their ability to act as *bona fide* GW182 proteins by mediating translational repression and cognate mRNA degradation. AIN-1 and AIN-2 are essential components of the miRNA effector complex in *C. elegans*. The phenotypes observed in *ain-2; ain-1* animals closely resemble those observed in *alg-1; alg-2* Argonaute deficient (Grishok et al., 2001) or *dcr-1* Dicer deficient animals (Grishok et al., 2001), except that both pre- and mature miRNA levels are not substantially affected (Zhang et al., 2007). Thus, AIN-1 and AIN-2 act downstream of miRNA biogenesis. Additionally, AIN-1 and AIN-2 were found to be associated with the miRNA-specific Argonaute proteins ALG-1 and ALG-2, a major fraction of annotated miRNAs, and a large number of candidate target mRNAs (Zhang et al., 2007). Consistent with a role as essential effector proteins in the miRNA pathway in *C. elegans*, we found that depletion of the GW182 proteins AIN-1 and AIN-2 severely impaired miRNA-mediated translational repression and target degradation (Ding and Grosshans, 2009). AIN-1 and AIN-2 were postulated to have a redundant function in the miRNA pathway (Zhang et al., 2007) and the expression pattern of transcriptional and translational fusions suggests that AIN-1 and AIN-2 are expressed in all somatic cells throughout development (Ding et al., 2005; Mounsey et al., 2002; Zhang et al., 2007), leading also to overlapping activities. However, given the relative low similarity of AIN-1 and AIN-2 at the protein level, it is not clear whether AIN-1 and AIN-2 have similar effector functions and/or recruit the same set of downstream effectors.

Analysis of polysome profiles and total mRNA level of *ain-1* and *ain-2* single mutant animals suggests that AIN-1 and AIN-2 are not completely redundant with respect to how they cause silencing of target genes. *ain-1(ku322)* prevents translational repression, but does only have a limited effect on target mRNA degradation. *ain-2(tm1863)* does not show a deficiency in miRNA function, suggesting that wild-type levels of AIN-1 can accomplish wild-type miRNA function. However, AIN-2 can substantially contribute to target mRNA degradation, as evidenced by the effect of *ain-2(RNAi)* on transcript levels in the *ain-1(ku322)* loss-of-function background.

The absence of an *ain-2(tm1863)* specific miRNA loss of function effect in our assays is not likely to be due to a residual *ain-2(tm1863)* activity. *ain-2(tm1863); ain-1(ku322)* animals show the same severe developmental phenotypes as *ain-1(ku322); ain-2(RNAi)* animals. Furthermore, *ain-2(tm1863); ain-2(RNAi)* animals show wild-type development, although western blotting confirms efficient depletion of AIN-2(tm1863) (not shown).

These data are consistent with a model in which AIN-1 mediates both translational repression and mRNA degradation, whereas AIN-2 primarily or exclusively engages in mRNA degradation. The single mutant analysis thus contrasts the initial speculation that AIN-2 complexes represent the "translationally repressed form of miRISC", since AIN-2 associated mRNAs have poly(A)-tails (Zhang et al., 2007). However, we find that AIN-2 is not intrinsically unable to mediate translational repression, since overexpression of AIN-2 from an extrachromosomal array rescues wild-type translational repression. This is not prerequisite for, but in line with the rescue of *ain-1(ku322)* specific developmental defects in *ain-1(ku322); Ex[ain-2]* animals. Our data thus proof the principle that AIN-1- and AIN-2-loaded miRISC can mediate translational repression as well as mRNA degradation. Nevertheless, we cannot rule out mechanistic differences in AIN-1 and AIN-2 mediated silencing.

Our current data may be explained by a scenario in which AIN-1 outnumbers AIN-2. Such a scenario may explain why only *ain-1(ku322)* shows a phenotype since mutation in AIN-2 would not critically affect the level of functional miRISC complexes. Alternatively, if AIN-1 and AIN-2 levels were similar, AIN-1 could out-compete AIN-2 in associating with AGO-1/2 or a limiting downstream factor, so that a large fraction of AIN-2 is idle in the presence of wild-type levels of AIN-1. These scenarios may explain the absence of a detectable phenotype in *ain-2(lf)*, the mild phenotype of *ain-1(ku322)* and the strong synergy observed in the combined loss-of-function. However, we did not yet establish the relative levels of AIN-1 and AIN-2.

In the long run, the relevant function of miRNA-mediated gene regulation is to prevent further accumulation of the proteins encoded by the target gene. We thus started to expand our studies to reporter gene assays and protein quantification by

western blotting. Unfortunately, our current data are not clear-cut. On one hand, detection of endogenous LIN-41 and LIN-28 hints for a synergistic effect of *ain-1(ku322); ain-2(RNAi)*. As exemplified by endogenous LIN-41, western blotting suggests that the combined loss of AIN-1 and AIN-2 is multiplying, rather than adding, the individual effects of *ain-1(ku322)* and *ain-2(RNAi)*. On the other hand, GFP expression from *daf-12* and *lin-41* 3' UTR reporter genes closely matches GFP expression from the *unc-54* 3' UTR control in *ain-1(ku322)*. Both assays will have to be optimized. The western blot shows hallmarks of a threshold effect which becomes most evident when GFP levels of the *lin-41* and *daf-12* 3' UTR reporters in Figure 4.6 are compared to each other and to the corresponding GFP signals Figure 4.5. In the case of reporter genes, the increased seam cell number in *ain-1(ku322); ain-2(RNAi)* adds to the GFP level detected on the western blot, as evidenced by the *unc-54* 3' UTR control. Future experiments will have to show whether protein levels in *ain-1(ku322)* animals are more comparable to *ain-1(ku322); ain-2(RNAi)* or wild-type situation. In this respect it may be rewarding to include genes that follow the pattern of endogenous DAF-12, for which *ain-1(ku322)* predominantly leads to a relief of translational repression. This may help to address the long-standing question as to how much translational repression contributes to miRNA mediated gene silencing in *C. elegans*.

In addition to our general interest in the mechanism of miRNA-mediated gene silencing in *C. elegans*, we also started this project with the specific question of whether translational repression and mRNA degradation are sequential or parallel events. Thus far we cannot answer that question. However, if translational repression and mRNA degradation were parallel events in *C. elegans*, the mechanism of inhibition is not determined by the identity of the GW182 protein in miRISC.

To finish with a clear statement, I favor the concept that translational repression and target degradation are mediated by the same sequence of events. I envision miRNA-mediated gene silencing as a three step process consisting of miRISC binding, mRNA deadeadenylation and mRNA degradation. Under conditions where translation initiation is the rate-liming step, translational repression is already a direct consequence of miRISC binding to the mRNA. The GW182 proteins likely mediate

translational repression by disturbing the interaction between PABPC1 and eIF4G. This interaction either interferes with the closed loop formation, or, since the closed loop formation is controversial, may impair tethering of eIF4F to the mRNA. In the latter scenario, eIF4F would be needed to be recruited *de novo* for another round of translation initiation. Translational repression occurring at this stage is readily reversible and does not require deadenylation. Although alternative 5' and 3' structures or internal ribosome entry sites (IRES) may render mRNAs insensitive to this form of repression, they do not prevent further regulatory steps to occur as long as miRISC remains associated. Deadenylation is induced by recruitment of the CAF1:CCR4:NOT1 complex to miRISC, which occurs independently of whether an mRNA is translated or not. Deadenylation is an additional source of translational repression, which becomes most detectable when deadenylation is not immediately followed by mRNA degradation, so that a deadenylated, translationally repressed mRNA species can accumulate. Deadenylation is followed by decapping and degradation of the mRNA by exonucleolytic digest. Therefore, context dependent kinetics of deadenylation and mRNA degradation may account for presence or absence of a translationally repressed species. In some contexts, mRNA deadenylation is reversible and is not followed by degradation which accounts for mRNAs that are exclusively regulated by translational repression. This may for instance apply to maternal mRNAs in embryonic tissues. However, this is due to an abruption of the chain of events that likely involves factors that prevent degradation and does not constitute a truly parallel mechanism.

4.4 Figures

Figure 4.1

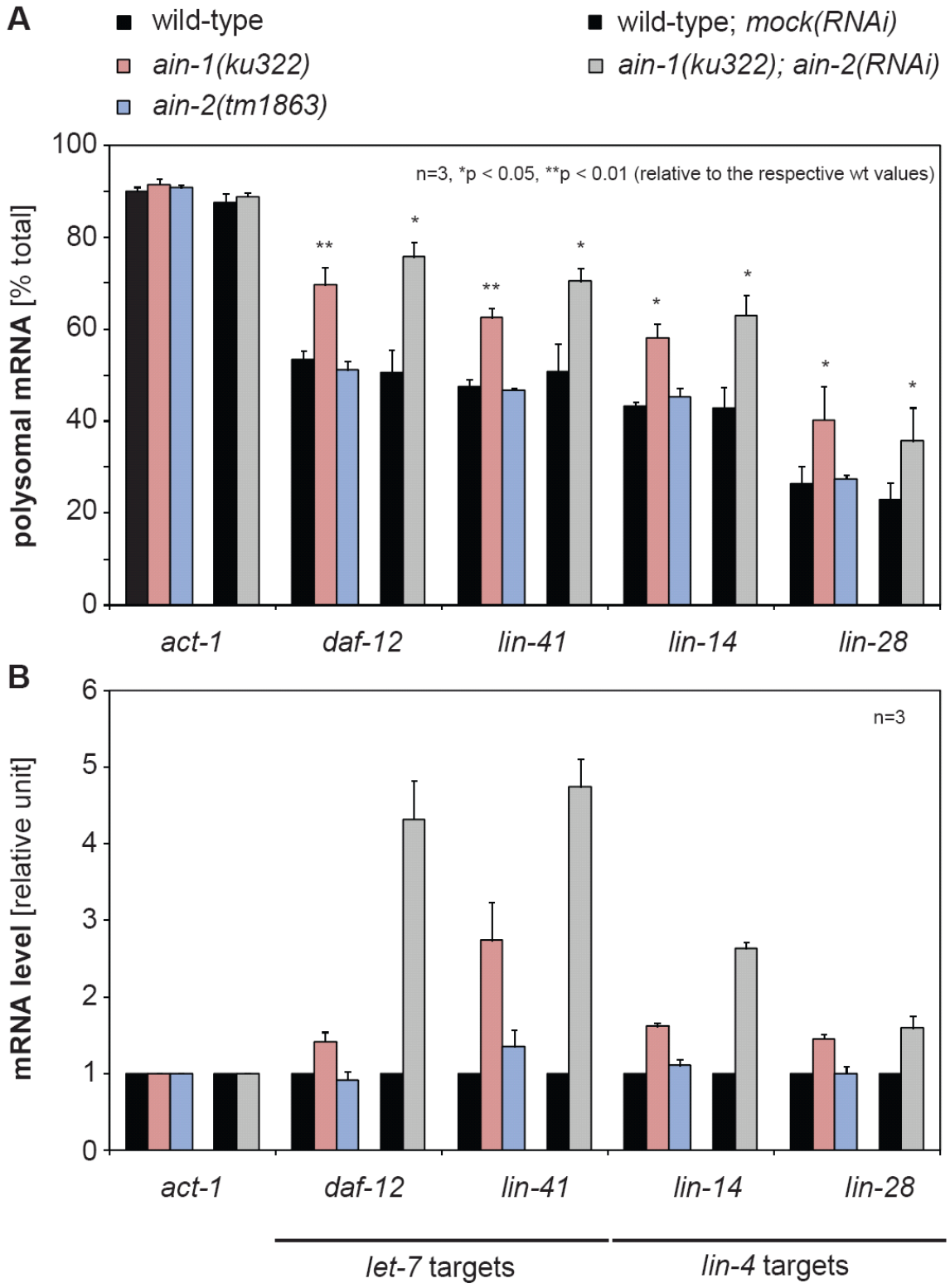
A
wild-type
ain-1(ku322)
ain-2(tm1863)
wild-type; mock(RNAi)
ain-1(ku322); ain-2(RNAi)
n=3, *p < 0.05, **p < 0.01 (relative to the respective wt values)
polysomal mRNA [% total]
100
80
60
40
20
0
act-1
daf-12
lin-41
lin-14
lin-28
B
n=3
mRNA level [relative unit]
6
5
4
3
2
1
0
act-1
daf-12
lin-41
lin-14
lin-28
let-7 targets
lin-4 targets

Figure 4.1 Translational repression of miRNA target genes is relieved in *ain-1(ku322)* animals. Polysome associated and total mRNA of synchronized late L4 animals grown at 25° C. mRNA levels were analyzed by qRT-PCR. (A) Polysomal fractions of indicated mRNAs are shown as percentage of total mRNA (=monosomal + polysomal fractions). (B) Total mRNA levels of the *let-7* targets *daf-12* and *lin-41* and the *lin-4* targets *lin-14* and *lin-28* normalized to *act-1*. The results presented here are from two independent series of experiments: data of wild-type, *ain-1(ku322)* and *ain-2(tm1863)* were acquired in a first set of experiments, data of wild-type grown on *mock(RNAi)* and *ain-1(ku322)* grown on *ain-2(RNAi)* were acquired in a second series of experiments. In this and subsequent figures, *mock(RNAi)* describes RNAi by feeding the insert-less L4440 vector. Error bars denote s.e.m. (X.C. Ding, unpublished).

Figure 4.2

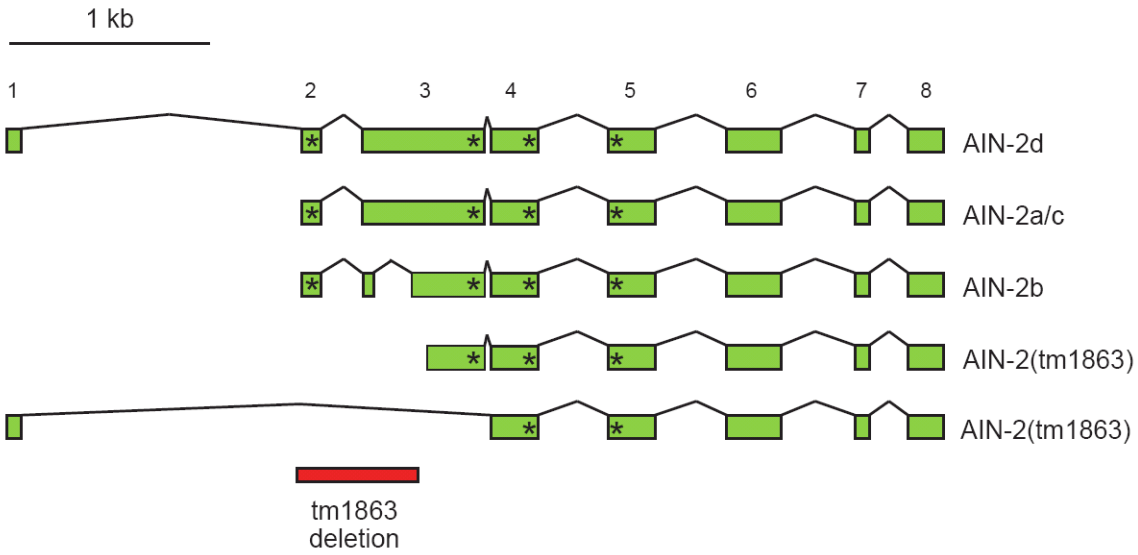

Figure 4.2 AIN-2 gene model based on comparison of annotated ESTs in wormbase (www.wormbase.org; release WS226) and the migration pattern of AIN-2 and AIN-2(tm1863) on our western blots. The asterisks denote GW or WG repeats. Wild-type AIN-2 migrates as three discrete bands. AIN-2d and AIN-2a/c appear to be equally expressed. AIN-2a and c differ in their 3' splice site in the 3rd exon, leading to a peptide sequence of 706 and 704 amino acids, respectively. AIN-2b is only detected at a lower level. AIN-2(tm1863) migrates as two discrete bands detected at the same level. The slightly higher running band may correspond to a truncated version of AIN-2 starting at an alternative in-frame ATG at the indicated position, which was also observed by Zhang et al. The lower running band may correspond to a partial deletion, in which exon 1 is directly spliced to exon 4. The epitope recognized by the antibody is encoded by exons 4 and 5.

Figure 4.3

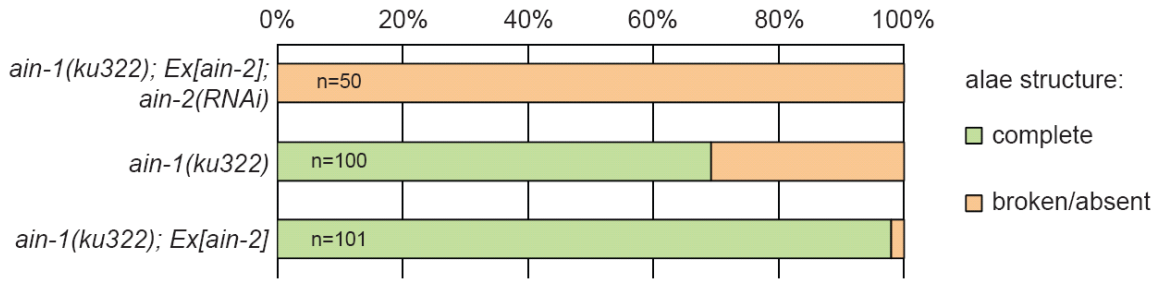

Figure 4.3 Over-expression of AIN-2 rescues *ain-1(ku322)*-specific alae defects. Partial or complete loss in miRNA function causes cell-differentiation defects which ultimately lead to a failure in the secretion of a wild-type alae structure. *ain-1(ku322)*, *ain-1(ku322); Ex[ain-2]; ain-2(RNAi)* and *ain-1(ku322); Ex[ain-2]* animals were grown at RT (~23° C). The alae structure was analyzed upon reaching young adult stage. *ain-1(ku322); Ex[ain-2]* grown on *ain-2(RNAi)* displayed fully penetrant alae defects. Parental *ain-1(ku322)*, i.e. animals that lost the rescue construct, displayed alae defects in 30% of animals. This value declined to less than 2% in *ain-1(ku322); Ex[ain-2]* animals. The total number of animals analyzed in two independent experiments are indicated.

Figure 4.4

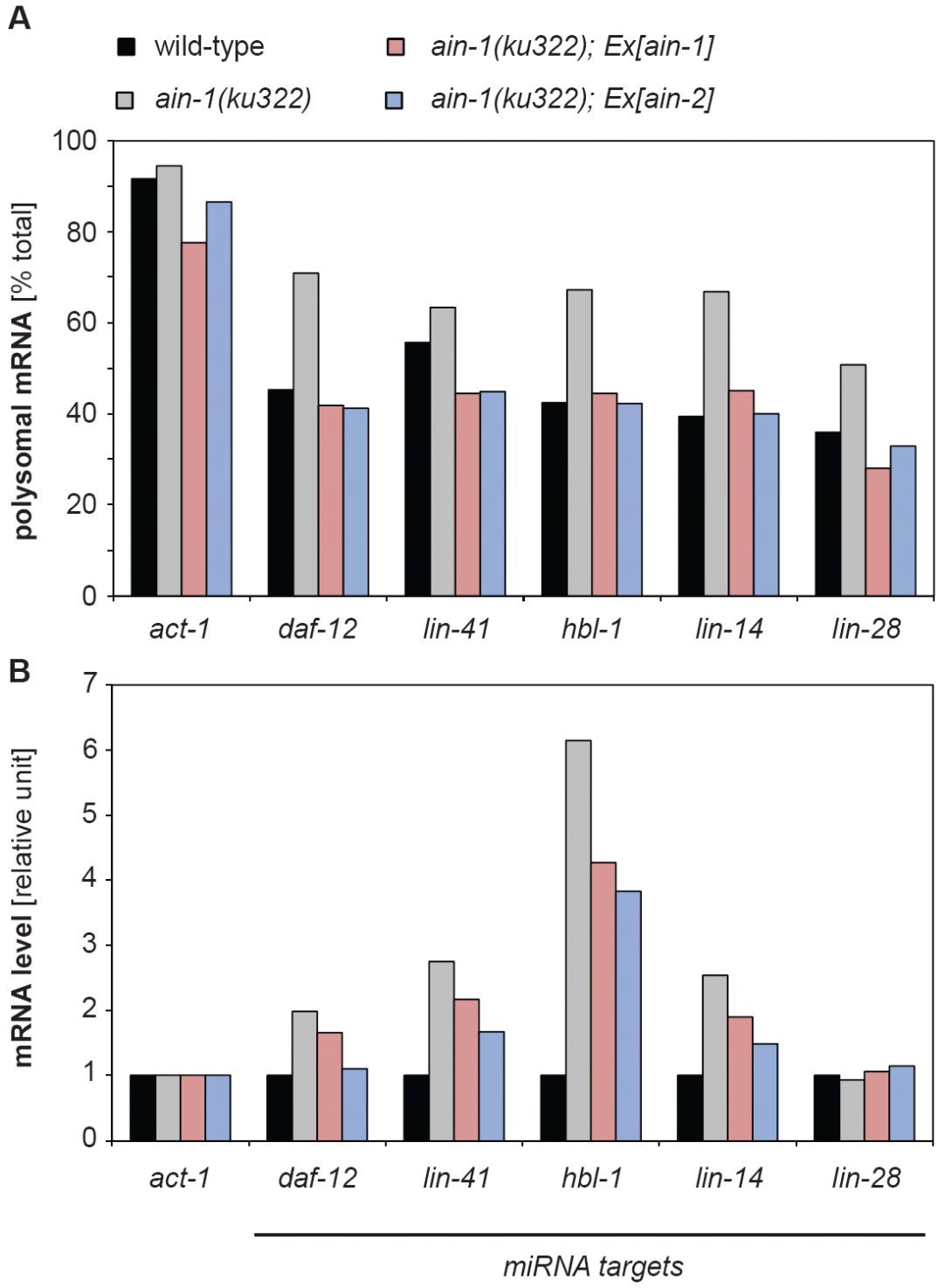
A
wild-type
ain-1(ku322)
ain-1(ku322); Ex[ain-1]
ain-1(ku322); Ex[ain-2]
polysomal mRNA [% total]
100
80
60
40
20
0
act-1
daf-12
lin-41
hbl-1
lin-14
lin-28
B
mRNA level [relative unit]
7
6
5
4
3
2
1
0
act-1
daf-12
lin-41
hbl-1
lin-14
lin-28
miRNA targets

Figure 4.4 AIN-2 over-expression restores translational repression of miRNA targets in *ain-1(ku322)*. Polysome associated and total mRNA of synchronized late L4 animals grown at 25° C. Wild-type, *ain-1(ku322)* and *ain-1(ku322)* expressing either additional AIN-1 or AIN-2 from an extrachromosomal array were used. mRNA levels were analyzed by qRT-PCR. (A) Polysomal fractions of mRNAs plotted as percentage of total mRNA. Additional expression of AIN-1 or AIN-2 restores wild-type like translational repression in *ain-1(ku322)* animals (B) Total mRNA level of the miRNA targets *daf-12*, *lin-41*, *hbl-1*, *lin-14* and *lin-28* normalized to *act-1*. Additional expression of AIN-1 or AIN-2 in *ain-1(ku322)* reduces miRNA target levels, albeit not to wild-type levels.

Figure 4.5

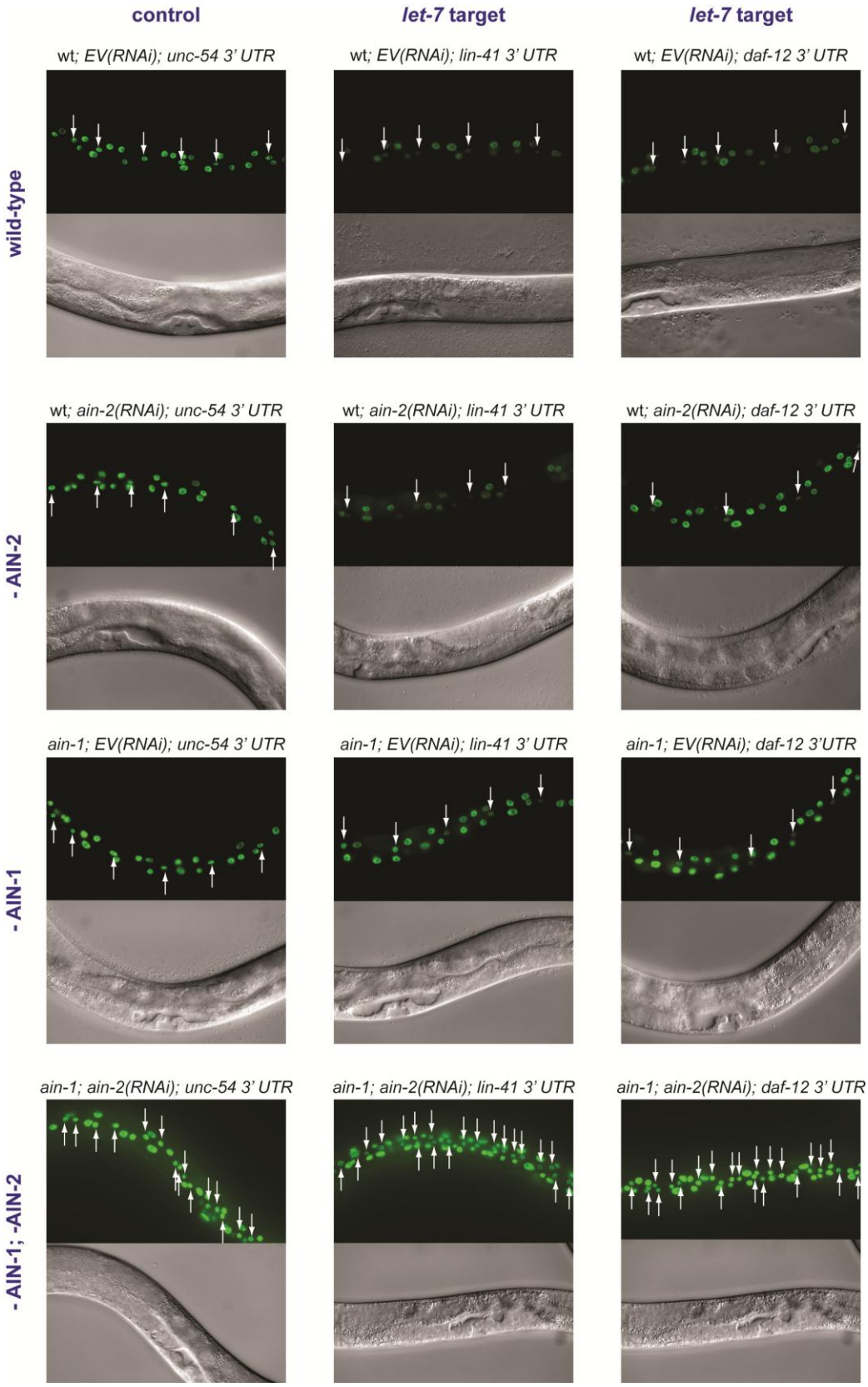
control
let-7 target
let-7 target
wt; EV(RNAi); unc-54 3' UTR
wt; EV(RNAi); lin-41 3' UTR
wt; EV(RNAi); daf-12 3' UTR
wild-type
wt; ain-2(RNAi); unc-54 3' UTR
wt; ain-2(RNAi); lin-41 3' UTR
wt; ain-2(RNAi); daf-12 3' UTR
- AIN-2
ain-1; EV(RNAi); unc-54 3' UTR
ain-1; EV(RNAi); lin-41 3' UTR
ain-1; EV(RNAi); daf-12 3'UTR
- AIN-1
ain-1; ain-2(RNAi); unc-54 3' UTR
ain-1; ain-2(RNAi); lin-41 3' UTR
ain-1; ain-2(RNAi); daf-12 3' UTR
- AIN-1; -AIN-2

Figure 4.5 Regulation of *lin-41* and *daf-12* 3' UTR reporter genes in wild-type and *ain-1*, *ain-2* single and double mutant situation. *Pwrt-2::gfp(pest)/h2b::unc-54* 3'UTR, *Pwrt-2::gfp(pest)/h2b::lin-41* 3'UTR, *Pwrt-2::gfp(pest)/h2b::daf-12* 3'UTR reporter genes were expressed in wild-type and *ain-1(ku322)* animals grown on either *mock(RNAi)* or *ain-2(RNAi)* until late L4 stage. All reporter genes are single copy integrated into chromosome II by MosSCI. The endogenous *wrt-2* promoter is active in seam cells and hyp-7 cells.

The upper panels show epifluorescent images and the lower panels show DIC images of the same animal at a different focal plane. White arrows in the epifluorescent images point to seam cell nuclei. Note that the combined depletion of AIN-1 and AIN-2 leads to a failure in terminal differentiation of seam cells, thus leading to an increased number of seam cells. No significant regulation of the *Pwrt-2::gfp(pest)/h2b::unc-54* 3'UTR can be observed, which served as a control gene. Down-regulation of the *let-7* target gene reporters *Pwrt2::gpf(pest)/h2b::lin-41* 3'UTR and *Pwrt-2::gfp(pest)/h2b::daf-12* 3'UTR is relieved in seam cell and hyp-7 nuclei of the indicated *ain-1* and *ain-2* mutant animals. GFP intensity of *let-7* reporters was observed as follows: *ain-1(ku322)*; *ain-2(RNAi)* > *ain-1(ku322)* > *ain-2(RNAi)* ≥ wild-type.

Figure 4.6

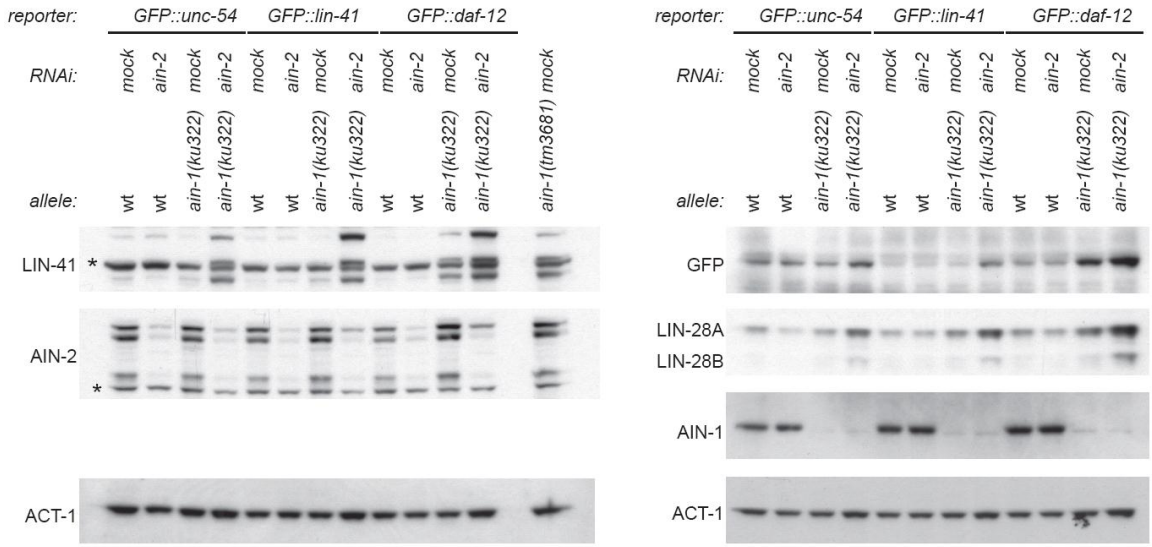

Figure 4.6 Combined loss of AIN-1 and AIN-2 shows a synergistic effect on the protein levels of endogenous target genes or reporter target genes. Western blotting of the same samples was performed in duplicate to avoid multiple stripping of the same membrane. Synchronized wild-type and *ain-1(ku322)* 3' UTR reporter strains were grown on either *mock(RNAi)* or *ain-2(RNAi)* until late L4 stage. The analyzed stage essentially corresponds to the stages in Figure 4.5. The single-copy integrated reporter genes express destabilized GFP(PEST)/H2B from the seam-cell and hyp-7 specific *wrt-2* promoter. The *lin-41* 3' UTR and *daf-12* 3' UTR are both regulated by *let-7*, the *unc-54* 3' UTR lacks miRNA binding sites. Blots for endogenous LIN-41, endogenous LIN28A and B and reporter GFP are shown. Blots for AIN-1 and AIN-2 confirm partial depletion of AIN-2 in *ain-2(RNAi)* or AIN-1 by the premature stop-codon in *ain-1(ku322)*. *ain-1(tm3681)*, a recently available deletion allele of *ain-1* was included for comparison. The asterisks indicate unspecific bands.

4.5 Future directions

The data presented in section 4.2 are based on hypothesis driven experiments. On one side, this was due to our concept that translational repression and mRNA degradation have a different requirement for AIN-1 and AIN-2. The obvious next step was to show that AIN-2 cannot rescue translational repression in absence of AIN-1. On the other side, there were only a few months left that I could invest and thus kept me from embarking on venturesome approaches. Nevertheless, I think that intrepid approaches may well pay off in the long run and should also be considered.

On the ground that AIN-1 and AIN-2 are more redundant than we previously anticipated, it is likely to be more rewarding to establish and evaluate a comprehensive network of AIN-1 and AIN-2 interacting factors, rather than focusing on AIN-1 and AIN-2 themselves. A comprehensive network of AIN-1 and AIN-2 interacting factors could be established by a combined approach of proteomic analyses and genetic screens. The first priority is to test a candidate list of genes for genetic interaction with *ain-1* and *ain-2*. Such a list can be obtained by literature search as well as immunoprecipitation of AIN-1 and AIN-2 and other methods to study protein-protein interaction. For instance, we have established expression vectors of AIN-1 and AIN-2 for a split-ubiquitin screen of a *C. elegans* protein library expressed in yeast. We have previously tested a literature based, small candidate list for genetic interaction (X.C. Ding, unpublished). Briefly, we tested candidate genes for causing miRNA loss-of-function phenotypes in wild-type animals and in the *ain-1(ku322)* sensitized background. Thereby, we identified a possible effector function of *pab-2, cgh-1* and *sqd-1* in miRNA-mediated gene regulation in *C. elegans*. Whereas RNAi-depletion of these factors had a minor or no effect on wild-type animals, it led to highly penetrant alae defects in *ain-1(ku322)* animals. Since we have established single-copy integrated GFP reporter genes for *daf-12*, *lin-41* and *unc-54* 3' UTRs in *ain-1(tm3681), ain-1(ku322)* and *ain-2(tm1863)* animals, we can study effects on the alae structure and reporter gene regulation in the same assay and also by using different genetic backgrounds.

A promissing opportunity to conduct genetic screens is provided by the fact that the extrachromomal arrays in *ain-1(ku322); Ex[ain-1]* or *ain-1(ku322); Ex[ain-2]* are transmitted at a low frequency. Thus it is conceivable to perform a mutagenesis screen for animals which are forced to retain the extrachromosomal array.

On the basis of work performed to study the function of Argonaute and GW182 proteins in drosophila or human cells, it may be possible to express ALG-1, ALG-2, AIN-1 and AIN-2 as fusions with λ N-peptide to specifically tether these proteins to box B hairpins inserted into the 3' UTR of reporter genes. Tethering of AIN-1 and AIN-2 allows to perform domain mapping studies as it was already done for drosophila and human GW182 proteins. Far-fetched, one could also tether drosophila or human dGW182 proteins or fragments thereof. Tethering of ALG-1 or ALG-2 is possibly a more elegant way to study full-length AIN-1 or AIN-2 function since the presence of an Argonaute protein more closely reflects a physiological miRISC complex. By crossing reporter lines with *ain-1(tm3681)* or a yet to be established *ain-2* deletion strain, *ain-1* and *ain-2* function can still be studied separately. Regarding the reporter mRNA, it will make sense to use the same promoter and the same 3' UTR with and without box B hairpins to express for instance GFP and RFP in the same tissue. The combination of two colors improves the ability to detect impaired or enhanced regulation of the reporter gene. Depending on the robustness of the system, expression could then be assessed by using a *C. elegans* adjusted *COPAS* large particle flow cytometry system ("worm sorter"), which would open a door to genome wide screens.

4.6 Methods

Caenorhabditis elegans strains and handling

Wild-type N2 and MH2385: *ain-1(ku322)* were provided by GCG. *ain-2(tm1863)* and *ain-1(tm3681)* were provided by S. Mitani (National Bioresource Project, Japan). HW767: *unc-119 (ed3) III; xeSi8[Pwrt-2::gfp(pest)/h2b::lin-41 3'UTR, unc-119 (+)] II*, HW784: *unc-119 (ed3) III; xeSi20[Pwrt-2::gfp(pest)/h2b::daf-12 3'UTR, unc-119 (+)] II*, HW786: *unc-119 (ed3) III; xeSi22[Pwrt-2::gfp(pest)/h2b::unc-54 3'UTR, unc-119 (+)]II* were established by M. Ecsedi and crossed into MH2385: *ain-1(ku322)* to obtain lines HW: *ain-1(ku322); unc-119 (ed3) III; xeSi8*[*Pwrt-2::gfp(pest)/h2b::lin-41 3'UTR, unc-119 (+)] II*, HW: *ain-1(ku322); unc-119 (ed3) III; xeSi20*[*Pwrt-2::gfp(pest)/h2b::daf-12 3'UTR, unc-119 (+)] II*, HW: *ain-1(ku322); unc-119 (ed3) III; xeSi22*[*Pwrt-2::gfp(pest)/h2b::unc-54 3'UTR, unc-119 (+)] II* to study reporter GFP expression in GW182 mutant situations. *ain-1(ku322)* rescue lines IK23: *ain-1(ku322); Ex[WRM0623aE03;pCFJ90(Pmyo-2::mCherry)]*, IK24: *ain-1(ku322); Ex[WRM0630aD07; pCFJ90(Pmyo-2::mCherry)]*, IK25: *ain-1(ku322); Ex[WRM063cE10; pCFJ90(Pmyo-2::mCherry)]* and IK26: *ain-1(ku322); Ex[WRM0641bE06;pCFJ90(Pmyo-2::mCherry)]* were established by Iskra Katic. Fosmids containing the full coding sequence and flanking 3' and 5' elements of *ain-1* and *ain-2* were obtained from the *C. elegans* fosmid library (Source BioScience LifeSciences). The fosmids were streaked onto LB plates containing 12.5 µg/ml cloramphenicol and single colonies were grown overnight in a 2 mL LB + 12.5 µg/ml cloramphenicol liquid culture. Fosmids were induced by culturing for five hours at 37 degrees in 4.5 ml of LB+cloramphenicol, 500 ul overnight culture, 50µl of 10% arabinose stock. Qiaprep Spin Miniprep Kit was used to isolate fosmid DNA. Restriction digests were performed to confirm the identity of each fosmid. *ain-1(ku322)* adults were microinjected with a DNA mix including 10 ng/µl fosmid, 2.5 ng/µl pCFJ90(*Pmyo-2::mCherry*) and 87.5 ng/µl 1 kb Plus DNA Ladder (invitrogen). The fosmids were as follows: Mix IK23, WRM0623aE03 (*ain-1*); Mix IK24, WRM0630aD07 (*ain-1*); Mix IK25, WRM063cE10 (*ain-2*); Mix IK26, WRM0641bE06 (*ain-2*). Multiple lines were obtained from each microinjection.

Polysome profiling and qRT-PCR

Polysome profiling and qRT-PCR for single mutant analysis was performed by X. Ding as described in (Ding and Grosshans, 2009). Polysome profiling for rescue analysis. Sample preparation: Worms of the rescue lines IK23, IK24, IK25, and IK26 were selected for pharyngeal *Pmyo-2::mCherry* expression using a *C. elegans* adjusted *COPAS* Biosort system (Union Biometrica; *wormsorter*). To this end, worms were grown on OP50 plates at 25° C for 26 hours. Test samples of worms were analyzed under a fluorescent dissecting microscope to adjust the gating parameters. After sorting, worms were washed 2x in M9 and seeded on OP50 plates for further development at 25° C until late L4 stage was reached. Due to the low amount of biological material which could be loaded on the gradients, quantitative extraction of RNA was not possible. Therefore, sucrose fractions were spiked with 2 µg of mouse total brain RNA (Agilent technologies, Catalog number 736501) prior to RNA extraction. The transcript level of each fraction was normalized to mouse CYTc and L13 mRNAs. Mouse mRNA was detected by using following primer pairs:
mmCYTc F1: 5' CTCTATTTCAACCCTTACTTTCCC 3';
mmCYTc R1: 5' TCAACAACATCTTGAGACCCA 3';
mmL13 F1: 5' CCTACCAGAAAGTTTGCTTACC 3';
mmL13 R1 5' CTTCCGATAGTGCATCTTGG 3'

Antibodies and western blotting

Protein samples were prepared by grinding worm pellets (~100 µl) resuspended in 500 µl lysis buffer (20 mM Tris-HCl pH 7.2, 150 mM KCl, 1 % Triton X-100, 1 mM DTT, 0.1 mM EDTA complemented with 10 mg/ml Complete Protease Inhibitor Cocktail (Roche Applied Science)) using mortar and pestle in presence of liquid nitrogen. Lysates were cleared by centrifugation at 4° C for 15 minutes at 12'000 RCF. Protein concentrations were adjusted using Pierce BCA Protein Assay Kit (Thermo Scientific, Cat. #23250). 40 µg of protein/sample were loaded on NuPAGE 4 %-12 % Bis-Tris gels (Invitrogen) and transferred to Immuno-Blot PVDF membranes (Biorad).

Mouse monoclonal antibodies [Clones 7.1 and 13.1] to GFP (Roche Applied Science) were used 1:1000. LIN-41 Q4796 affinity purified rabbit polyclonal serum to LIN-41 was provided by M. Rausch and used 1:2000. LIN-28 unpurified rabbit serum was provided by E. Moss and used 1:2000. AIN-2 Q4352 affinity purified rabbit polyclonal antibodies to epitope MERCPSHLKKKALNEEALRRRLTSENPQ-IVAQAQQQAEEEANAMMRIGRRPIVPSGWGDIPSEISTDKSDSEFDQSSSRGW DEGSISGGGSGRHPSHHQS produced by SDI (Newark USA) was used 1:2000. MAB1501 monoclonal mouse to Actin (Chemicon International) was used 1:1000. HRP-conjugated anti-mouse (NA931V, GE Healthcare) was used 1:7500. HRP-conjugated anit-rabbit (NA934, GE Healthcare) was used 1:7500. Super Signal West Dura (Thermo Scientific) and ECL (GE Healthcare) ECL kits were used for signal detection.

5. References

Abbott, A.L., Alvarez-Saavedra, E., Miska, E.A., Lau, N.C., Bartel, D.P., Horvitz, H.R., and Ambros, V. (2005). The let-7 MicroRNA family members mir-48, mir-84, and mir-241 function together to regulate developmental timing in Caenorhabditis elegans. Dev Cell *9*, 403-414.

Abrahante, J.E., Daul, A.L., Li, M., Volk, M.L., Tennessen, J.M., Miller, E.A., and Rougvie, A.E. (2003). The Caenorhabditis elegans hunchback-like gene lin-57/hbl-1 controls developmental time and is regulated by microRNAs. Dev Cell *4*, 625-637.

Ambros, V. (1989). A hierarchy of regulatory genes controls a larva-to-adult developmental switch in C. elegans. Cell *57*, 49-57.

Ambros, V., and Horvitz, H.R. (1984). Heterochronic mutants of the nematode Caenorhabditis elegans. Science *226*, 409-416.

Ambros, V., and Horvitz, H.R. (1987). The lin-14 locus of Caenorhabditis elegans controls the time of expression of specific postembryonic developmental events. Genes Dev *1*, 398-414.

Aza-Blanc, P., Cooper, C.L., Wagner, K., Batalov, S., Deveraux, Q.L., and Cooke, M.P. (2003). Identification of modulators of TRAIL-induced apoptosis via RNAi-based phenotypic screening. Mol Cell *12*, 627-637.

Babiarz, J.E., Ruby, J.G., Wang, Y., Bartel, D.P., and Blelloch, R. (2008). Mouse ES cells express endogenous shRNAs, siRNAs, and other Microprocessor-independent, Dicer-dependent small RNAs. Genes Dev *22*, 2773-2785.

Baek, D., Villen, J., Shin, C., Camargo, F.D., Gygi, S.P., and Bartel, D.P. (2008). The impact of microRNAs on protein output. Nature *455*, 64-71.

Baillat, D., and Shiekhattar, R. (2009). Functional dissection of the human TNRC6 (GW182-related) family of proteins. Mol Cell Biol *29*, 4144-4155.

Behm-Ansmant, I., Rehwinkel, J., Doerks, T., Stark, A., Bork, P., and Izaurralde, E. (2006). mRNA degradation by miRNAs and GW182 requires both CCR4:NOT deadenylase and DCP1:DCP2 decapping complexes. Genes Dev *20*, 1885-1898.

Beitzinger, M., Peters, L., Zhu, J.Y., Kremmer, E., and Meister, G. (2007). Identification of human microRNA targets from isolated argonaute protein complexes. RNA Biol *4*, 76-84.

Bernstein, E., Caudy, A.A., Hammond, S.M., and Hannon, G.J. (2001). Role for a bidentate ribonuclease in the initiation step of RNA interference. Nature *409*, 363-366.

Betel, D., Wilson, M., Gabow, A., Marks, D.S., and Sander, C. (2008). The microRNA.org resource: targets and expression. Nucleic Acids Res *36*, D149-153.

Blumenthal, T. (2005). Trans-splicing and operons. WormBook, 1-9.

Bohnsack, M.T., Czaplinski, K., and Gorlich, D. (2004). Exportin 5 is a RanGTP-dependent dsRNA-binding protein that mediates nuclear export of pre-miRNAs. RNA *10*, 185-191.

Borchert, G.M., Lanier, W., and Davidson, B.L. (2006). RNA polymerase III transcribes human microRNAs. Nat Struct Mol Biol *13*, 1097-1101.

Bracht, J., Hunter, S., Eachus, R., Weeks, P., and Pasquinelli, A.E. (2004). Trans-splicing and polyadenylation of let-7 microRNA primary transcripts. RNA *10*, 1586-1594.

Brennecke, J., Stark, A., Russell, R.B., and Cohen, S.M. (2005). Principles of microRNA-target recognition. PLoS Biol *3*, e85.

Britten, R.J., and Davidson, E.H. (1969). Gene regulation for higher cells: a theory. Science *165*, 349-357.

Bussing, I., Yang, J.S., Lai, E.C., and Grosshans, H. (2010). The nuclear export receptor XPO-1 supports primary miRNA processing in C. elegans and Drosophila. EMBO J *29*, 1830-1839.

Cai, X., Hagedorn, C.H., and Cullen, B.R. (2004). Human microRNAs are processed from capped, polyadenylated transcripts that can also function as mRNAs. RNA *10*, 1957-1966.

Cakmakci, N.G., Lerner, R.S., Wagner, E.J., Zheng, L., and Marzluff, W.F. (2008). SLIP1, a factor required for activation of histone mRNA translation by the stem-loop binding protein. Mol Cell Biol *28*, 1182-1194.

Chalfie, M., Horvitz, H.R., and Sulston, J.E. (1981). Mutations that lead to reiterations in the cell lineages of C. elegans. Cell *24*, 59-69.

Chatterjee, S., Fasler, M., Bussing, I., and Grosshans, H. (2011). Target-mediated protection of endogenous microRNAs in C. elegans. Dev Cell *20*, 388-396.

Chatterjee, S., and Grosshans, H. (2009). Active turnover modulates mature microRNA activity in Caenorhabditis elegans. Nature *461*, 546-549.

Chekulaeva, M., Filipowicz, W., and Parker, R. (2009). Multiple independent domains of dGW182 function in miRNA-mediated repression in Drosophila. RNA *15*, 794-803.

Chekulaeva, M., Parker, R., and Filipowicz, W. (2010). The GW/WG repeats of Drosophila GW182 function as effector motifs for miRNA-mediated repression. Nucleic Acids Res *38*, 6673-6683.

Chendrimada, T.P., Gregory, R.I., Kumaraswamy, E., Norman, J., Cooch, N., Nishikura, K., and Shiekhattar, R. (2005). TRBP recruits the Dicer complex to Ago2 for microRNA processing and gene silencing. Nature *436*, 740-744.

Chi, S.W., Zang, J.B., Mele, A., and Darnell, R.B. (2009). Argonaute HITS-CLIP decodes microRNA-mRNA interaction maps. Nature *460*, 479-486.

Corcoran, D.L., Pandit, K.V., Gordon, B., Bhattacharjee, A., Kaminski, N., and Benos, P.V. (2009). Features of mammalian microRNA promoters emerge from polymerase II chromatin immunoprecipitation data. PLoS One *4*, e5279.

Davis, E., Caiment, F., Tordoir, X., Cavaille, J., Ferguson-Smith, A., Cockett, N., Georges, M., and Charlier, C. (2005). RNAi-mediated allelic trans-interaction at the imprinted Rtl1/Peg11 locus. Curr Biol *15*, 743-749.

Denli, A.M., Tops, B.B., Plasterk, R.H., Ketting, R.F., and Hannon, G.J. (2004). Processing of primary microRNAs by the Microprocessor complex. Nature *432*, 231-235.

Deppe, U., Schierenberg, E., Cole, T., Krieg, C., Schmitt, D., Yoder, B., and von Ehrenstein, G. (1978). Cell lineages of the embryo of the nematode Caenorhabditis elegans. Proc Natl Acad Sci U S A *75*, 376-380.

Ding, L., and Han, M. (2007). GW182 family proteins are crucial for microRNA-mediated gene silencing. Trends Cell Biol *17*, 411-416.

Ding, L., Spencer, A., Morita, K., and Han, M. (2005). The developmental timing regulator AIN-1 interacts with miRISCs and may target the argonaute protein ALG-1 to cytoplasmic P bodies in C. elegans. Mol Cell *19*, 437-447.

Ding, X.C., and Grosshans, H. (2009). Repression of C. elegans microRNA targets at the initiation level of translation requires GW182 proteins. EMBO J *28*, 213-222.

Ding, X.C., Slack, F.J., and Grosshans, H. (2008). The let-7 microRNA interfaces extensively with the translation machinery to regulate cell differentiation. Cell Cycle *7*, 3083-3090.

Ding, X.C., Weiler, J., and Grosshans, H. (2009). Regulating the regulators: mechanisms controlling the maturation of microRNAs. Trends Biotechnol *27*, 27-36.

Doench, J.G., and Sharp, P.A. (2004). Specificity of microRNA target selection in translational repression. Genes Dev *18*, 504-511.

Easow, G., Teleman, A.A., and Cohen, S.M. (2007). Isolation of microRNA targets by miRNP immunopurification. Rna.

Elbashir, S.M., Harborth, J., Lendeckel, W., Yalcin, A., Weber, K., and Tuschl, T. (2001). Duplexes of 21-nucleotide RNAs mediate RNA interference in cultured mammalian cells. Nature *411*, 494-498.

Ender, C., Krek, A., Friedlander, M.R., Beitzinger, M., Weinmann, L., Chen, W., Pfeffer, S., Rajewsky, N., and Meister, G. (2008). A human snoRNA with microRNA-like functions. Mol Cell *32*, 519-528.

Esquela-Kerscher, A., Johnson, S.M., Bai, L., Saito, K., Partridge, J., Reinert, K.L., and Slack, F.J. (2005). Post-embryonic expression of C. elegans microRNAs belonging to the lin-4 and let-7 families in the hypodermis and the reproductive system. Dev Dyn *234*, 868-877.

Eulalio, A., Helms, S., Fritzsch, C., Fauser, M., and Izaurralde, E. (2009a). A C-terminal silencing domain in GW182 is essential for miRNA function. RNA *15*, 1067-1077.

Eulalio, A., Huntzinger, E., and Izaurralde, E. (2008). GW182 interaction with Argonaute is essential for miRNA-mediated translational repression and mRNA decay. Nat Struct Mol Biol *15*, 346-353.

Eulalio, A., Huntzinger, E., Nishihara, T., Rehwinkel, J., Fauser, M., and Izaurralde, E. (2009b). Deadenylation is a widespread effect of miRNA regulation. RNA *15*, 21-32.

Eulalio, A., Rehwinkel, J., Stricker, M., Huntzinger, E., Yang, S.F., Doerks, T., Dorner, S., Bork, P., Boutros, M., and Izaurralde, E. (2007). Target-specific requirements for enhancers of decapping in miRNA-mediated gene silencing. Genes Dev *21*, 2558-2570.

Eulalio, A., Tritschler, F., Buttner, R., Weichenrieder, O., Izaurralde, E., and Truffault, V. (2009c). The RRM domain in GW182 proteins contributes to miRNA-mediated gene silencing. Nucleic Acids Res *37*, 2974-2983.

Eulalio, A., Tritschler, F., and Izaurralde, E. (2009d). The GW182 protein family in animal cells: new insights into domains required for miRNA-mediated gene silencing. RNA *15*, 1433-1442.

Eystathioy, T., Chan, E.K., Tenenbaum, S.A., Keene, J.D., Griffith, K., and Fritzler, M.J. (2002). A phosphorylated cytoplasmic autoantigen, GW182, associates with a unique population of human mRNAs within novel cytoplasmic speckles. Mol Biol Cell *13*, 1338-1351.

Fabian, M.R., Mathonnet, G., Sundermeier, T., Mathys, H., Zipprich, J.T., Svitkin, Y.V., Rivas, F., Jinek, M., Wohlschlegel, J., Doudna, J.A., *et al.* (2009). Mammalian miRNA RISC recruits CAF1 and PABP to affect PABP-dependent deadenylation. Mol Cell *35*, 868-880.

Fabian, M.R., Sonenberg, N., and Filipowicz, W. (2010). Regulation of mRNA translation and stability by microRNAs. Annu Rev Biochem *79*, 351-379.

Fichelson, P., Moch, C., Ivanovitch, K., Martin, C., Sidor, C.M., Lepesant, J.A., Bellaiche, Y., and Huynh, J.R. (2009). Live-imaging of single stem cells within their niche reveals that a U3snoRNP component segregates asymmetrically and is required for self-renewal in Drosophila. Nat Cell Biol *11*, 685-693.

Fire, A., Xu, S., Montgomery, M.K., Kostas, S.A., Driver, S.E., and Mello, C.C. (1998). Potent and specific genetic interference by double-stranded RNA in Caenorhabditis elegans. Nature *391*, 806-811.

Forstemann, K., Horwich, M.D., Wee, L., Tomari, Y., and Zamore, P.D. (2007). Drosophila microRNAs are sorted into functionally distinct argonaute complexes after production by dicer-1. Cell *130*, 287-297.

Forstemann, K., Tomari, Y., Du, T., Vagin, V.V., Denli, A.M., Bratu, D.P., Klattenhoff, C., Theurkauf, W.E., and Zamore, P.D. (2005). Normal microRNA maturation and germ-line stem cell maintenance requires Loquacious, a double-stranded RNA-binding domain protein. PLoS Biol *3*, e236.

Friedman, R.C., Farh, K.K., Burge, C.B., and Bartel, D.P. (2009). Most mammalian mRNAs are conserved targets of microRNAs. Genome Res *19*, 92-105.

Gaidatzis, D., van Nimwegen, E., Hausser, J., and Zavolan, M. (2007). Inference of miRNA targets using evolutionary conservation and pathway analysis. BMC Bioinformatics *8*, 69.

Gregory, R.I., Yan, K.P., Amuthan, G., Chendrimada, T., Doratotaj, B., Cooch, N., and Shiekhattar, R. (2004). The Microprocessor complex mediates the genesis of microRNAs. Nature *432*, 235-240.

Griffiths-Jones, S., Saini, H.K., van Dongen, S., and Enright, A.J. (2008). miRBase: tools for microRNA genomics. Nucleic Acids Res *36*, D154-158.

Grimson, A., Farh, K.K., Johnston, W.K., Garrett-Engele, P., Lim, L.P., and Bartel, D.P. (2007). MicroRNA Targeting Specificity in Mammals: Determinants beyond Seed Pairing. Mol Cell *27*, 91-105.

Grishok, A., Pasquinelli, A.E., Conte, D., Li, N., Parrish, S., Ha, I., Baillie, D.L., Fire, A., Ruvkun, G., and Mello, C.C. (2001). Genes and mechanisms related to RNA interference regulate expression of the small temporal RNAs that control C. elegans developmental timing. Cell *106*, 23-34.

Grosshans, H., and Chatterjee, S. (2010). MicroRNases and the Regulated Degradation of Mature Animal miRNAs. Adv Exp Med Biol *700*, 140-155.

Grosshans, H., Johnson, T., Reinert, K.L., Gerstein, M., and Slack, F.J. (2005). The temporal patterning microRNA let-7 regulates several transcription factors at the larval to adult transition in C. elegans. Dev Cell *8*, 321-330.

Grzechnik, P., and Kufel, J. (2008). Polyadenylation linked to transcription termination directs the processing of snoRNA precursors in yeast. Mol Cell *32*, 247-258.

Gu, S., Jin, L., Zhang, F., Sarnow, P., and Kay, M.A. (2009a). Biological basis for restriction of microRNA targets to the 3' untranslated region in mammalian mRNAs. Nat Struct Mol Biol *16*, 144-150.

Gu, T.J., Yi, X., Zhao, X.W., Zhao, Y., and Yin, J.Q. (2009b). Alu-directed transcriptional regulation of some novel miRNAs. BMC Genomics *10*, 563.

Guo, H., Ingolia, N.T., Weissman, J.S., and Bartel, D.P. (2010). Mammalian microRNAs predominantly act to decrease target mRNA levels. Nature *466*, 835-840.

Guo, S., and Kemphues, K.J. (1995). par-1, a gene required for establishing polarity in C. elegans embryos, encodes a putative Ser/Thr kinase that is asymmetrically distributed. Cell *81*, 611-620.

Haase, A.D., Jaskiewicz, L., Zhang, H., Laine, S., Sack, R., Gatignol, A., and Filipowicz, W. (2005). TRBP, a regulator of cellular PKR and HIV-1 virus expression, interacts with Dicer and functions in RNA silencing. EMBO Rep *6*, 961-967.

Hagan, J.P., Piskounova, E., and Gregory, R.I. (2009). Lin28 recruits the TUTase Zcchc11 to inhibit let-7 maturation in mouse embryonic stem cells. Nat Struct Mol Biol *16*, 1021-1025.

Hamilton, A.J., and Baulcombe, D.C. (1999). A species of small antisense RNA in posttranscriptional gene silencing in plants. Science *286*, 950-952.

Hammell, M., Long, D., Zhang, L., Lee, A., Carmack, C.S., Han, M., Ding, Y., and Ambros, V. (2008). mirWIP: microRNA target prediction based on microRNA-containing ribonucleoprotein-enriched transcripts. Nat Methods *5*, 813-819.

Hammond, S.M., Bernstein, E., Beach, D., and Hannon, G.J. (2000). An RNA-directed nuclease mediates post-transcriptional gene silencing in Drosophila cells. Nature *404*, 293-296.

Han, J., Lee, Y., Yeom, K.H., Kim, Y.K., Jin, H., and Kim, V.N. (2004). The Drosha-DGCR8 complex in primary microRNA processing. Genes Dev *18*, 3016-3027.

Han, J., Lee, Y., Yeom, K.H., Nam, J.W., Heo, I., Rhee, J.K., Sohn, S.Y., Cho, Y., Zhang, B.T., and Kim, V.N. (2006). Molecular basis for the recognition of primary microRNAs by the Drosha-DGCR8 complex. Cell *125*, 887-901.

Hastings, K.E. (2005). SL trans-splicing: easy come or easy go? Trends Genet *21*, 240-247.

Hayes, G.D., Frand, A.R., and Ruvkun, G. (2006). The mir-84 and let-7 paralogous microRNA genes of Caenorhabditis elegans direct the cessation of molting via the conserved nuclear hormone receptors NHR-23 and NHR-25. Development *133*, 4631-4641.

Hendrickson, D.G., Hogan, D.J., Herschlag, D., Ferrell, J.E., and Brown, P.O. (2008). Systematic identification of mRNAs recruited to argonaute 2 by specific microRNAs and corresponding changes in transcript abundance. PLoS One *3*, e2126.

Henke, J.I., Goergen, D., Zheng, J., Song, Y., Schuttler, C.G., Fehr, C., Junemann, C., and Niepmann, M. (2008). microRNA-122 stimulates translation of hepatitis C virus RNA. EMBO J *27*, 3300-3310.

Heo, I., Joo, C., Cho, J., Ha, M., Han, J., and Kim, V.N. (2008). Lin28 mediates the terminal uridylation of let-7 precursor MicroRNA. Mol Cell *32*, 276-284.

Heo, I., Joo, C., Kim, Y.K., Ha, M., Yoon, M.J., Cho, J., Yeom, K.H., Han, J., and Kim, V.N. (2009). TUT4 in concert with Lin28 suppresses microRNA biogenesis through pre-microRNA uridylation. Cell *138*, 696-708.

Hocine, S., Singer, R.H., and Grunwald, D. (2010). RNA processing and export. Cold Spring Harb Perspect Biol *2*, a000752.

Hong, X., Hammell, M., Ambros, V., and Cohen, S.M. (2009). Immunopurification of Ago1 miRNPs selects for a distinct class of microRNA targets. Proc Natl Acad Sci U S A *106*, 15085-15090.

Horvitz, H.R., and Sulston, J.E. (1980). Isolation and genetic characterization of cell-lineage mutants of the nematode Caenorhabditis elegans. Genetics *96*, 435-454.

Hsu, R.J., Yang, H.J., and Tsai, H.J. (2009). Labeled microRNA pull-down assay system: an experimental approach for high-throughput identification of microRNA-target mRNAs. Nucleic Acids Res *37*, e77.

Huntzinger, E., Braun, J.E., Heimstadt, S., Zekri, L., and Izaurralde, E. (2010). Two PABPC1-binding sites in GW182 proteins promote miRNA-mediated gene silencing. EMBO J *29*, 4146-4160.

Hurschler, B.A., Harris, D.T., and Grosshans, H. (2011). The type II poly(A)-binding protein PABP-2 genetically interacts with the let-7 miRNA and elicits heterochronic phenotypes in Caenorhabditis elegans. Nucleic Acids Res *39*, 5647-5657.

Hutvagner, G., McLachlan, J., Pasquinelli, A.E., Balint, E., Tuschl, T., and Zamore, P.D. (2001). A cellular function for the RNA-interference enzyme Dicer in the maturation of the let-7 small temporal RNA. Science *293*, 834-838.

Iwasaki, S., Kobayashi, M., Yoda, M., Sakaguchi, Y., Katsuma, S., Suzuki, T., and Tomari, Y. (2010). Hsc70/Hsp90 chaperone machinery mediates ATP-dependent RISC loading of small RNA duplexes. Mol Cell *39*, 292-299.

Jackson, R.J., Hellen, C.U., and Pestova, T.V. (2010). The mechanism of eukaryotic translation initiation and principles of its regulation. Nat Rev Mol Cell Biol *11*, 113-127.

Jakymiw, A., Lian, S., Eystathioy, T., Li, S., Satoh, M., Hamel, J.C., Fritzler, M.J., and Chan, E.K. (2005). Disruption of GW bodies impairs mammalian RNA interference. Nat Cell Biol *7*, 1267-1274.

Jiang, F., Ye, X., Liu, X., Fincher, L., McKearin, D., and Liu, Q. (2005). Dicer-1 and R3D1-L catalyze microRNA maturation in Drosophila. Genes Dev *19*, 1674-1679.

Jinek, M., and Doudna, J.A. (2009). A three-dimensional view of the molecular machinery of RNA interference. Nature *457*, 405-412.

Jinek, M., Fabian, M.R., Coyle, S.M., Sonenberg, N., and Doudna, J.A. (2010). Structural insights into the human GW182-PABC interaction in microRNA-mediated deadenylation. Nat Struct Mol Biol *17*, 238-240.

Johnson, S.M., Lin, S.Y., and Slack, F.J. (2003). The time of appearance of the C. elegans let-7 microRNA is transcriptionally controlled utilizing a temporal regulatory element in its promoter. Dev Biol 259, 364-379.

Johnston, R.J., Jr., Chang, S., Etchberger, J.F., Ortiz, C.O., and Hobert, O. (2005). MicroRNAs acting in a double-negative feedback loop to control a neuronal cell fate decision. Proc Natl Acad Sci U S A *102*, 12449-12454.

Jones, M.R., Quinton, L.J., Blahna, M.T., Neilson, J.R., Fu, S., Ivanov, A.R., Wolf, D.A., and Mizgerd, J.P. (2009). Zcchc11-dependent uridylation of microRNA directs cytokine expression. Nat Cell Biol *11*, 1157-1163.

Karginov, F.V., Conaco, C., Xuan, Z., Schmidt, B.H., Parker, J.S., Mandel, G., and Hannon, G.J. (2007). A biochemical approach to identifying microRNA targets. Proc Natl Acad Sci U S A *104*, 19291-19296.

Kawahara, Y., Zinshteyn, B., Sethupathy, P., Iizasa, H., Hatzigeorgiou, A.G., and Nishikura, K. (2007). Redirection of silencing targets by adenosine-to-inosine editing of miRNAs. Science *315*, 1137-1140.

Kedde, M., Strasser, M.J., Boldajipour, B., Oude Vrielink, J.A., Slanchev, K., le Sage, C., Nagel, R., Voorhoeve, P.M., van Duijse, J., Orom, U.A., *et al.* (2007). RNA-binding protein Dnd1 inhibits microRNA access to target mRNA. Cell *131*, 1273-1286.

Kennerdell, J.R., and Carthew, R.W. (1998). Use of dsRNA-mediated genetic interference to demonstrate that frizzled and frizzled 2 act in the wingless pathway. Cell *95*, 1017-1026.

Kertesz, M., Iovino, N., Unnerstall, U., Gaul, U., and Segal, E. (2007). The role of site accessibility in microRNA target recognition. Nat Genet *39*, 1278-1284.

Ketting, R.F., Fischer, S.E., Bernstein, E., Sijen, T., Hannon, G.J., and Plasterk, R.H. (2001). Dicer functions in RNA interference and in synthesis of small RNA involved in developmental timing in C. elegans. Genes Dev *15*, 2654-2659.

Khvorova, A., Reynolds, A., and Jayasena, S.D. (2003). Functional siRNAs and miRNAs exhibit strand bias. Cell *115*, 209-216.

Kim, Y.K., and Kim, V.N. (2007). Processing of intronic microRNAs. EMBO J *26*, 775-783.

Kimble, J., and Hirsh, D. (1979). The postembryonic cell lineages of the hermaphrodite and male gonads in Caenorhabditis elegans. Dev Biol *70*, 396-417.

Kiss, T., Fayet, E., Jady, B.E., Richard, P., and Weber, M. (2006). Biogenesis and intranuclear trafficking of human box C/D and H/ACA RNPs. Cold Spring Harb Symp Quant Biol 71, 407-417.

Knight, S.W., and Bass, B.L. (2001). A role for the RNase III enzyme DCR-1 in RNA interference and germ line development in Caenorhabditis elegans. Science *293*, 2269-2271.

Kozlov, G., Menade, M., Rosenauer, A., Nguyen, L., and Gehring, K. (2010a). Molecular determinants of PAM2 recognition by the MLLE domain of poly(A)-binding protein. J Mol Biol *397*, 397-407.

Kozlov, G., Safaee, N., Rosenauer, A., and Gehring, K. (2010b). Structural basis of binding of P-body-associated proteins GW182 and ataxin-2 by the Mlle domain of poly(A)-binding protein. J Biol Chem *285*, 13599-13606.

Krol, J., Busskamp, V., Markiewicz, I., Stadler, M.B., Ribi, S., Richter, J., Duebel, J., Bicker, S., Fehling, H.J., Schubeler, D., *et al.* (2010a). Characterizing light-regulated retinal microRNAs reveals rapid turnover as a common property of neuronal microRNAs. Cell *141*, 618-631.

Krol, J., Loedige, I., and Filipowicz, W. (2010b). The widespread regulation of microRNA biogenesis, function and decay. Nat Rev Genet *11*, 597-610.

Lagos-Quintana, M., Rauhut, R., Lendeckel, W., and Tuschl, T. (2001). Identification of novel genes coding for small expressed RNAs. Science *294*, 853-858.

Lagos-Quintana, M., Rauhut, R., Meyer, J., Borkhardt, A., and Tuschl, T. (2003). New microRNAs from mouse and human. RNA *9*, 175-179.

Lall, S., Friedman, C.C., Jankowska-Anyszka, M., Stepinski, J., Darzynkiewicz, E., and Davis, R.E. (2004). Contribution of trans-splicing, 5' -leader length, cap-poly(A) synergism, and initiation factors to nematode translation in an Ascaris suum embryo cell-free system. J Biol Chem *279*, 45573-45585.

Lall, S., Grun, D., Krek, A., Chen, K., Wang, Y.L., Dewey, C.N., Sood, P., Colombo, T., Bray, N., Macmenamin, P., *et al.* (2006). A genome-wide map of conserved microRNA targets in C. elegans. Curr Biol *16*, 460-471.

Landthaler, M., Gaidatzis, D., Rothballer, A., Chen, P.Y., Soll, S.J., Dinic, L., Ojo, T., Hafner, M., Zavolan, M., and Tuschl, T. (2008). Molecular characterization of human Argonaute-containing ribonucleoprotein complexes and their bound target mRNAs. Rna *14*, 2580-2596.

Landthaler, M., Yalcin, A., and Tuschl, T. (2004). The human DiGeorge syndrome critical region gene 8 and Its D. melanogaster homolog are required for miRNA biogenesis. Curr Biol *14*, 2162-2167.

Lau, N.C., Lim, L.P., Weinstein, E.G., and Bartel, D.P. (2001). An abundant class of tiny RNAs with probable regulatory roles in Caenorhabditis elegans. Science *294*, 858-862.

Lazzaretti, D., Tournier, I., and Izaurralde, E. (2009). The C-terminal domains of human TNRC6A, TNRC6B, and TNRC6C silence bound transcripts independently of Argonaute proteins. RNA *15*, 1059-1066.

Lee, R.C., and Ambros, V. (2001). An extensive class of small RNAs in Caenorhabditis elegans. Science *294*, 862-864.

Lee, Y., Ahn, C., Han, J., Choi, H., Kim, J., Yim, J., Lee, J., Provost, P., Radmark, O., Kim, S., *et al.* (2003). The nuclear RNase III Drosha initiates microRNA processing. Nature *425*, 415-419.

Lee, Y., Hur, I., Park, S.Y., Kim, Y.K., Suh, M.R., and Kim, V.N. (2006). The role of PACT in the RNA silencing pathway. EMBO J *25*, 522-532.

Lee, Y., Jeon, K., Lee, J.T., Kim, S., and Kim, V.N. (2002). MicroRNA maturation: stepwise processing and subcellular localization. EMBO J *21*, 4663-4670.

Lee, Y., Kim, M., Han, J., Yeom, K.H., Lee, S., Baek, S.H., and Kim, V.N. (2004). MicroRNA genes are transcribed by RNA polymerase II. EMBO J *23*, 4051-4060.

Lehrbach, N.J., Armisen, J., Lightfoot, H.L., Murfitt, K.J., Bugaut, A., Balasubramanian, S., and Miska, E.A. (2009). LIN-28 and the poly(U) polymerase PUP-2 regulate let-7 microRNA processing in Caenorhabditis elegans. Nat Struct Mol Biol *16*, 1016-1020.

Lemay, J.F., D'Amours, A., Lemieux, C., Lackner, D.H., St-Sauveur, V.G., Bahler, J., and Bachand, F. (2010). The nuclear poly(A)-binding protein interacts with the exosome to promote synthesis of noncoding small nucleolar RNAs. Mol Cell *37*, 34-45.

Lemieux, C., and Bachand, F. (2009). Cotranscriptional recruitment of the nuclear poly(A)-binding protein Pab2 to nascent transcripts and association with translating mRNPs. Nucleic Acids Res.

Lewis, B.P., Burge, C.B., and Bartel, D.P. (2005). Conserved seed pairing, often flanked by adenosines, indicates that thousands of human genes are microRNA targets. Cell *120*, 15-20.

Lewis, B.P., Shih, I.H., Jones-Rhoades, M.W., Bartel, D.P., and Burge, C.B. (2003). Prediction of mammalian microRNA targets. Cell *115*, 787-798.

Li, S., Lian, S.L., Moser, J.J., Fritzler, M.L., Fritzler, M.J., Satoh, M., and Chan, E.K. (2008). Identification of GW182 and its novel isoform TNGW1 as translational repressors in Ago2-mediated silencing. J Cell Sci *121*, 4134-4144.

Lin, S.Y., Johnson, S.M., Abraham, M., Vella, M.C., Pasquinelli, A., Gamberi, C., Gottlieb, E., and Slack, F.J. (2003). The C elegans hunchback homolog, hbl-1, controls temporal patterning and is a probable microRNA target. Dev Cell *4*, 639-650.

Liu, J., Rivas, F.V., Wohlschlegel, J., Yates, J.R., 3rd, Parker, R., and Hannon, G.J. (2005). A role for the P-body component GW182 in microRNA function. Nat Cell Biol *7*, 1261-1266.

Lund, E., Guttinger, S., Calado, A., Dahlberg, J.E., and Kutay, U. (2004). Nuclear export of microRNA precursors. Science *303*, 95-98.

Maroney, P.A., Denker, J.A., Darzynkiewicz, E., Laneve, R., and Nilsen, T.W. (1995). Most mRNAs in the nematode Ascaris lumbricoides are trans-spliced: a role for spliced leader addition in translational efficiency. RNA *1*, 714-723.

Mavrakis, K.J., Wolfe, A.L., Oricchio, E., Palomero, T., de Keersmaecker, K., McJunkin, K., Zuber, J., James, T., Khan, A.A., Leslie, C.S., *et al.* (2010). Genome-wide RNA-mediated interference screen identifies miR-19 targets in Notch-induced T-cell acute lymphoblastic leukaemia. Nat Cell Biol *12*, 372-379.

Meister, G., Landthaler, M., Peters, L., Chen, P.Y., Urlaub, H., Luhrmann, R., and Tuschl, T. (2005). Identification of novel argonaute-associated proteins. Curr Biol *15*, 2149-2155.

Miranda, K.C., Huynh, T., Tay, Y., Ang, Y.S., Tam, W.L., Thomson, A.M., Lim, B., and Rigoutsos, I. (2006). A pattern-based method for the identification of MicroRNA binding sites and their corresponding heteroduplexes. Cell *126*, 1203-1217.

Miyoshi, T., Takeuchi, A., Siomi, H., and Siomi, M.C. (2010). A direct role for Hsp90 in pre-RISC formation in Drosophila. Nat Struct Mol Biol *17*, 1024-1026.

Morlando, M., Ballarino, M., Gromak, N., Pagano, F., Bozzoni, I., and Proudfoot, N.J. (2008). Primary microRNA transcripts are processed co-transcriptionally. Nat Struct Mol Biol *15*, 902-909.

Mounsey, A., Bauer, P., and Hope, I.A. (2002). Evidence suggesting that a fifth of annotated Caenorhabditis elegans genes may be pseudogenes. Genome Res *12*, 770-775.

Nakamura, R., Takeuchi, R., Takata, K., Shimanouchi, K., Abe, Y., Kanai, Y., Ruike, T., Ihara, A., and Sakaguchi, K. (2008). TRF4 is involved in polyadenylation of snRNAs in Drosophila melanogaster. Mol Cell Biol *28*, 6620-6631.

Napoli, C., Lemieux, C., and Jorgensen, R. (1990). Introduction of a Chimeric Chalcone Synthase Gene into Petunia Results in Reversible Co-Suppression of Homologous Genes in trans. Plant Cell *2*, 279-289.

Newman, M.A., Thomson, J.M., and Hammond, S.M. (2008). Lin-28 interaction with the Let-7 precursor loop mediates regulated microRNA processing. RNA *14*, 1539-1549.

Nielsen, C.B., Shomron, N., Sandberg, R., Hornstein, E., Kitzman, J., and Burge, C.B. (2007). Determinants of targeting by endogenous and exogenous microRNAs and siRNAs. RNA *13*, 1894-1910.

Okamura, K., Hagen, J.W., Duan, H., Tyler, D.M., and Lai, E.C. (2007). The mirtron pathway generates microRNA-class regulatory RNAs in Drosophila. Cell *130*, 89-100.

Orom, U.A., and Lund, A.H. (2007). Isolation of microRNA targets using biotinylated synthetic microRNAs. Methods *43*, 162-165.

Orom, U.A., and Lund, A.H. (2009). Experimental identification of microRNA targets. Gene *451*, 1-5.

Orom, U.A., Nielsen, F.C., and Lund, A.H. (2008). MicroRNA-10a binds the 5'UTR of ribosomal protein mRNAs and enhances their translation. Mol Cell *30*, 460-471.

Ozsolak, F., Poling, L.L., Wang, Z., Liu, H., Liu, X.S., Roeder, R.G., Zhang, X., Song, J.S., and Fisher, D.E. (2008). Chromatin structure analyses identify miRNA promoters. Genes Dev *22*, 3172-3183.

Pasquinelli, A.E., Reinhart, B.J., Slack, F., Martindale, M.Q., Kuroda, M.I., Maller, B., Hayward, D.C., Ball, E.E., Degnan, B., Muller, P., *et al.* (2000). Conservation of the sequence and temporal expression of let-7 heterochronic regulatory RNA. Nature *408*, 86-89.

Pawlicki, J.M., and Steitz, J.A. (2008). Primary microRNA transcript retention at sites of transcription leads to enhanced microRNA production. J Cell Biol *182*, 61-76.

Peters, L., and Meister, G. (2007). Argonaute proteins: mediators of RNA silencing. Mol Cell *26*, 611-623.

Ramachandran, V., and Chen, X. (2008). Degradation of microRNAs by a family of exoribonucleases in Arabidopsis. Science *321*, 1490-1492.

Rehwinkel, J., Natalin, P., Stark, A., Brennecke, J., Cohen, S.M., and Izaurralde, E. (2006). Genome-wide analysis of mRNAs regulated by Drosha and Argonaute proteins in Drosophila melanogaster. Mol Cell Biol *26*, 2965-2975.

Reinhart, B.J., Slack, F.J., Basson, M., Pasquinelli, A.E., Bettinger, J.C., Rougvie, A.E., Horvitz, H.R., and Ruvkun, G. (2000). The 21-nucleotide let-7 RNA regulates developmental timing in Caenorhabditis elegans. Nature *403*, 901-906.

Resnick, T.D., McCulloch, K.A., and Rougvie, A.E. (2010). miRNAs give worms the time of their lives: small RNAs and temporal control in Caenorhabditis elegans. Dev Dyn *239*, 1477-1489.

Romano, N., and Macino, G. (1992). Quelling: transient inactivation of gene expression in Neurospora crassa by transformation with homologous sequences. Mol Microbiol *6*, 3343-3353.

Rougvie, A.E., and Ambros, V. (1995). The heterochronic gene lin-29 encodes a zinc finger protein that controls a terminal differentiation event in Caenorhabditis elegans. Development *121*, 2491-2500.

Roy, G., De Crescenzo, G., Khaleghpour, K., Kahvejian, A., O'Connor-McCourt, M., and Sonenberg, N. (2002). Paip1 interacts with poly(A) binding protein through two independent binding motifs. Mol Cell Biol *22*, 3769-3782.

Ruby, J.G., Jan, C.H., and Bartel, D.P. (2007a). Intronic microRNA precursors that bypass Drosha processing. Nature *448*, 83-86.

Ruby, J.G., Stark, A., Johnston, W.K., Kellis, M., Bartel, D.P., and Lai, E.C. (2007b). Evolution, biogenesis, expression, and target predictions of a substantially expanded set of Drosophila microRNAs. Genome Res *17*, 1850-1864.

Ruvkun, G., and Giusto, J. (1989). The Caenorhabditis elegans heterochronic gene lin-14 encodes a nuclear protein that forms a temporal developmental switch. Nature *338*, 313-319.

Rybak, A., Fuchs, H., Smirnova, L., Brandt, C., Pohl, E.E., Nitsch, R., and Wulczyn, F.G. (2008). A feedback loop comprising lin-28 and let-7 controls pre-let-7 maturation during neural stem-cell commitment. Nat Cell Biol *10*, 987-993.

Saito, K., Ishizuka, A., Siomi, H., and Siomi, M.C. (2005). Processing of pre-microRNAs by the Dicer-1-Loquacious complex in Drosophila cells. PLoS Biol *3*, e235.

Schwarz, D.S., Hutvagner, G., Du, T., Xu, Z., Aronin, N., and Zamore, P.D. (2003). Asymmetry in the assembly of the RNAi enzyme complex. Cell *115*, 199-208.

Selbach, M., Schwanhausser, B., Thierfelder, N., Fang, Z., Khanin, R., and Rajewsky, N. (2008). Widespread changes in protein synthesis induced by microRNAs. Nature *455*, 58-63.

Slack, F.J., Basson, M., Liu, Z., Ambros, V., Horvitz, H.R., and Ruvkun, G. (2000). The lin-41 RBCC gene acts in the C. elegans heterochronic pathway between the let-7 regulatory RNA and the LIN-29 transcription factor. Mol Cell *5*, 659-669.

Stark, A., Brennecke, J., Bushati, N., Russell, R.B., and Cohen, S.M. (2005). Animal MicroRNAs confer robustness to gene expression and have a significant impact on 3'UTR evolution. Cell *123*, 1133-1146.

Stark, A., Brennecke, J., Russell, R.B., and Cohen, S.M. (2003). Identification of Drosophila MicroRNA targets. PLoS Biol *1*, E60.

Steiner, F.A., Hoogstrate, S.W., Okihara, K.L., Thijssen, K.L., Ketting, R.F., Plasterk, R.H., and Sijen, T. (2007). Structural features of small RNA precursors determine Argonaute loading in Caenorhabditis elegans. Nat Struct Mol Biol *14*, 927-933.

Su, H., Meng, S., Lu, Y., Trombly, M.I., Chen, J., Lin, C., Turk, A., and Wang, X. (2011). Mammalian hyperplastic discs homolog EDD regulates miRNA-mediated gene silencing. Mol Cell *43*, 97-109.

Sulston, J.E., and Horvitz, H.R. (1977). Post-embryonic cell lineages of the nematode, Caenorhabditis elegans. Dev Biol *56*, 110-156.

Thomas, M., Lieberman, J., and Lal, A. (2010). Desperately seeking microRNA targets. Nat Struct Mol Biol *17*, 1169-1174.

Till, S., Lejeune, E., Thermann, R., Bortfeld, M., Hothorn, M., Enderle, D., Heinrich, C., Hentze, M.W., and Ladurner, A.G. (2007). A conserved motif in Argonaute-interacting proteins mediates functional interactions through the Argonaute PIWI domain. Nat Struct Mol Biol *14*, 897-903.

Tomari, Y., Du, T., and Zamore, P.D. (2007). Sorting of Drosophila small silencing RNAs. Cell *130*, 299-308.

Tritschler, F., Huntzinger, E., and Izaurralde, E. (2010). Role of GW182 proteins and PABPC1 in the miRNA pathway: a sense of deja vu. Nat Rev Mol Cell Biol *11*, 379-384.

van der Krol, A.R., Lenting, P.E., Jetty, V., van der Meer, I.M., Koes, R.E., Gerats, A.G.M., Mol, J.N.M., and Stutje, A.R. (1988). An anti-sense chalcone synthase gene in transgenic plants inhibits flower pigmentation. Nature *333*, 866-869.

van der Krol, A.R., Mur, L.A., Beld, M., Mol, J.N., and Stuitje, A.R. (1990). Flavonoid genes in petunia: addition of a limited number of gene copies may lead to a suppression of gene expression. Plant Cell *2*, 291-299.

Vella, M.C., Choi, E.Y., Lin, S.Y., Reinert, K., and Slack, F.J. (2004). The C. elegans microRNA let-7 binds to imperfect let-7 complementary sites from the lin-41 3'UTR. Genes Dev *18*, 132-137.

Vinther, J., Hedegaard, M.M., Gardner, P.P., Andersen, J.S., and Arctander, P. (2006). Identification of miRNA targets with stable isotope labeling by amino acids in cell culture. Nucleic Acids Res *34*, e107.

Viswanathan, S.R., Daley, G.Q., and Gregory, R.I. (2008). Selective Blockade of MicroRNA Processing by Lin-28. Science.

Wang, P.P., and Ruvinsky, I. (2010). Computational prediction of Caenorhabditis box H/ACA snoRNAs using genomic properties of their host genes. RNA *16*, 290-298.

Wang, Y., Juranek, S., Li, H., Sheng, G., Tuschl, T., and Patel, D.J. (2008a). Structure of an argonaute silencing complex with a seed-containing guide DNA and target RNA duplex. Nature *456*, 921-926.

Wang, Y., Sheng, G., Juranek, S., Tuschl, T., and Patel, D.J. (2008b). Structure of the guide-strand-containing argonaute silencing complex. Nature *456*, 209-213.

Wen, J., Parker, B.J., Jacobsen, A., and Krogh, A. (2011). MicroRNA transfection and AGO-bound CLIP-seq data sets reveal distinct determinants of miRNA action. RNA *17*, 820-834.

Wightman, B., Burglin, T.R., Gatto, J., Arasu, P., and Ruvkun, G. (1991). Negative regulatory sequences in the lin-14 3'-untranslated region are necessary to generate a temporal switch during Caenorhabditis elegans development. Genes Dev *5*, 1813-1824.

Wightman, B., Ha, I., and Ruvkun, G. (1993). Posttranscriptional regulation of the heterochronic gene lin-14 by lin-4 mediates temporal pattern formation in C. elegans. Cell *75*, 855-862.

Yekta, S., Shih, I.H., and Bartel, D.P. (2004). MicroRNA-directed cleavage of HOXB8 mRNA. Science *304*, 594-596.

Yi, R., Doehle, B.P., Qin, Y., Macara, I.G., and Cullen, B.R. (2005). Overexpression of exportin 5 enhances RNA interference mediated by short hairpin RNAs and microRNAs. RNA *11*, 220-226.

Zamore, P.D., Tuschl, T., Sharp, P.A., and Bartel, D.P. (2000). RNAi: double-stranded RNA directs the ATP-dependent cleavage of mRNA at 21 to 23 nucleotide intervals. Cell *101*, 25-33.

Zekri, L., Huntzinger, E., Heimstadt, S., and Izaurralde, E. (2009). The silencing domain of GW182 interacts with PABPC1 to promote translational repression and degradation of microRNA targets and is required for target release. Mol Cell Biol *29*, 6220-6231.

Zeng, Y., and Cullen, B.R. (2005). Efficient processing of primary microRNA hairpins by Drosha requires flanking nonstructured RNA sequences. J Biol Chem *280*, 27595-27603.

Zhang, L., Ding, L., Cheung, T.H., Dong, M.Q., Chen, J., Sewell, A.K., Liu, X., Yates, J.R., 3rd, and Han, M. (2007). Systematic identification of C. elegans miRISC proteins, miRNAs, and mRNA targets by their interactions with GW182 proteins AIN-1 and AIN-2. Mol Cell *28*, 598-613.

Zipprich, J.T., Bhattacharyya, S., Mathys, H., and Filipowicz, W. (2009). Importance of the C-terminal domain of the human GW182 protein TNRC6C for translational repression. RNA *15*, 781-793.

6. Appendix

A quantitative targeted proteomics approach to validate predicted microRNA targets in *C. elegans*

Marko Jovanovic[1–3,11], Lukas Reiter[1–3,10,11], Paola Picotti[4], Vinzenz Lange[4,5,10], Erica Bogan[1,2], Benjamin A Hurschler[6], Cherie Blenkiron[7,8,10], Nicolas J Lehrbach[7,8], Xavier C Ding[6], Manuel Weiss[1–3], Sabine P Schrimpf[1,3], Eric A Miska[7,8], Helge Großhans[6], Ruedi Aebersold[4,5,9] & Michael O Hengartner[1,3]

Efficient experimental strategies are needed to validate computationally predicted microRNA (miRNA) target genes. Here we present a large-scale targeted proteomics approach to validate predicted miRNA targets in *Caenorhabditis elegans*. Using selected reaction monitoring (SRM), we quantified 161 proteins of interest in extracts from wild-type and *let-7* mutant worms. We demonstrate by independent experimental downstream analyses such as genetic interaction, as well as polysomal profiling and luciferase assays, that validation by targeted proteomics substantially enriched for biologically relevant let-7 interactors. For example, we found that the zinc finger protein ZTF-7 was a bona fide let-7 miRNA target. We also validated predicted miR-58 targets, demonstrating that this approach is adaptable to other miRNAs. We propose that targeted mass spectrometry can be applied generally to validate candidate lists generated by computational methods or in large-scale experiments, and that the described strategy should be readily adaptable to other organisms.

MicroRNA (miRNAs) are short noncoding RNAs that bind to target mRNAs and negatively regulate gene expression. miRNAs are important in many developmental and disease-related processes[1]. A full understanding of miRNA function requires knowledge of their target mRNAs. In recent years much progress has been made experimentally and computationally to identify miRNA targets. One of the most widely used approaches to identify potential miRNA targets is to apply different target prediction algorithms[1]. However, the many algorithms available predict target sets with only limited overlap and cumulatively identify several hundred potential target mRNAs per miRNA. In addition, large-scale experiments undertaken to identify target mRNAs, such as studies based on mRNA profiling, pulldown of target mRNAs and to a certain extent based on genetics, also identified many potential miRNA targets[2,3]. Recent publications have clearly shown that using multiple independent experimental approaches greatly improves the reliability of the results obtained[4,5], but large-scale experiments are often cumbersome and time intensive. Therefore we aimed to establish a targeted quantification method to rapidly validate large numbers of potential miRNA targets.

We reasoned that such a method should measure the most relevant output of gene expression, namely miRNA-dependent changes in protein amounts from potential target genes. Moreover, to be worthwhile, the method should be easy to use, fast, sensitive, reproducible, quantitative and scalable, as several hundred proteins have to be tested for each miRNA. A technique that promises to fulfill most of those criteria is proteomics. Indeed several groups have shown that shotgun proteomics can be used to screen for miRNA targets[4,6]. However, with available shotgun proteomics approaches, the bulk of measurement time is spent on signals not arising from the desired candidate proteins. Moreover, many of the desired proteins might not be assayed owing to the stochastic sampling of the peptide ions that is common to this method. This results in loss of sensitivity and reproducibility to the extent that high-confidence data on candidate targets can only be achieved at a high cost of time and labor. In contrast, a targeted proteomics approach such as selected reaction monitoring (SRM)[7,8] has the potential for fast and reliable protein quantification of candidate genes. By limiting the measurement to the proteins of interest, the sensitivity and the reproducibility of the measurements increase dramatically. SRM assays can be developed by selecting for each candidate protein one or several proteotypic peptides that unambiguously identify a protein of interest and have favorable detection properties by mass spectrometry[9].

Here we describe the application of SRM and isotope-coded affinity tag (ICAT)[10] quantification to screen potential let-7 targets in *Caenorhabditis elegans*. Our targeted proteomics approach provided high-confidence quantification data, which we then mined to identify miRNA targets of biological importance. Independent downstream

[1]Institute of Molecular Life Sciences, University of Zurich, Zurich, Switzerland. [2]Doctorate Program in Molecular Life Sciences Zurich, Zurich, Switzerland. [3]Quantitative Model Organism Proteomics, University of Zurich, Zurich, Switzerland. [4]Institute of Molecular Systems Biology, ETH Zurich, Zurich, Switzerland. [5]Competence Center for Systems Physiology and Metabolic Diseases, Zurich, Switzerland. [6]Friedrich Miescher Institute for Biomedical Research, Basel, Switzerland. [7]Department of Biochemistry, University of Cambridge, Cambridge, UK. [8]Wellcome Trust/Cancer Research UK Gurdon Institute, University of Cambridge, Cambridge, UK. [9]Faculty of Science, University of Zurich, Zurich, Switzerland. [10]Present addresses: Biognosys AG, Zurich, Switzerland (L.R.), DKMS Life Science Lab, Dresden, Germany (V.L.) and Department of Molecular Medicine and Pathology, University of Auckland, Auckland, New Zealand (C.B.). [11]These authors contributed equally to this work. Correspondence should be addressed to M.O.H. (michael.hengartner@imls.uzh.ch) or R.A. (aebersold@imsb.biol.ethz.ch).

RECEIVED 26 JANUARY; ACCEPTED 23 AUGUST; PUBLISHED ONLINE 12 SEPTEMBER 2010; CORRECTED AFTER PRINT 9 NOVEMBER 2010; DOI:10.1038/NMETH.1504

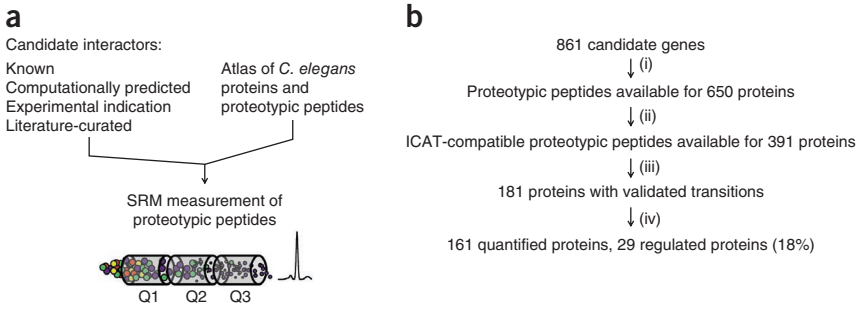

Figure 1 | Strategy and workflow for quantification of potential *C. elegans* let-7–interacting genes. (**a**) Proteins of interest were compiled based on predictions, literature search and previous experiments. Proteotypic peptides for these proteins of interest were selected from the *C. elegans* proteome atlas[14]. The selected proteotypic peptides were used as probes for reproducible quantification by SRM on a QTrap mass spectrometer operated as a triple quadrupole instrument. (**b**) From the initial 861 genes, 650 proteins had proteotypic peptides in the *C. elegans* proteome atlas (i), of which 391 had cysteine-containing peptides and were quantifiable by ICAT (ii). Validated transitions were derived for 181 proteins (iii), of which 161 could be quantified (iv). Of these, 29 proteins showed significant changes in abundance ($P < 0.01$) between wild type and *let-7(n2853)* mutants (iv).

experiments, including genetic studies, polysomal profiling and luciferase assays, confirmed that the candidate genes classified as regulated by let-7 based on our protein quantification data were indeed enriched in let-7 interactors. In addition, we showed that the described method was easily adaptable to another miRNA, miR-58, and quantification strategies other than ICAT, such as metabolic labeling.

RESULTS

SRM-based validation of potential let-7 target genes

To quantify proteins of interest in a complex whole-worm extract generated from *C. elegans*, we developed a protocol combining ICAT sample labeling and SRM mass spectrometry (**Supplementary Fig. 1** and **Supplementary Results 1**). To test the utility of this protocol, we applied it to screen several hundred potential let-7 miRNA targets. We focused on *let-7* because it is highly conserved from *C. elegans* to humans[11] and is one of the best studied nematode miRNAs[12]. We used for our studies the hypomorphic allele *let-7(n2853)*, which contains a point mutation in the mature *let-7* seed sequence that also results in reduced *let-7* expression[13].

We outline the experimental strategy used to quantify potential let-7 targets in **Figure 1**. Briefly, we compiled a list of potential let-7 targets based on predictions from five different algorithms, experimental data (for example, microarray analysis, RNA interference (RNAi) screens and others) and published literature, including known let-7 target genes. We also included control genes that we knew to be altered in *let-7* mutant worms owing to secondary effects (B.A.H. and H.G., unpublished data) and randomly chosen genes which served as 'neutral controls'; the final list comprised 861 candidate genes (**Supplementary Table 1** and Online Methods). Proteotypic peptides for 650 proteins of these 861 genes of interest were present in the *C. elegans* proteome atlas[14,15], a recently published large *C. elegans* proteomics dataset, in which 8,608 proteins, or about 40% of the proteome, had been identified by shotgun proteomics experiments. For 391 of these, we observed cysteine-containing peptides, a prerequisite for applying ICAT quantification. We experimentally confirmed the presence of 181 (46%) of these 391 proteins by SRM-triggered product ion scan (MS2) measurements in fractionated extracts from synchronized fourth larval stage (L4) worms.

We next compared the abundance of these 181 proteins in synchronized *let-7 (n2853)* mutants and wild-type late L4 larvae (when let-7 expression is highest) in three biological replicates. Most target proteins (139) could be quantified in all three biological replicates, another 15 in two replicates and seven in one replicate, yielding quantification data for a majority of the identified proteins (161 of 181; 89%) and confirming the high reproducibility of this method (**Fig. 2a** and **Supplementary Table 2**). We computed normalized $\log_2$ ratios (*let-7(n2853)* versus wild type) and corresponding *P* values for all 161 proteins (**Fig. 2b** and **Supplementary Table 2**).

Twenty-nine proteins had a significant difference in expression in *let-7(n2853)* mutants when compared to wild-type worms ($P < 0.01$, one-sample Student's *t*-test; **Fig. 2c** and **Supplementary Table 3**): 10 proteins were downregulated and 19 proteins upregulated in *let-7(n2853)* worms. As expected, the two control genes *vit-2* and *vit-6*, which had greatly reduced mRNA amounts in *let-7(n2853)* mutants (B.A.H. and H.G., unpublished data) were also strongly downregulated in our assay (13-fold and 23-fold, respectively; **Supplementary Table 3**). The upregulated proteins included LET-526 (also known as LSS-4), the only previously reported let-7 target[16] whose abundance we could measure. Our SRM measurements suggest that the two splice variants of LET-526 responded differently to let-7: whereas a peptide specific for the LET-526a splice form showed a strong, 3.1-fold upregulation, a second peptide, matching to a region common to both splice isoforms, displayed only a weak 1.2-fold upregulation in *let-7(n2853)* mutants when compared to wild-type worms (**Supplementary Fig. 2a**,**b**). We confirmed and validated this splice variant–specific response by polysomal profiling (**Supplementary Fig. 2c** and **Supplementary Results 2**).

Also among the proteins that had significant changes ($P < 0.01$) in expression were 15 of the 66 computationally predicted let-7 targets, and 9 of the 53 proteins whose mRNA do not contain a predicted let-7 target site but that have been linked to *let-7* through other experimental approaches or the literature (**Supplementary Table 3**). By contrast, only 2 of the 39 of the randomly picked 'neutral controls' had a significant abundance change ($P < 0.01$). The 'neutral controls' were the only significantly underrepresented group among the regulated proteins ($P = 0.016$, Fisher's exact test). This low 'hit rate' for these randomly tested proteins confirmed that our initial candidate list was enriched for let-7 miRNA target genes.

Whether the regulated candidates are primary or secondary targets of let-7 cannot be determined from the protein ratios. Although the most straightforward explanation for proteins downregulated in *let-7(n2853)* mutants is secondary effects, miRNAs have recently been reported to act as positive regulators under certain conditions[17]. A gain of function caused by the point mutation in the seed region of the mature let-7 miRNA in *let-7(n2853)* mutants, resulting in better binding to a suboptimal seed sequence, also cannot be excluded at this point.

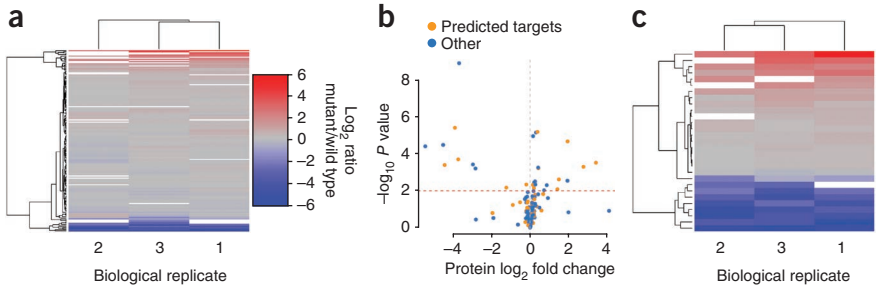

Figure 2 | Identification of proteins regulated by let-7. (**a**) Heat map and hierarchical clustering of the 161 quantified proteins in three biological replicates. Red and blue indicate up- and downregulated proteins in *let-7(n2853)* mutants, respectively. (**b**) Volcano plot showing normalized mean $\log_2$ ratios (vertical gray line indicates no change in expression: $\log_2$ ratio(*let-7(n2853)*/wild type) = 0) and probability of regulation (−log(*P* value)) of the measured proteins. All proteins above the dotted red line ($P = 0.01$) were considered to be significantly regulated ($P < 0.01$). (**c**) Heat map and hierarchical clustering of the 29 significantly regulated proteins ($P < 0.01$). Color bar as in **a**.

SRM-based validation enriches for let-7 genetic interactors

let-7(n2853) mutant worms grown at 25 °C die at the adult stage because of vulval bursting. RNAi knockdown of known let-7 miRNA targets has been shown in some cases to rescue this lethality to different extents[16]. To determine whether the positive hits in our proteomics screen are indeed enriched in let-7 targets, we knocked down all 29 genes that showed protein changes in *let-7(n2853)* mutants (up- or downregulated) to determine whether they could suppress the *let-7(n2853)* lethal phenotype. Six of the 29 genes knocked down by RNAi caused either larval arrest or lethality, and thus could not be scored for suppression of vulval bursting. For the remaining 23 genes tested, ten reproducibly rescued the lethality to at least 20%, whereas less than 5% of the *let-7(n2853)* worms treated with negative control RNAi survived as adults (**Fig. 3a** and **Supplementary Table 4**). As expected, the vast majority (9/10) of the suppressors were genes that were upregulated in *let-7(n2853)* mutants (and whose overexpression could thus be compensated via RNAi knockdown). As a control, we performed a similar experiment using 29 candidate genes that did not show significant protein changes ($P > 0.1$) in our targeted proteomics assay. Again, five genes either caused early larval arrest or lethality and could not be characterized further. Only three out of the remaining 24 candidates rescued the lethality (**Fig. 3b** and **Supplementary Table 5**), demonstrating that the regulated protein set is significantly enriched for genes that genetically interact with let-7 ($P = 0.024$ for all regulated genes, $P = 0.013$ considering only the upregulated genes, Fischer's exact test; **Supplementary Fig. 3**). We conclude that our targeted proteomics method can indeed be used to enrich for miRNA interaction partners from a list of candidate genes.

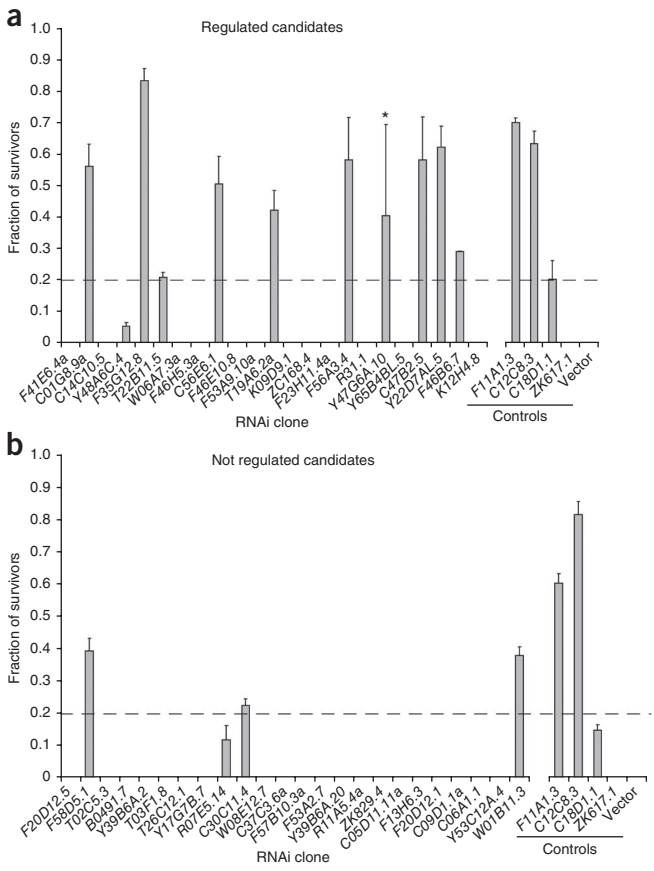

Figure 3 | Genes displaying protein changes in *let-7(n2853)* mutants are enriched in *let-7* suppressors. (**a**) RNAi knockdown of 23 genes that showed significant protein changes ($P < 0.01$) and 5 control genes. The controls included two negative controls (vector and *ZK617.1* (*unc-22*) RNAi) and three positive controls (*F11A1.3* (*daf-12*), *C12C8.3* (*lin-41*) and *C18D1.1* (*die-1*) RNAi). Only survival rates above 5% are shown. (**b**) As a control, 24 candidates that did not show a significant protein amount change ($P > 0.1$) in the *let-7(n2853)* mutant worms in our targeted proteomics assay were tested as in **a**, including the same positive and negative controls. Error bars, s.e.m. ($n = 3$). *, suppression in two out of three replicate experiments. The candidate was regarded as positive as the average survival rate over all three replicates was above the threshold. Dashed lines indicate survival rate of 20%.

Partial correlation between protein and mRNA abundances

In addition to causing translational repression, miRNAs can also lead to degradation of their targets[1]. To determine whether the changes in protein levels that we observed could also be captured at the mRNA level, we determined by reverse transcription–quantitative PCR transcript amounts of all 161 proteins as well as of the well established let-7 targets *daf-12* and *lin-41*, in wild-type and *let-7(n2853)* worms (**Supplementary Table 6**). The amounts of both *daf-12* and *lin-41* mRNA were significantly upregulated in *let-7(n2853)* mutants ($P = 0.006$ and 0.048, respectively, one-sided one sample Student's *t*-test), as has been reported previously[18,19]. Whereas some proteins had very good correlation between changes in amounts of mRNA and protein, others, including the known let-7 target *let-526*, showed substantial changes in protein amounts but no strong changes in mRNA amounts (**Fig. 4a**). As our method cannot distinguish primary from secondary targets, we do not know at this point whether the proteins that showed strong protein changes but no mRNA changes are primary let-7 targets.

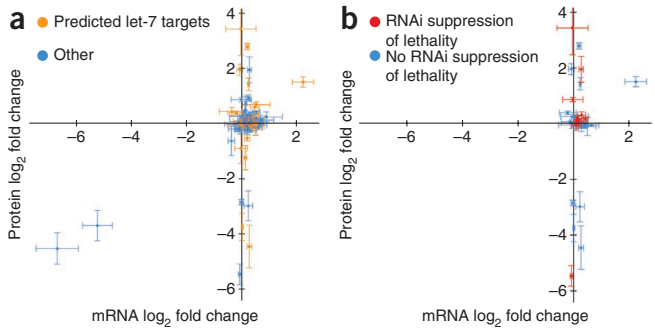

Figure 4 | Comparison of let-7–dependent changes in protein and transcript amounts of candidate let-7 miRNA targets. (**a**,**b**) Log_2 fold changes at the mRNA (*x* axis) and protein (*y* axis) level between *let-7(n2853)* mutant and wild-type worms for all 161 proteins measured (**a**) and the subgroup of the 47 candidates scored by RNAi (**b**). Error bars, s.e.m. ($n = 3$).

We next focused our attention on the 47 genes that we previously tested for suppression of *let-7(n2853)* lethality (see above). Whereas many of the 13 RNAi suppressors showed large changes in protein amounts in *let-7(n2853)* mutants, their mRNA levels varied only weakly, if at all (**Fig. 4b**). We conclude that many of the protein changes we detected in our targeted proteomics approach are not recapitulated on the mRNA level, and that although mRNA profiling can identify many primary targets[4,5], it would not detect several of the biologically important candidates revealed by protein quantification.

zft-7 is a bona fide let-7 target gene

One of the most interesting candidates from our RNAi screen was *ztf-7* (F46B6.7), a gene belonging to the zinc finger transcription factor family, as knockdown of this gene not only suppressed lethality (**Fig. 3** and **Supplementary Table 4**) but also the sterility observed in *let-7(n2853)* mutants at 25 °C (data not shown). Of the genes that we tested, only the two positive controls *daf-12* and *lin-41* could also suppress both defects. Consistent with our RNAi results, lethality was strongly reduced in *ztf-7(tm600);let-7(n2853)* double mutant worms when compared to the *let-7(n2853)* single mutants (**Fig. 5a**).

Our SRM measurements had indicated that ZTF-7 protein levels are elevated by ~10% in *let-7(n2853)* mutants when compared to wild-type worms. Although this increase is admittedly mild, it was reproducible across all three biological replicates and significant ($P = 0.005$, one-sample Student's *t*-test; **Supplementary Table 3**).

As *ztf-7* is predicted to contain a conserved perfect seed complementary let-7 binding site in its 3′ untranslated region (UTR)[20,21] we next tested whether the *ztf-7* 3′ UTR could confer let-7–dependent regulation of a reporter transcript. It has been reported that certain *C. elegans* 3′ UTRs can elicit an miRNA-dependent response in human cell lines[22]. As the sequence of the mature let-7 miRNA is identical in worms and in humans[11], we could rapidly test the effect of both overexpression and depletion of human let-7a miRNA in HeLa cells, which we transfected with a dual luciferase plasmid in which the *ztf-7* 3′ UTR was cloned directly downstream of the firefly luciferase gene (*luciferase::ztf-7 3′ UTR*). Indeed, we observed a strong response of the *luciferase::ztf-7 3′ UTR* reporter to both human let-7a up- and downregulation (**Fig. 5b**).

Taken together, our proteomic, genetic and reporter assays strongly suggest that *ztf-7* is a bona fide let-7 miRNA target. Moreover, *ztf-7* also has been identified recently as a potential let-7 target by a new approach[23], providing independent support for our claim. Additionally that method also allowed mapping of the binding site, which overlapped perfectly with the predicted conserved seed site. Further work will be required to understand the function of ZTF-7 in *C. elegans* development.

A streamlined pipeline for miRNA target validation

To test the generality of our targeted proteomics approach, we performed a second experiment to validate predicted targets of miR-58. *mir-58* is of particular interest as it is part of an miRNA gene family. Whereas the single *mir-58* family mutants show no obvious defect, the whole-family knockout is severely sick[24]. Therefore, it was unclear whether predicted miR-58 targets would show substantial changes in single mutants.

In this second experiment we introduced several technical improvements. First, to target the full peptide repertoire of *C. elegans* and not just cysteine-containing peptides, we used metabolically heavy isotope–labeled worms[25] as a quantification standard. Second, we used crude chemically synthesized peptides to establish and optimize the SRM assays[26]. Third, we applied a newly developed algorithm that automatically assigns peak groups to their corresponding peptides and controls the false discovery rate (FDR) of those assignments (L.R., O. Rinner, P.P., R. Hüttenhain, M. Beck, M. Brusniak *et al.*, unpublished data).

The TargetScan[20,21] program predicted 118 miR-58 target genes in *C. elegans*. To validate this candidate list, we used crude synthetic peptides for all 118 proteins to develop and optimize SRM assays. We also developed SRM assays for 42 'neutral control' genes that we randomly selected from 5,000 genes that were well expressed in L4 hermaphrodites (data not shown). We next measured the relative amounts of as many of these proteins as possible directly in complex, unfractionated extracts derived from staged L4 wild-type and *mir-58(n4640)* mutant worms. Applying a 5% FDR cutoff for the correct peak assignment, we quantified 27 of the 118 predicted targets and 24 of the 42 randomly chosen proteins in at least one replicate pair

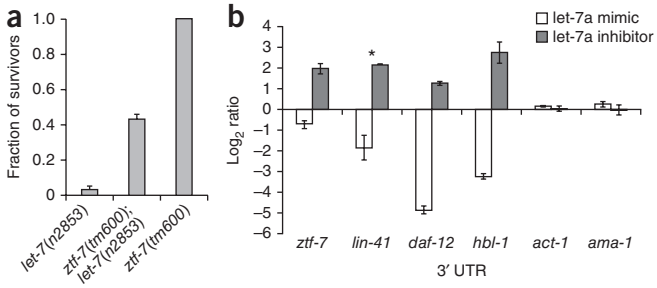

Figure 5 | *ztf-7* (*F46B6.7*) is a bona fide let-7 target gene. (**a**) Analysis of worm survival 12 h after L4 in the indicated mutants. Error bars, s.e.m. ($n = 4$). (**b**) Relative luciferase activities for reporter constructs containing the indicated 3′-UTR sequences. The let-7a readouts (mimics and inhibitors) were normalized to their respective oligo controls. The 3′ UTRs of the known targets *C12C8.3* (*lin-41*), *F11A1.3* (*daf-12*) and *F13D11.2* (*hbl-1*) were positive controls, and the 3′ UTRs of *F36A4.7* (*ama-1*) and *T04C12.6* (*act-1*) were negative controls[16]. Transfections were performed in triplicate for all candidates but *lin-41* (*), which was only transfected in duplicate. Error bars, s.e.m.

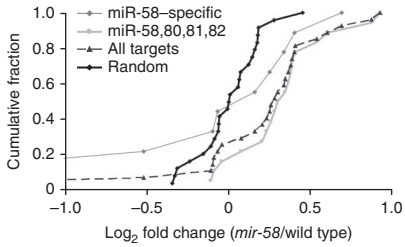

Figure 6 | Predicted miR-58 targets are significantly upregulated in *mir-58(n4640)* mutants. Cumulative fraction plots of the protein response of all 27 measured, predicted miR-58 targets (predicted by TargetScan[20,21]) as well as of the two subgroups of only miR-58–specific targets (9 of 27) and targets common to all miR-58 family members (miR-58, -80, -81 and -82; 18 of 27) and of a random gene group upon *mir-58* knockout. Data are shown as $\log_2$ ratios (*mir-58(n4640)* to wild type). Both the overall group as well as the whole family subgroup were significantly upregulated in *mir-58(n4640)* mutant worms when compared to the proteins that we randomly chose ($P < 10^{-3}$, Kolmogorov-Smirnov test).

(**Supplementary Table 7**). Predicted miR-58 targets were, as a group, significantly more likely to be upregulated in *mir-58(n4640)* mutant worms when compared to the randomly chosen control group (**Fig. 6**; $P < 10^{-3}$, Kolmogorov-Smirnov test). Consistent with this observation, we found that 4 of 27 predicted targets, compared to 1 of 24 control proteins, were significantly upregulated in *mir-58(n4640)* mutant worms ($P < 0.05$, one-sided, one-sample Student's *t*-test; **Supplementary Table 7**).

miR-58 is a member of a highly abundant miRNA family that also includes miR-80, miR-81, miR-82 and the recently discovered miR-1834 (ref. 24). As expected, TargetScan predicts largely overlapping sets of targets for the various miR-58 family members. Thus, the miR-58 family might show substantial redundancy, as loss of a single miRNA might be compensated by the other family members. Consistent with this hypothesis, single *mir-58* family mutants are all overtly wild type, whereas the *mir-58,80,81,82* quadruple mutant is severely sick. Despite this redundancy at the organismal level, we found that targets predicted to be bound by all miR-58 family members (18 of 27) still showed a significant increase in abundance in *mir-58(n4640)* mutants (**Fig. 6**; $P < 10^{-3}$, Kolmogorov-Smirnov test). Analysis of protein amounts in the family knockout will be necessary to determine the exact extent of compensation that occurs, if any, in this miRNA family.

DISCUSSION

Our results demonstrate that a targeted proteomics approach can be used to find biologically relevant candidate miRNA targets. First, our method measures changes in protein levels, arguably the most relevant assay for miRNA activity. Second, our approach allows for quantification of several hundred proteins and thus has a much higher throughput than traditional protein quantification methods such as immunoblotting. Additionally, it is much faster and cheaper to develop suitable mass spectrometric assays than immunoassays[26]. Moreover, once an SRM assay is established for a protein, it becomes universally useful and exportable[8,27]. Thus, others can readily use the SRM assays we established for the 312 *C. elegans* proteins that we measured (**Supplementary Tables 8** and **9**). Third, because it focuses on highly responsive peptides, our SRM-based approach is highly sensitive and reproducible. Indeed, we reproducibly measured changes as small as 10% in total protein abundance, as exemplified with ZTF-7. This high accuracy is particularly important in the analysis of potential miRNA targets, as miRNAs have been shown to mostly induce small changes in target gene expression[4,6].

Despite the clear value of our targeted proteomics approach, several challenges remain. First, although we achieved high sensitivity, we still did not quantify a substantial fraction of the proteins in our target list. Technical improvements, such as using a combination of chemically synthesized peptides and sample fractionation, could potentially boost the sensitivity by an order of magnitude, as has previously been shown in yeast[7]. Second, the targeted proteomics approach cannot be used to distinguish primary from secondary targets. Additional experiments will thus invariably be necessary to establish which hits are direct targets, as we did for *ztf-7*.

We also stress that the applicability of our targeted proteomics method to whole organs or whole animals is particularly challenging, as the miRNA of interest might be of low abundance or have a highly restricted expression pattern. We therefore conclude that our method will function best in situations in which sufficient material can readily be obtained and the sample is homogenous (for example, cell lines; **Supplementary Discussion**).

The targeted proteomics approach described here should be considered complementary to the shotgun proteomics approaches recently reported to identify miRNA targets[4,6]. Whereas shotgun proteomics should be regarded as one of several discovery tools that can be used to find potential new miRNA target candidates, a targeted proteomics approach should be perceived as a validation and hypothesis–driven tool with high sensitivity, reproducibility and accuracy.

Although here we validated miRNA targets in *C. elegans*, the targeted proteomics method is broadly applicable and could be readily adapted to study other organisms and other biological questions. Many quantification methods are available[28], suitable for nearly every extract composition. In addition, public proteomics databases for many organisms are available, from which experimentally identified proteins and their corresponding proteotypic peptides can be easily mined[29,30]. Even for organisms for which such proteomics data are not readily accessible, sophisticated proteotypic peptide prediction algorithms[9] can be used to target the right peptides. Thus, the targeted proteomics approach described here can be applied generally to measure protein abundances of candidate lists generated by computational methods or in large-scale experiments.

METHODS

Methods and any associated references are available in the online version of the paper at http://www.nature.com/naturemethods/.

Note: Supplementary information is available on the Nature Methods website.

ACKNOWLEDGMENTS

We thank R.F. Ketting (Hubrecht Institute, Utrecht) and B.B. Tops (Utrecht University, Utrecht) for providing the metabolically labeled *C. elegans* sample, A. Stark (Research Institute of Molecular Pathology, Vienna) for sharing miRNA target predictions for *C. elegans*, M. Moser for the assistance with the reverse transcription–quantitative PCR assays, B. Roschitzky and B. Gerrits for technical support, H. Rehrauer for statistical support, R. Schlapbach for access to the Functional Genomics Center Zurich, members of the Hengartner, Aebersold, Grosshans and Miska laboratories and E. Brunner and the whole Quantitative Model Organism Proteomics team for insightful discussion and comments on the

manuscript. This work was funded in part by the University of Zurich Research Priority Program in Systems Biology/Functional Genomics, the Swiss National Science Foundation, the Gerbert Rüf Foundation, the Swiss initiative for systems biology, SystemsX, the Ernst Hadorn Foundation and the ETH Zurich. R.A. was supported by the European Research Council grant ERC-2008-AdG 233226. M.J. and L.R. were supported by a grant from the Research Foundation of the University of Zurich. M.J. was also supported by a fellowship from the Roche Research Foundation. P.P. was supported by the Marie Curie Intra-European fellowship. V.L. was supported by a grant from F. Hoffmann-La Roche Ltd. to the Competence Center for Systems Physiology and Metabolic Diseases. H.G. was supported by the Swiss National Research Foundation, the Novartis Research Foundation and by an ERC Starting Investigator grant (miRTurn). X.C.D. was supported by a Boehringer Ingelheim Funds PhD Student fellowship. C.B., N.J.L. and E.A.M. were supported by a Cancer Research UK Programme grant to E.A.M.

AUTHOR CONTRIBUTIONS

M.J., L.R., M.O.H. and R.A. designed the experiments and wrote the paper. L.R. and M.J. did the majority of the data analysis. M.J. did the majority of the experiments. P.P. and V.L. contributed to and supervised the SRM experiments. E.B. contributed to the RNAi and reverse transcription–quantitative PCR experiments. B.A.H. and X.C.D. performed the polysomal profiling experiments. C.B. and N.J.L. contributed to the reporter assays. S.P.S. and M.W. provided the *C. elegans* proteome atlas. H.G. and E.A.M. provided critical input on the manuscript, contributed to the experimental design and the data analysis. M.O.H. and R.A. supervised the project.

COMPETING FINANCIAL INTERESTS

The authors declare no competing financial interests.

Published online at http://www.nature.com/naturemethods/.
Reprints and permissions information is available online at http://npg.nature.com/reprintsandpermissions/.

1. Bartel, D.P. MicroRNAs: target recognition and regulatory functions. *Cell* **136**, 215–233 (2009).
2. Lai, E.C. miRNAs: whys and wherefores of miRNA-mediated regulation. *Curr. Biol.* **15**, R458–R460 (2005).
3. Ørom, U.A. & Lund, A.H. Experimental identification of microRNA targets. *Gene* **451**, 1–5 (2010).
4. Baek, D. *et al.* The impact of microRNAs on protein output. *Nature* **455**, 64–71 (2008).
5. Hendrickson, D.G. *et al.* Concordant regulation of translation and mRNA abundance for hundreds of targets of a human microRNA. *PLoS Biol.* **7**, e1000238 (2009).
6. Selbach, M. *et al.* Widespread changes in protein synthesis induced by microRNAs. *Nature* **455**, 58–63 (2008).
7. Picotti, P., Bodenmiller, B., Mueller, L.N., Domon, B. & Aebersold, R. Full dynamic range proteome analysis of *S. cerevisiae* by targeted proteomics. *Cell* **138**, 795–806 (2009).
8. Picotti, P. *et al.* A database of mass spectrometric assays for the yeast proteome. *Nat. Methods* **5**, 913–914 (2008).
9. Mallick, P. *et al.* Computational prediction of proteotypic peptides for quantitative proteomics. *Nat. Biotechnol.* **25**, 125–131 (2007).
10. Gygi, S.P. *et al.* Quantitative analysis of complex protein mixtures using isotope-coded affinity tags. *Nat. Biotechnol.* **17**, 994–999 (1999).
11. Pasquinelli, A.E. *et al.* Conservation of the sequence and temporal expression of let-7 heterochronic regulatory RNA. *Nature* **408**, 86–89 (2000).
12. Bussing, I., Slack, F. & Großhans, H. let-7 microRNAs in development, stem cells and cancer. *Trends Mol. Med.* **14**, 400–409 (2008).
13. Reinhart, B.J. *et al.* The 21-nucleotide let-7 RNA regulates developmental timing in *Caenorhabditis elegans*. *Nature* **403**, 901–906 (2000).
14. Schrimpf, S.P. *et al.* Comparative functional analysis of the *Caenorhabditis elegans* and *Drosophila melanogaster* proteomes. *PLoS Biol.* **7**, e48 (2009).
15. Reiter, L. *et al.* Protein identification false discovery rates for very large proteomics data sets generated by tandem mass spectrometry. *Mol. Cell. Proteomics* **8**, 2405–2417 (2009).
16. Großhans, H., Johnson, T., Reinert, K., Gerstein, M. & Slack, F. The temporal patterning microRNA regulates several transcription factors at the larval to adult transition in *C. elegans*. *Dev. Cell* **8**, 321–330 (2005).
17. Vasudevan, S., Tong, Y. & Steitz, J.A. Switching from repression to activation: microRNAs can up-regulate translation. *Science* **318**, 1931–1934 (2007).
18. Bagga, S. *et al.* Regulation by let-7 and lin-4 miRNAs results in target mRNA degradation. *Cell* **122**, 553–563 (2005).
19. Ding, X.C. & Großhans, H. Repression of *C. elegans* microRNA targets at the initiation level of translation requires GW182 proteins. *EMBO J.* **28**, 213–222 (2009).
20. Lewis, B.P., Burge, C.B. & Bartel, D.P. Conserved seed pairing, often flanked by adenosines, indicates that thousands of human genes are microRNA targets. *Cell* **120**, 15–20 (2005).
21. Ruby, J.G. *et al.* Large-scale sequencing reveals 21U-RNAs and additional microRNAs and endogenous siRNAs in *C. elegans*. *Cell* **127**, 1193–1207 (2006).
22. Nottrott, S., Simard, M.J. & Richter, J.D. Human let-7a miRNA blocks protein production on actively translating polyribosomes. *Nat. Struct. Mol. Biol.* **13**, 1108–1114 (2006).
23. Andachi, Y. A novel biochemical method to identify target genes of individual microRNAs: Identification of a new *Caenorhabditis elegans* let-7 target. *RNA* **14**, 2440–2451 (2008).
24. Alvarez-Saavedra, E. & Horvitz, H.R. Many families of *C. elegans* microRNAs are not essential for development or viability. *Curr. Biol.* **20**, 367–373 (2010).
25. Krijgsveld, J. *et al.* Metabolic labeling of *C. elegans* and *D. melanogaster* for quantitative proteomics. *Nat. Biotechnol.* **21**, 927–931 (2003).
26. Picotti, P. *et al.* High-throughput generation of selected reaction-monitoring assays for proteins and proteomes. *Nat. Methods* **7**, 43–46 (2010).
27. Addona, T.A. *et al.* Multi-site assessment of the precision and reproducibility of multiple reaction monitoring-based measurements of proteins in plasma. *Nat. Biotechnol.* **27**, 633–641 (2009).
28. Mueller, L.N., Brusniak, M., Mani, D.R. & Aebersold, R. An assessment of software solutions for the analysis of mass spectrometry based quantitative proteomics data. *J. Proteome Res.* **7**, 51–61 (2008).
29. Brunner, E. *et al.* A high-quality catalog of the *Drosophila melanogaster* proteome. *Nat. Biotechnol.* **25**, 576–583 (2007).
30. Baerenfaller, K. *et al.* Genome-scale proteomics reveals *Arabidopsis* thaliana gene models and proteome dynamics. *Science* **320**, 938–941 (2008).

ONLINE METHODS

Mutations and strains. All mutants used in this study were derived from the wild-type variety Bristol strain N2. The following mutations were used: LGIII, *unc-119(ed3)* (ref. 31); LGIV, *miR-58(n4640)* (ref. 32); LGV, *ztf-7(tm600)* (http://www.wormbase.org/); LGX, *let-7(n2853)* (ref. 13); *ain-1(ku322)* (ref. 33); *alg-1(tm492)*; and transgene, *opIs205* ($P_{eft\text{-}3}$::TAPtag::*alg-1*(genomics+3′UTR);*unc-119*(+)). The *alg-1 (tm492)* mutant was obtained from the laboratory of S. Mitani (Tokyo Women's Medical University Hospital) and outcrossed four times. The 610-bp deletion was confirmed by PCR amplification.

For the miR-58–related experiments only, the transgenic line carrying *opIs205* was crossed into *alg-1(tm492)* mutant worms to generate the strain WS4303 (*alg-1(tm492);opIs205*), to which we refer as 'wild type'. WS4303 was also crossed into *mir-58(n4640)* worms to generate the strain WS5041 (*mir-58(n4640); alg-1(tm492); opIs205*), to which we refer to as '*mir-58(n4640)*'.

Sample preparation for let-7–related experiments. *C. elegans* strains were grown as described previously[34] at either 15 °C or 25 °C.

C. elegans wild-type strain N2 (Bristol) and the *let-7(n2853)* mutant strain MT7626 were grown on 9-cm nematode growth medium (NGM) agar plates seeded with a lawn of the *Escherichia coli* strain OP50. N2 and *let-7(n2853)* worms were always grown in parallel (three biological replicates total). Protein extracts were generated from synchronized late L4 larval stage worms (before vulval bursting), which were grown at 25 °C. Worms were collected and washed three times in M9 medium. Generation of the protein extract has been described previously[14]. The protein concentrations of the purified extracts were determined by using the Bradford reagent (Sigma-Aldrich). The protein concentrations of N2 and *let-7(n2853)* extracts were adjusted to each other to minimize biases for the subsequent ICAT (Applied Biosystems) labeling[10].

ICAT labeling, tryptic digestion of the samples, and the isolation and clean up of ICAT labeled cysteine-containing peptides were performed as described previously[35]. N2 extracts were always labeled with the heavy ICAT reagent and *let-7(n2853)* extracts with the light ICAT reagent. A total of 5 mg per sample and replicate was labeled, resulting in ~500 µg of ICAT-labeled peptides. The resulting peptide samples were separated according to the isoelectric point of the peptides by off-gel electrophoresis and then cleaned as previously described[7]. All peptide samples were dried in a vacuum centrifuge, resolubilized in 2% acetonitrile and 0.1% formic acid and frozen at –20 °C until analyzed on the mass spectrometer.

Reverse transcription–quantitative PCR (RT-qPCR). Before protein isolation, a small aliquot of intact worms of each biological replicate (three times N2 wild-type worms and three times *let-7(n2853)* worms; see above) was frozen, and then used for total RNA isolation. Total RNA was isolated using the Nucleo Spin RNA II kit (Macherey-Nagel) according to the manufacturer's instructions. After total RNA isolation, genomic DNA was further digested by DNase I using the Turbo DNA-free kit (Ambion) according to the manufacturer's instructions. Total RNA concentrations were determined with the Nanodrop device (Thermo Fisher Scientific). RNA reverse transcription was performed using the Transcriptor High Fidelity cDNA Synthesis kit (Roche) with oligo-(dT) primers, according to the manufacturer's recommendations using equal amounts of RNA (4 × 2 µg) for each sample. qPCR reactions were performed in technical duplicate for each of the biological triplicates using MESA Green qPCR Mastermix Plus for SYBR Assay (Eurogentec), according to the manufacturer's recommendations, on an ABI 7900 HT Sequence Detection System coupled to ABI Prism 7900 SDS 2.2 Software (Applied Biosystems). Relative transcript amouts were calculated using the $2^{-\Delta\Delta Ct}$ method[36]. The following genes were used as internal control genes for normalization: *F11C3.3* (*unc-54*), *T03F1.3* (*pgk-1*), *F43C1.2* (*mpk-1*), *T20B12.2* (*tbp-1*) and *F36A4.7* (*ama-1*). Most primer pairs were designed via the Roche Universal Probe Library. All the primer pairs used are listed in **Supplementary Table 10**.

Polysomal profile analysis and subsequent RT-qPCR. The polysomal profile analysis and subsequent RT-qPCR was performed using the same polysomal fractions and protocols as previously described[19]. The experiments were performed in triplicate.

We could not develop an RT-qPCR assay specific for *let-526b* only, as there is just a small region (<50 bp) in this splice form that is not present in *let-526a*. Instead we used primers specific for both splice forms. The primers used for *let-526a* specifically were 5′-accacgaccaccatatccat-3′ and 5′-cgggcattgtagaagagagc-3′. The primers for both *let-526a* and *let-526b* were 5′-tcgccgagagat tactcgtt-3′ and 5′-agaagcgatgcaaagagcat-3′.

RNAi experiments. The suppression of *let-7(n2853)* lethality by RNAi knockdown of candidate genes was tested as previously described[16]. Briefly, gene knockdown was achieved through RNAi by feeding[37–40]. Media supplements were used at the following concentrations: 200 µg ml^{-1} ampicillin and 2 mM isopropyl-β-D-thiogalactopyranoside (IPTG). All the experiments were performed at 25 °C. About 100–150 synchronized L1 worms were placed on IPTG and AMP NGM agarose plates seeded with 200 µl *E. coli* expressing dsRNA. The worms were scored 72 h later (adult stage) for suppression of lethality. Clones were regarded as positive when at least 20% of the worms were viable as adults. All the clones used were verified by sequencing for their correct insert. All RNAi plasmids used are listed in **Supplementary Table 11**.

Lethality assays for *C. elegans* mutant strains. All the experiments were performed at 25 °C and in quadruplicate. About 100–150 synchronized L1 worms were placed on NGM agarose plates seeded with 250 µl of OP50 *E. coli* bacteria. The worms were scored 48 h later (12 h after L4) for suppression of lethality. Following strains were tested: *MT7626* (*let-7(n2853)*), *FX00600* (*ztf-7(tm600)*) and *WS5673* (*ztf-7(tm600);let-7(n2853)*). At least 20% of the worms had to be viable in the double-mutant worms (WS5673) to be regarded as a successful suppressor.

Most double-mutant worms (WS5673) were dead 24 h after L4, suggesting more a lethality delay than a true suppression. A developmental delay in WS5673 worms could be excluded as the survivors at the 12 h after L4 time point had fully developed gonads with oocytes and at least 60% of the survivors also had embryos.

Cloning of 3′ UTRs from candidate genes. pEM393 is a dual luciferase Gateway (Invitrogen) compatible vector, adapted from the psiCHECK-II vector (Promega). The 3′ UTRs of *F46B6.7* (*ztf-7*), *C12C8.3* (*lin-41*), *F11A1.3a* (*daf-12*), *F13D11.2* (*hbl-1*), *F36A4.7* (*ama-1*) and *T04C12.6* (*act-1*) were cloned directly downstream of the firefly luciferase gene. The 3′ UTRome *C. elegans* database[41] (http://www.utrome.org/) and Wormbase (http://www.wormbase.org/) were used to retrieve the sequences for the 3′ UTRs of interest. The primers used for PCR and the length of each putative 3′ UTR sequence cloned are listed in **Supplementary Table 12**. Gateway cloning was performed according to the manufacturer's instructions (Invitrogen). Briefly, the sequences of interest were amplified using the *attB* adaptor primer PCR protocol to generate PCR clones containing the 3′ UTR flanked by respective *attB* sites (*attB1* site at the 5′ end and the *attB2* site the 3′ end). The PCR product was recombined into pDONR221 by the BP reaction to create the entry clone set (**Supplementary Table 12**). The entry clones were verified by sequencing and then recombined with the destination vector pEM393 to generate the expression clones via the LR reaction (**Supplementary Table 12**). The expression clones were again verified by sequencing and used for the subsequent luciferase assays.

Luciferase assay. The reactions were performed in 96-well plates. miRNA mimics or inhibitors were ordered from Dharmacon. We transfected 150 ng of the dual luciferase expression clone containing the 3′ UTR of interest and 10 pmol of either the human let-7a mimic, the control mimic (*C. elegans* miR-67), the human let-7a inhibitor or the control inhibitor (against *C. elegans* miR-67) into HeLa cells (10,000 cells per reaction) in triplicate. The Dual-Glo Luciferase assay system (Promega) was used 48 h after transfection, according to the manufacturer's instructions. All the firefly luciferase readouts were first normalized to their matching renilla luciferase readouts. Those readouts were then normalized to empty vector (pEM393 vector without any 3′ UTR) controls and then the let-7a readouts (mimics and inhibitors) were normalized to their respective oligo controls.

Selection of let-7 candidates. We selected 861 genes of interest based on computational prediction algorithms[16,42–45], experimental evidence, published literature, including known let-7 target genes[13,16,46–52] and mass spectrometry detectability[14] (random controls). The predicted targets from the computational prediction algorithms were (i) from miRBase: based on the miRanda prediction algorithm version 3.0 (ref. 44) (let-7 targets were downloaded on 25 April 2006; a *P*-value cutoff of 0.005 was applied); (ii) from Pictar: all let-7 targets available at http://pictar.mdc-berlin.de/cgi-bin/new_PicTar_nematode.cgi?species=nematode downloaded 26 April 2006 (ref. 42); (iii) our 'Stark targets': let-7 target prediction for *C. elegans* based on the algorithm described in reference 43 (A. Stark provided the target list); (iv) all the let-7 targets published in reference 16; (v) all the let-7 targets published in reference 45.

Design of SRM assays for let-7–related experiments. SRM assays were designed as previously described[7] with minor adjustments. Briefly, proteotypic peptides (PTPs) were selected based on a large shotgun proteomics dataset[14]. This *C. elegans* proteome atlas dataset was filtered for a peptide-spectrum match false discovery rate of 0.17% corresponding to a protein identification false discovery rate of 5% using Mayu[15]. Proteotypic peptides needed to contain at least one cysteine[10], and doubly charged peptides with a high number of identifications were preferred. Four to eight fragment ions from the *y*-ion series were computed for each peptide. Fragment ions (Q3) with a mass-to-charge ratio (*m/z*) above the peptide ion (Q1) and with a defined minimal distance to the peptide ion were chosen ($m/z_{Q3} - m/z_{Q1} \geq 50$ Thomson). The peptide ion/fragment ion (Q1/Q3) transitions were used to trigger the acquisition of MS2 spectra of the peptides of interest in *C. elegans* whole-worm extracts and in off-gel electrophoresis–fractionated samples (see below for SRM assay validation). Proteotypic peptides for additional 19 proteins not contained in the *C. elegans* proteome atlas were found using SRM-triggered MS2. For the samples derived from the off-gel electrophoresis fractionations, the isoelectric points of the peptides were predicted using BioPerl[53] and peptides were targeted in the predicted fraction and in the two neighboring fractions if available.

Database search and extraction of optimal SRM transitions for let-7–related experiments. The data were converted from the raw .wiff to the .mzXML format using the program mzWiff (version 3.5.3, build 16 April 2008 14:40:24). The MS2 spectra from the SRM-triggered MS2 experiments were searched against wormpep140 (http://www.wormbase.org/) using Sequest on a Sorcerer machine (3.10.4 release, SageN Research) with light ICAT as static modification and heavy ICAT and/or oxidized methionine as variable modifications. Precursor mass tolerance was set to 1.5 Da, and the data were searched fully tryptic (peptides with both ends corresponding to either N or C terminus of the corresponding protein or trypsin cleavage sites (after arginine or lysine not followed by proline) with maximal two missed cleavages. The data were filtered with a peptide-spectrum match FDR of 2.5% using PeptideProphet[54]. Three transitions for each proteotypic peptide were generated by extracting the three highest fragment ions and the retention time of the peptide from the triple quadrupole MS2. All transitions used for quantification in this study are listed in **Supplementary Table 8**.

Mass spectrometry analysis of let-7–related experiments. The same instruments, a hybrid triple quadrupole–ion trap mass spectrometer (4000QTrap, ABI/MDS-Sciex) equipped with a nanoelectrospray ion source coupled to a Tempo nano LC system (Applied Biosystems) and settings were used as in reference 7. Briefly, for validations of SRM assays, the mass spectrometer was operated in SRM mode, triggering acquisition of a full MS2 spectrum upon detection of an SRM trace (MRM-triggered MS2, threshold 200 ion counts). The SRM transitions, generated as described above, were split and analyzed in several runs (an average of 60 transitions per run with a dwell time of 20 ms per transition). Each SRM acquisition was performed with Q1 and Q3 operated at unit resolution (0.7 *m/z* half-maximum peak width). MS2 spectra were acquired in enhanced product ion (EPI) mode for the two highest SRM transitions, using dynamic fill time, Q1 resolution low, scan speed 4000 amu s^{-1}, *m/z* range 300–1,400.

The complete transition list used for the quantifications is shown in **Supplementary Table 8**. An average of 60 transitions per run was used for the measurements. The quantification measurements were done in scheduled SRM mode (retention time window, 900 s and target scan time, 2 s).

doi:10.1038/nmeth.1504

Quantitative and statistical analysis of the let-7–related experiments. Peak height for the transitions associated to the *let-7(n2853)* (light ICAT label) and wild-type (heavy ICAT label) derived peptides were quantified using the software MultiQuant v. 1.1 Beta (Applied Biosystems). Log_2 fold changes (*let-7(n2853)*/wild type) were calculated for each transition separately. These values were then normalized using 11 proteotypic peptides (**Supplementary Figs. 1a** and **4**) on each biological replicate separately. To test for statistically significant abundance changes, a two-sided, one-sample *t*-test was done on the normalized log_2 fold changes of the transitions grouped according to protein (mean of null hypothesis (μ) equal to zero). To generate our list of regulated candidates we used a $P \leq 0.01$ cutoff.

Sample preparation for miR-58–related experiments. WS4303 and WS5041 worms were always grown in parallel for each biological replicate at 25 °C. Four biological replicates of synchronized late L4 larvae were generated.

The protein samples were derived as has been described previously[55]. We adapted the protocol accordingly. Briefly, after we collected the worms, we separated them from the bacteria by several washes in ice-cold buffer A (20 mM Tris–HCl (pH 8.0), 140 mM KCl, 1.8 mM $MgCl_2$, 0.1% Nonidet P-40 (NP-40) and 0.1 mg ml^{-1} heparin), froze them in liquid nitrogen, and stored them at −80 °C until further use. One milliliter of frozen worm pellet was resuspended in 5 ml buffer B (buffer A plus 1.5 mM dithiothreitol (DTT), 1 mM phenylmethylsulfonylfluoride, 0.5 μg ml^{-1} leupeptin, 0.8 μg ml^{-1} pepstatin, 20 U ml^{-1} DNase I, 100 U ml^{-1} RNaseOUT (Invitrogen) and 0.2 mg ml^{-1} heparin). The resuspended worms were dropwise refrozen in liquid nitrogen and homogenized by a TissueLyser instrument (Qiagen) by four cycles of 4 min, each with a setting of 30 Hz; the metal containers with the samples were always refrozen in liquid nitrogen between the cycles. The purified worm extracts were incubated with 400 μl slurry (50% (v/v)) IgG–agarose beads (Sigma) for 2 h at 4 °C. The supernatant representing the total extract was separated, and the beads were then used for the isolation of the TAP∷ALG-1 containing complex. We used the supernatant for additional processing, as it was nearly identical to the total clarified lysates (only about 50% of the TAP∷ALG-1 containing complex was missing).

Thereafter, the proteins were precipitated by acetone and resuspended in buffer (50 mM Tris-HCl (pH 8.3) and 8 M Urea) and the protein concentrations of the purified extracts were determined using the Bradford reagent (Sigma-Aldrich). The protein concentrations of the different extracts were adjusted to each other to minimize any bias for the further processing steps. Afterwards, 50 μg of total protein of each sample was mixed with 50 μg of total protein derived from ^{15}N heavy isotope metabolically labeled adult worms (provided by R.F. Ketting and B.B. Tops)[25]. The same metabolically labeled sample was mixed into all the 8 samples (four replicates of WS4303 and WS5041 worms). The metabolically labeled proteins were used as a normalization standard for all samples (for details, see below).

Finally, the tryptic digest and the following cation-exchange chromatography were performed as described previously[35]. The peptide mixtures were cleaned by Sep-Pak tC18 cartridges (Waters) and eluted with 60% acetonitrile. All peptide samples were dried in a vacuum centrifuge, resolubilized in 2% acetonitrile and 0.1% formic acid and frozen at −20 °C until they were analyzed on the mass spectrometer.

Design of SRM assays of miR-58–related experiments. We started with two protein lists of interest: 118 potential targets of miR-58 predicted with the TargetScan algorithm (http://www.targetscan.org/cgi-bin/targetscan/worm_12/targetscan.cgi?gid=&mir_c=miR-58&mir_nc=)[20,21] and 44 randomly selected proteins as negative controls (from a set of 5,000 genes that are well expressed in L4 hermaphrodites, based on microarray data; unpublished data). We used the large *C. elegans* proteome atlas to determine peptides with good properties for mass spectrometric analysis[14]. For proteins with no or less than three PTPs available in the *C. elegans* proteome atlas, additional peptides with good MS properties were derived by bioinformatic prediction as previously[26], using the publicly available tool PeptideSieve[9]. PTPs had to be 7–18 amino acids long, must not have contained methionine or cysteine, had to be between 700–2,500 Da and had to map to one gene locus. To select the 'best' three PTPs, the priorities were number of charge 2 peptide-spectrum matches (descending), peptide length (ascending), peptide predicted isoelectric point (ascending) and PeptideSieve score (descending). Based on this filtering, we ordered peptides, synthesized them on a small scale in an unpurified format using the SPOT synthesis technology (JPT Peptide Technology), for 115 predicted targets (TargetScan) and 42 random control proteins. These peptides were prepared according to ref. 26 and were used to derive the optimal coordinates of the corresponding SRM assays (that is, best responding fragment ions, chromatographic elution time) by SRM-triggered MS2 (ref. 26). For each peptide (precursor charge 2 and 3) a transition corresponding to the first singly charged y ion above the precursor *m/z* greater than ($m/z_{precursor}$ + 20 Th) was generated and used as a trigger for a full MS2 spectrum.

Database search and extraction of optimal SRM transitions for miR-58 related experiments. Resulting raw MS2 .wiff data, generated by the SRM triggered MS2 runs, were converted to .mzXML format with the program mzWiff and searched against a database containing all the protein sequences of the targeted proteins (wormpep 140) using mascot (Version 2.1.0). A decoy database was generated by randomly reshuffling amino acids in between tryptic cleavage sites and appended to the target database. Precursor mass tolerance was set at 2 Da. The data were searched with full tryptic cleavage (maximally two missed cleavages) and filtered for a peptide-spectrum match FDR of 0.01 using Mayu[15]. For each peptide, the spectrum with the highest ion score was used to extract the five most intense fragment ions corresponding to the transitions used for quantification (doubly and triply charged). Fragments with *m/z* values close to the precursor ion *m/z* were discarded. Transitions corresponding to the metabolically heavy labeled proteins were calculated and added as well as decoy transitions that were used in the automated analysis of the data (**Supplementary Table 9**). The process was automated using in-house written Perl and R scripts (R Development Core Team. R: A Language and Environment for Statistical Computing).

Mass spectrometry analysis for miR-58–related experiments. The same instruments and settings as for the let-7-related experiments were used. Minor differences were that in the SRM

assays validation phase around 200 transitions (dwell time = 10 ms per transition) per run were targeted. Moreover, peptides that were not positively validated in the first set of runs were targeted again two more times.

The complete transition list used for quantifications is available in **Supplementary Table 9**. An average of 300 transitions per run was used for the measurements. The quantification measurements were done in the scheduled SRM mode (retention time window, 360 s and target scan time, 2.5 s).

SRM data processing for quantification of miR-58–related experiments. Raw SRM .wiff data were converted to .mzXML format with the program mzWiff. A peak detection algorithm was run on the data and several criteria of the signals were extracted to derive a score for the signal. Among the scores was a correlation score for expected relative intensities when compared to the relative intensities of the synthetic peptide measurement. Correlation of shape and coelution among light and of the light to the heavy transitions was also scored. A null model was derived from the measurement of negative controls (nonsense transitions or decoy transitions) included in the measurements. The scores were combined and a confidence score was calculated for the signals using the null model (L.R., O. Rinner, P.P., R. Hüttenhain, M. Beck, M. Brusniak *et al.*, unpublished data).

For quantification, the peak heights for one peptide were summed up. The summed peak heights were normalized using the signal of the isotopically heavy labeled peptide. After that, the $\log_2$ ratios of mutant to wild-type worms were calculated for each peptide measurement. For each protein, the average of this $\log_2$ ratio was calculated using the $\log_2$ ratios of all the peptides, charge states and biological replicates. A one sample Student's *t*-test (one-sided) was used to estimate a *P* value of regulation for the proteins.

31. Riddle, D.L., Blumenthal, T., Meyer, B.J. & Priess, J.R. *C. elegans II* (CSHL Press, 1997).
32. Miska, E.A. *et al.* Most *Caenorhabditis elegans* microRNAs are individually not essential for development or viability. *PLoS Genet.* **3**, e215 (2007).
33. Ding, L., Spencer, A., Morita, K. & Han, M. The developmental timing regulator AIN-1 interacts with miRISCs and may target the Argonaute protein ALG-1 to cytoplasmic P bodies in *C. elegans*. *Mol. Cell* **19**, 437–447 (2005).
34. Brenner, S. The genetics of *Caenorhabditis elegans*. *Genetics* **77**, 71–94 (1974).
35. Shiio, Y. & Aebersold, R. Quantitative proteome analysis using isotope-coded affinity tags and mass spectrometry. *Nat. Protoc.* **1**, 139–145 (2006).
36. Livak, K.J. & Schmittgen, T.D. Analysis of relative gene expression data using real-time quantitative PCR and the 2(-Delta Delta C(T)) Method. *Methods* **25**, 402–408 (2001).
37. Fraser, A.G. *et al.* Functional genomic analysis of *C. elegans* chromosome I by systematic RNA interference. *Nature* **408**, 325–330 (2000).
38. Kamath, R.S. *et al.* Systematic functional analysis of the *Caenorhabditis elegans* genome using RNAi. *Nature* **421**, 231–237 (2003).
39. Timmons, L. & Fire, A. Specific interference by ingested dsRNA. *Nature* **395**, 854 (1998).
40. Rual, J.F. *et al.* Toward improving *Caenorhabditis elegans* phenome mapping with an ORFeome-based RNAi library. *Genome Res.* **14**, 2162–2168 (2004).
41. Mangone, M., Macmenamin, P., Zegar, C., Piano, F. & Gunsalus, K.C. UTRome.org: a platform for 3'UTR biology in *C. elegans*. *Nucleic Acids Res.* **36**, D57–D62 (2008).
42. Lall, S. *et al.* A genome-wide map of conserved microRNA targets in *C. elegans*. *Curr. Biol.* **16**, 460–471 (2006).
43. Stark, A., Brennecke, J., Bushati, N., Russell, R. & Cohen, S. Animal microRNAs confer robustness to gene expression and have a significant impact on 3' UTR evolution. *Cell* **123**, 1133–1146 (2005).
44. Griffiths-Jones, S., Saini, H.K., Dongen, S.V. & Enright, A.J. miRBase: tools for microRNA genomics. *Nucleic Acids Res.* **36**, D154–D158 (2008).
45. Watanabe, Y. *et al.* Computational analysis of microRNA targets in *Caenorhabditis elegans*. *Gene* **365**, 2–10 (2006).
46. Johnson, S.M. *et al.* RAS is regulated by the let-7 microRNA family. *Cell* **120**, 635–647 (2005).
47. Ding, X.C., Slack, F.J. & Grosshans, H. The let-7 microRNA interfaces extensively with the translation machinery to regulate cell differentiation. *Cell Cycle* **7**, 3083–3090 (2008).
48. Abrahante, J.E. *et al.* The *Caenorhabditis elegans* hunchback-like gene lin-57/hbl-1 controls developmental time and is regulated by microRNAs. *Dev. Cell* **4**, 625–637 (2003).
49. Slack, F.J. *et al.* The lin-41 RBCC gene acts in the *C. elegans* heterochronic pathway between the let-7 regulatory RNA and the LIN-29 transcription factor. *Mol. Cell* **5**, 659–669 (2000).
50. Lin, S.Y. *et al.* The C elegans hunchback homolog, hbl-1, controls temporal patterning and is a probable microRNA target. *Dev. Cell* **4**, 639–650 (2003).
51. Papadopoulos, G.L., Reczko, M., Simossis, V.A., Sethupathy, P. & Hatzigeorgiou, A.G. The database of experimentally supported targets: a functional update of TarBase. *Nucleic Acids Res.* **37**, D155–D158 (2009).
52. Xiao, F. *et al.* miRecords: an integrated resource for microRNA-target interactions. *Nucleic Acids Res.* **37**, D105–D110 (2009).
53. Stajich, J.E. *et al.* The Bioperl toolkit: Perl modules for the life sciences. *Genome Res.* **12**, 1611–1618 (2002).
54. Keller, A., Eng, J., Zhang, N., Li, X. & Aebersold, R. A uniform proteomics MS/MS analysis platform utilizing open XML file formats. *Mol. Syst. Biol.* **1**, 2005.0017 (2005).
55. Gerber, A.P., Herschlag, D. & Brown, P.O. Extensive association of functionally and cytotopically related mRNAs with Puf family RNA-binding proteins in yeast. *PLoS Biol.* **2**, E79 (2004).

doi:10.1038/nmeth.1504